# Numerical Relativity

## From Breakthrough to the Next Decade of Multimessenger Astronomy

Manuela Campanelli

RIT | College of Science
Center for Computational Relativity and Gravitation

# The GW150914 “Golden” Binary

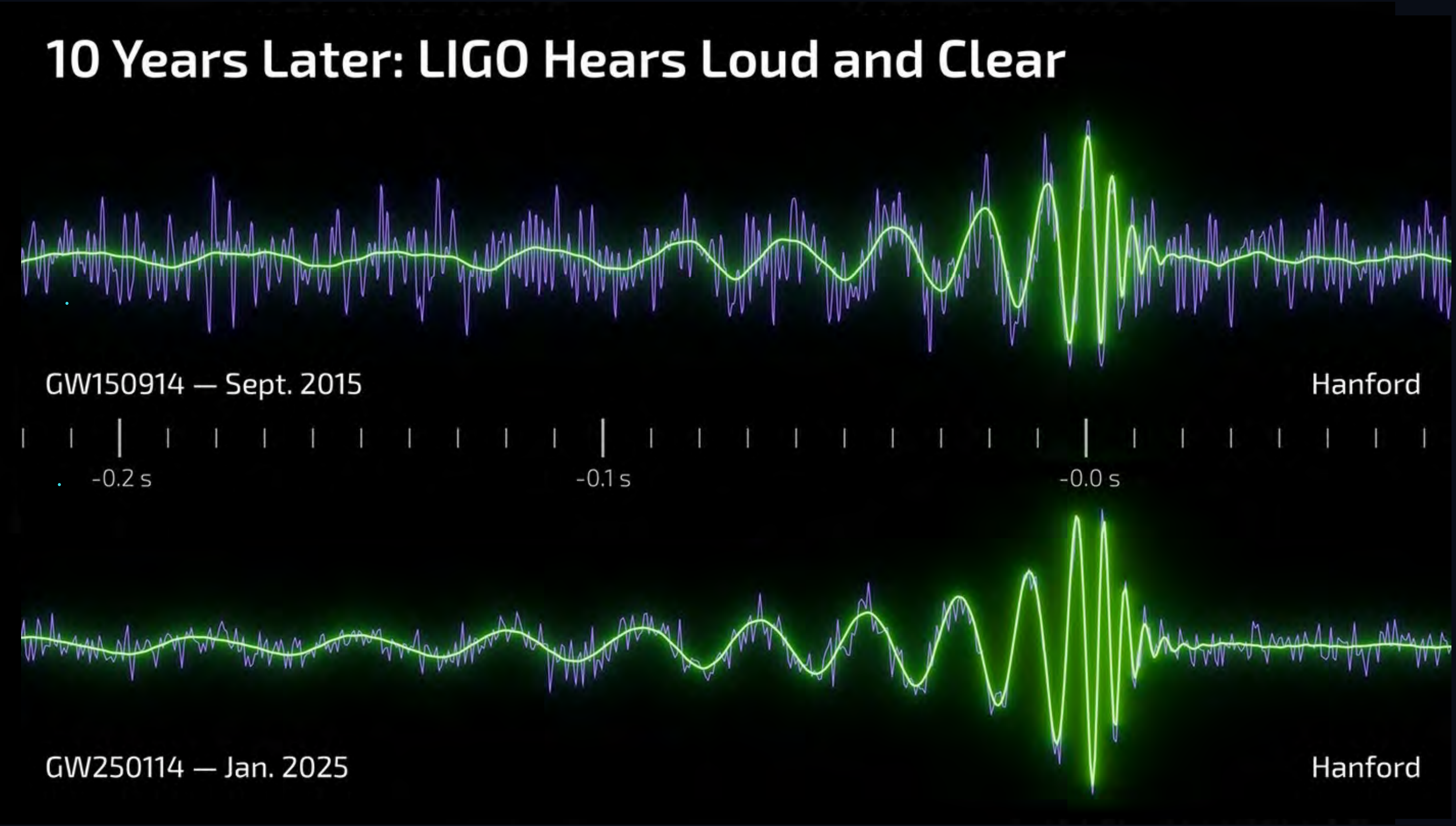


Analytical Relativity (AR) and Numerical Relativity (NR) were essential to interpreting gravitational-wave (GW) observations.

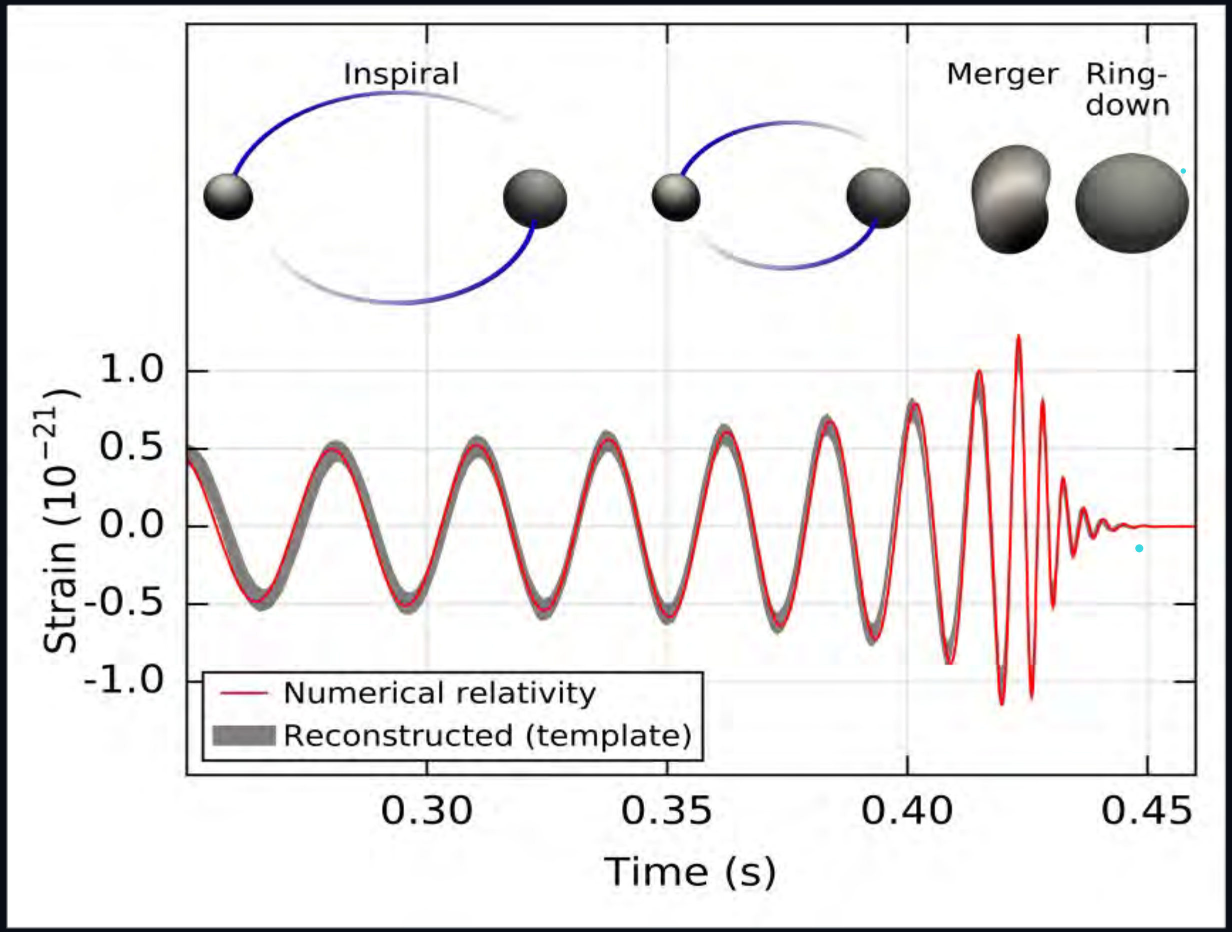


Abbott +2016 and many more ...

Is black-hole research a story of giant leaps roughly every decade?

# The Foundations for Numerical Relativity

- 1915: **General Relativity's Challenge** The field equations are too complex for most manual calculations, limiting solutions to approximations.
- 1916–1940s: **The Analytical Gap** Progress is limited to simple, pen-and-paper solutions; dynamic, real-world problems remain out of reach.
- 1952: **The Theoretical "Green Light"** Choquet-Bruhat proves the equations form a well-posed initial-value problem — confirming that simulation is mathematically viable.
- 1957: **The Call for Computation** At the Chapel Hill Conference, Bryce DeWitt argues for using computers to solve the equations.
- 1959–1962: **The Computational Blueprint** The ADM formalism (Arnowitt, Deser & Misner) creates the practical "3+1" equations, providing the essential framework for computation.

MISNER summarized the discussion of this session: "First we assume that you have a computing machine better than anything we have now, and many programmers and a lot of money, and you want to look at a nice pretty solution of the Einstein equations. The computer wants to know from you what are the values of $g_{\mu\nu}$ and $\frac{\partial g_{\mu\nu}}{\partial t}$ at some initial surface, say at $t = 0$. Now, if you don't watch out when you specify these initial conditions, then either the programmer will shoot himself or the machine will blow up. In order to avoid this calamity you must make sure that the initial conditions which you prescribe are in accord with certain differential equations in their dependence on x, y, z at the initial time. These are what are called the "constraints." They are the equations analogous to but much more com-

Charlie Misner (1957)

GR 1: Conference on the role of gravitation in physics
University of North Carolina, Chapel Hill [January 18-23, 1957]

What was analytically impossible in 1915 became mathematically viable by 1952.

By 1957, the field had its theoretical proof, its computational framework, and its marching orders: use computers.

But the predictions were alarming!

FIRST ATTEMPTS

# Pioneering Simulations & Problems

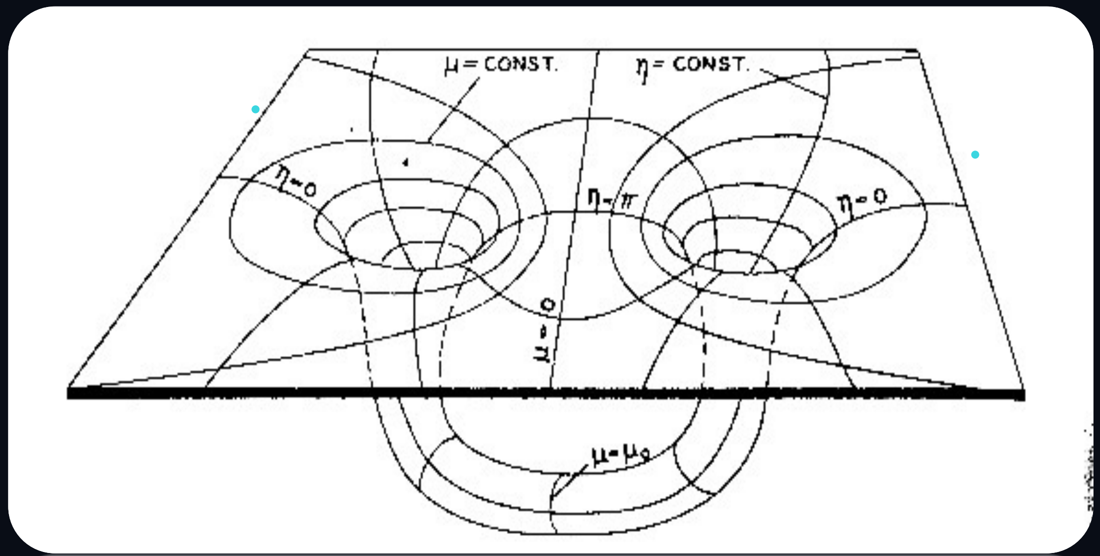


- 1964: Hahn & Lindquist attempt the "**first computer simulation**" of Einstein's equations to model a black hole collision.
- 1970s: **"The Singularity Problem"** becomes a major hurdle, as simulations "crash when encountering black hole singularities." Unruh's BH excision, York's formulation.
- 1977: Larry Smarr develops the first numerical code to model the **head-on (axisymmetric) collision** of two black holes (Smarr & Eppley).
- 1980s: Stark & Piran "simulate a rotating stellar collapse and extract the predicted gravitational waves," a crucial proof of concept.

**Underlying Challenge**

Progress in the field remains severely "hindered by the lack of sufficient computational power" for the highly complex, nonlinear equations.

*"Most had done all of their research relying on exact analytic solutions. I was arguing for computational science and that the only way to understand the dynamics was to use computers."*

NCSA's "Pioneers" series, Larry Smarr

# The Grand Challenge

- 1990s: **The Grand Challenge** collaboration is formed to tackle the complex problem of orbiting black holes.
- "Head-on Collision of Two Equal Mass Black Holes", Anninos, Hobill, Seidel, Smarr & Suen, 1993

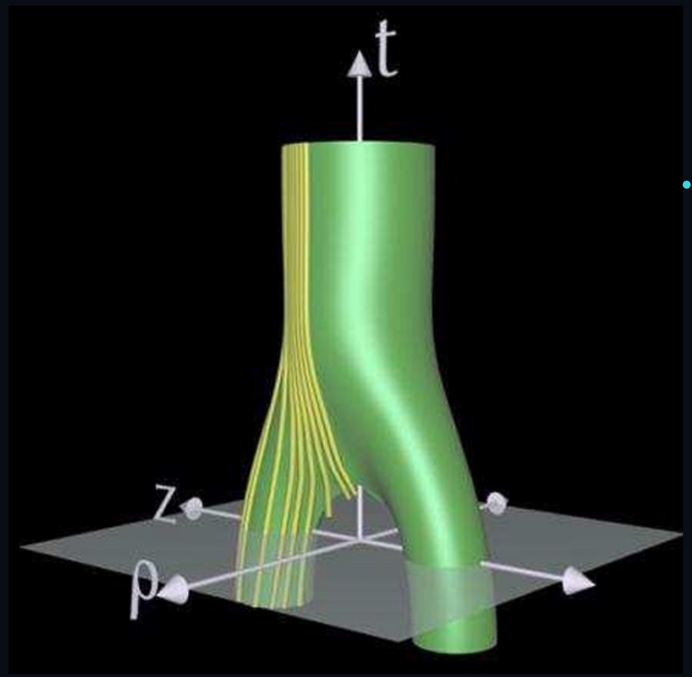


"Pair-of-pants" Cover of Science, 1995
Binary Black Hole Grand Challenge Alliance
(Matzner et al)

> " ... there are a substantial number of unresolved issues which the alliance must deal with before a successful simulation of black-hole binary in-spiral is in hand ... From a conceptual viewpoint, perhaps the most pressing of these is the question of coordinate system choice. "
>
> Choptuik, M. W. (1997).
> The Binary Black Hole Grand Challenge Project.
> ASP Conference Series, 123, 305.

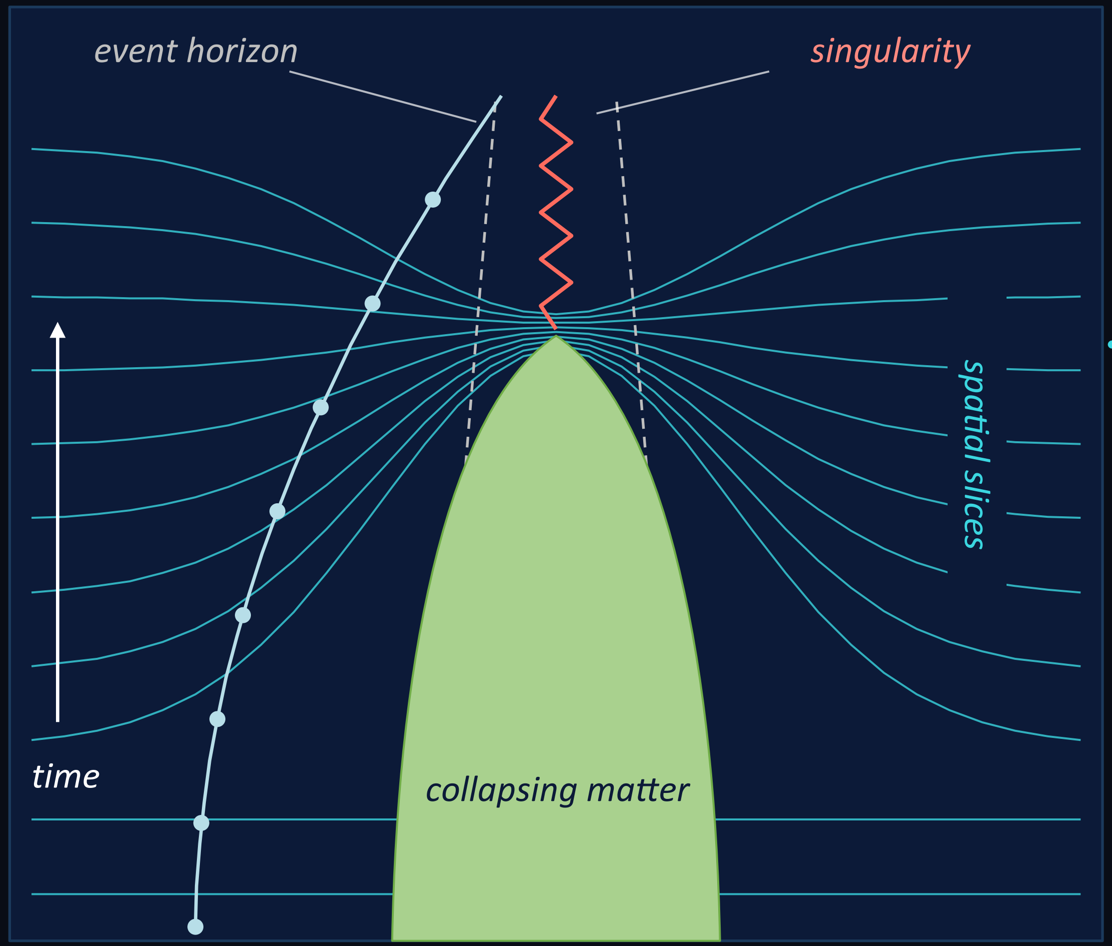


Grid stretching

**The 1990s reality:** 3D black-hole runs crashed at t ~ 10–100 M regardless of resolution — a formulation problem, not a coding problem.

SIMULATION VS. OBSERVATION

# The "Race" Between Simulation and Observation

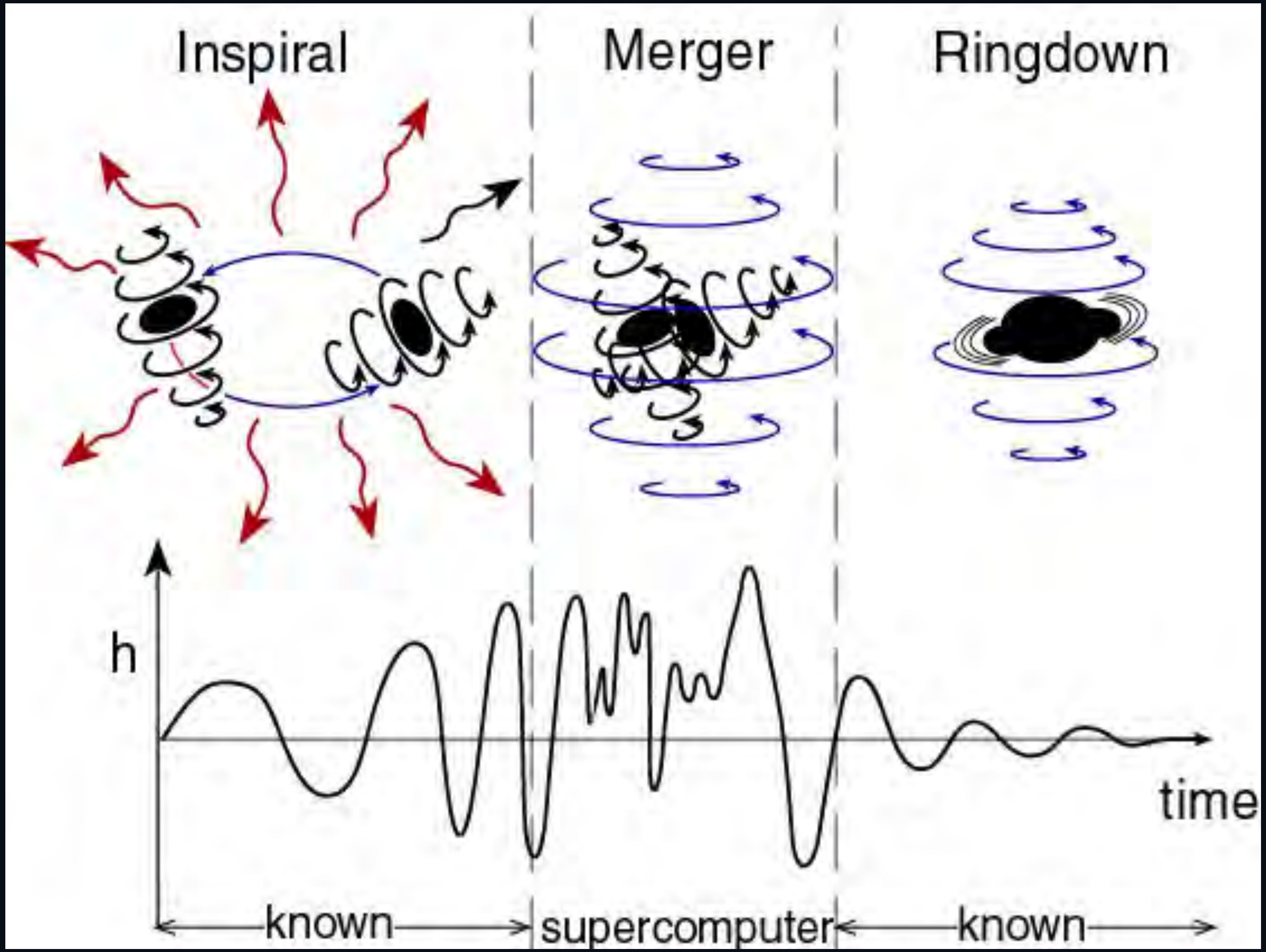


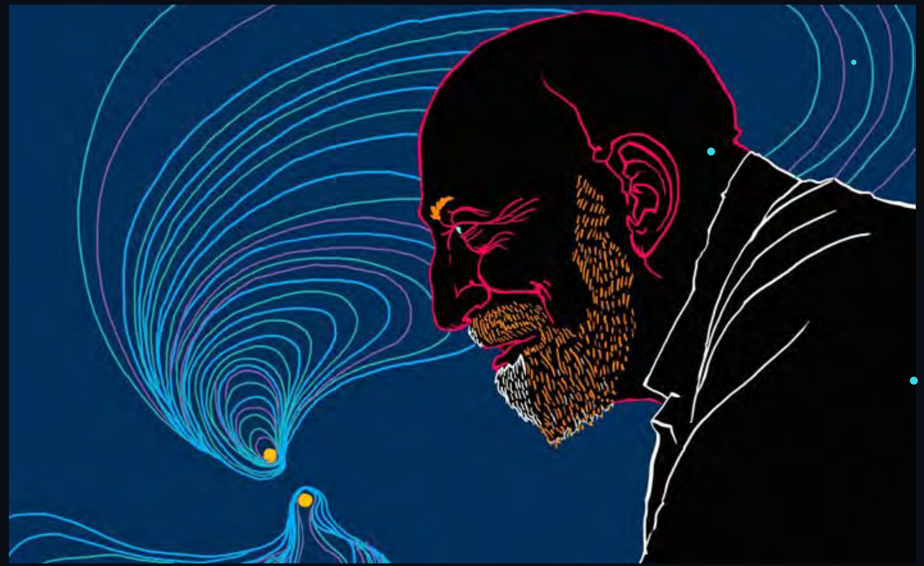

"I have bet these numerical relativists that gravitational waves will be detected from black-hole collisions before their computations are sophisticated enough to simulate them.

I expect to win … but hope to lose, because the simulation results are crucial to interpreting the observed waves.

…I heaved a sigh of relief; perhaps I would actually lose my bet!"

K.S. Thorne, *The Future of Spacetime* (2002).

# The Post Grand Challenge Era

- 1995: Evolution with conformal BSSN *(Shibata & Nakamura 1995, Baumgarte & Shapiro 1999).*
- 1997: Represented black holes as **"punctures"** (Brandt & Bruegmann) addressing the singular behavior of the conformal factor to solve the Hamiltonian constraint. The method was simple and required no excision!
- 1999: The grazing collision (Alcubierre+ 1999) with the singularity avoiding slice
    - ➢ BSSN, freeze the punctures on the computational grid
    - ➢ Variety of slicing conditions *and vanishing shift*
- 2003: Miguel Alcubierre proposes to use the singularity avoiding slicing (e.g. 1+log) (Alcubierre, 2003) and the gamma driver shift (Alcubierre+ 2003)
- 2004: Bernd Bruegmann achieves the one orbit mark (Bruegmann+ 2004)

This work set the stage for the Breakthrough Era …

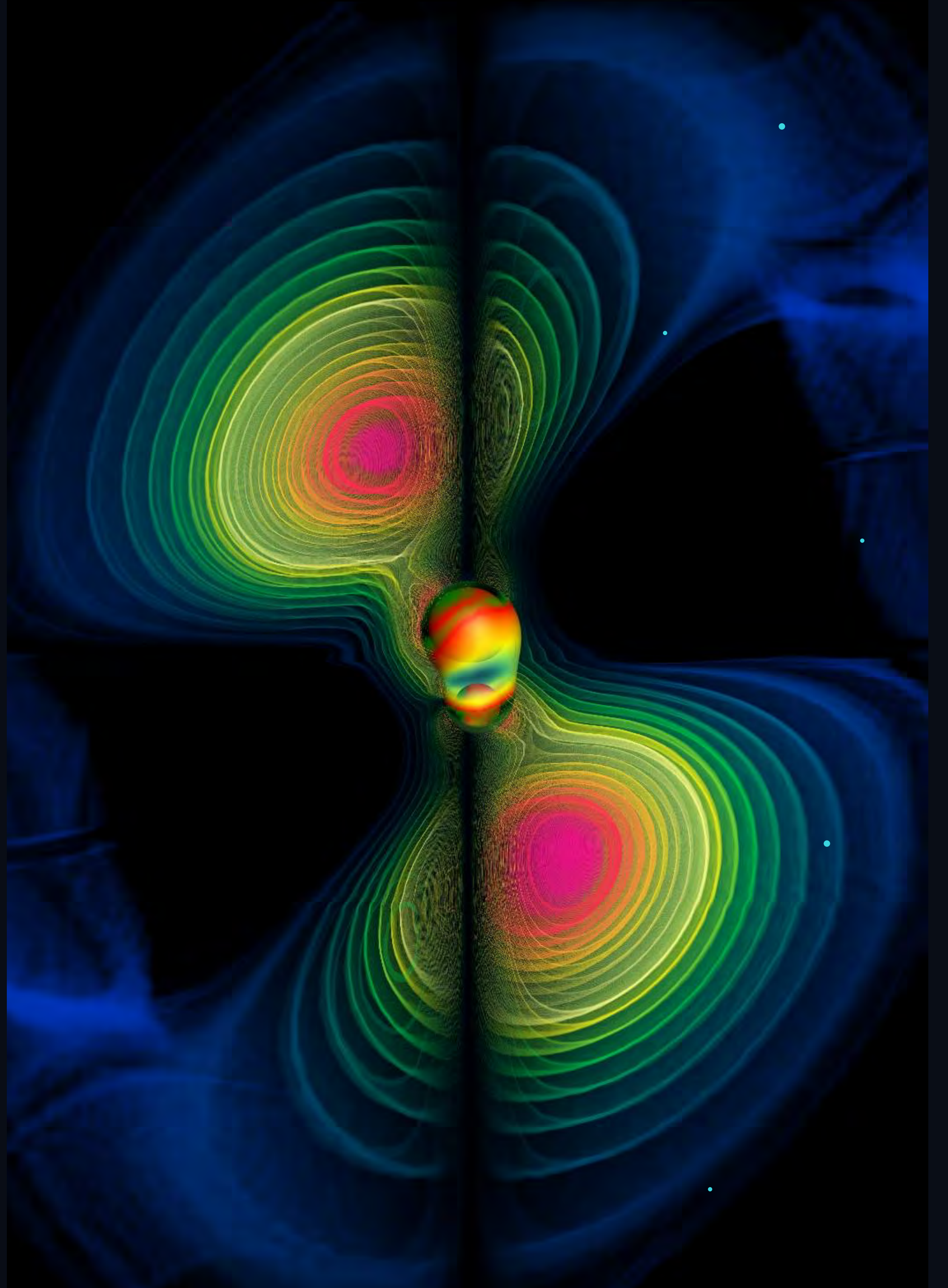

The grazing collision, visualization: Werner Benger

# Reviving the "Code Crash"

**The Lazarus Project (2001-2005).** A hybrid approach combines numerical relativity with black hole perturbation theory to model the final moments of a merger. (Baker+2001; Baker+2002; Baker, Campanelli+2004; Campanelli+2005)

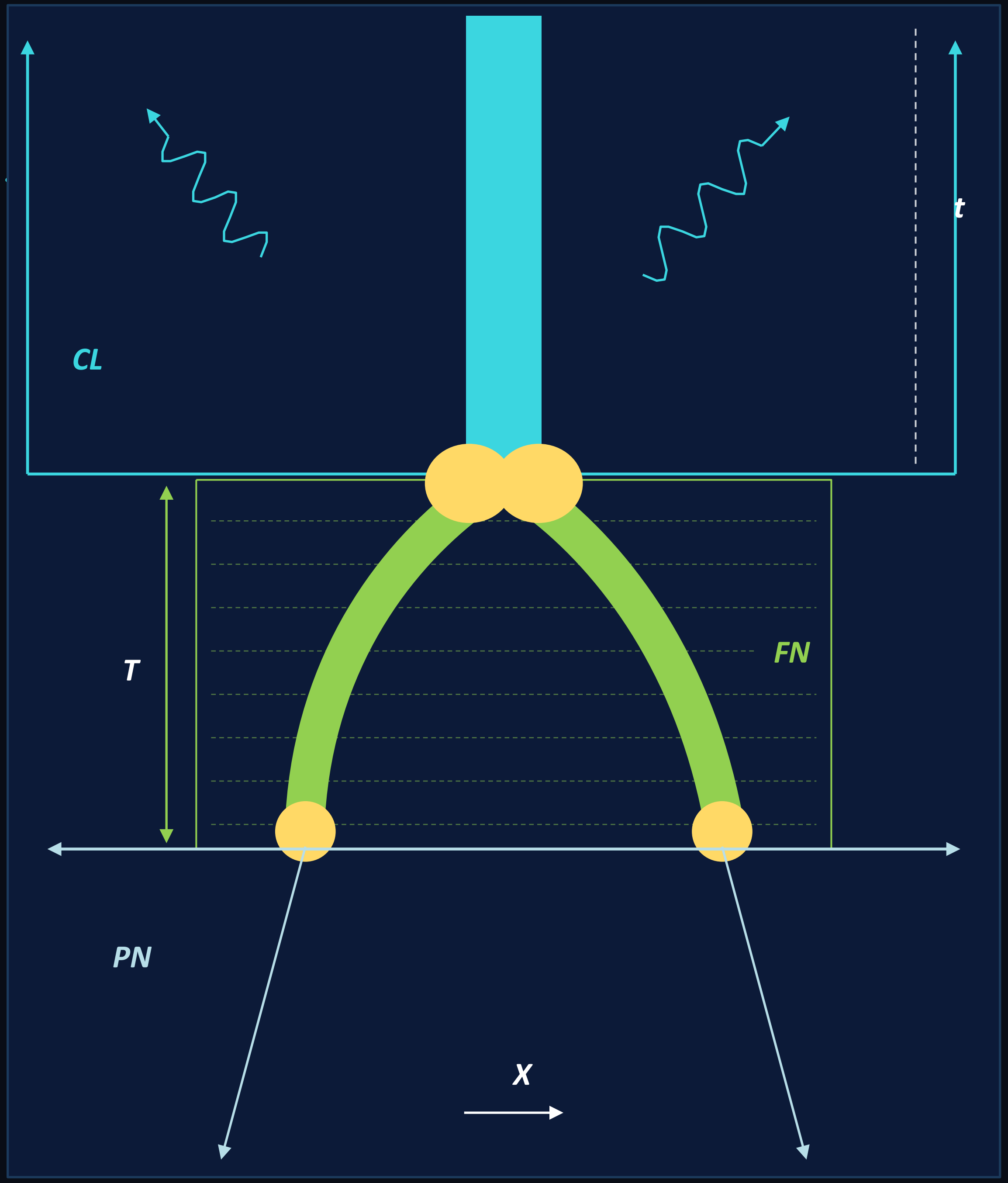


Stemming from Close Limit Approximation (Price & Pullin 1994): Treats the late-stage merger as a single, perturbed black hole.
Imposition of initial data in the Teukolsky equation (Campanelli+1997,1998)

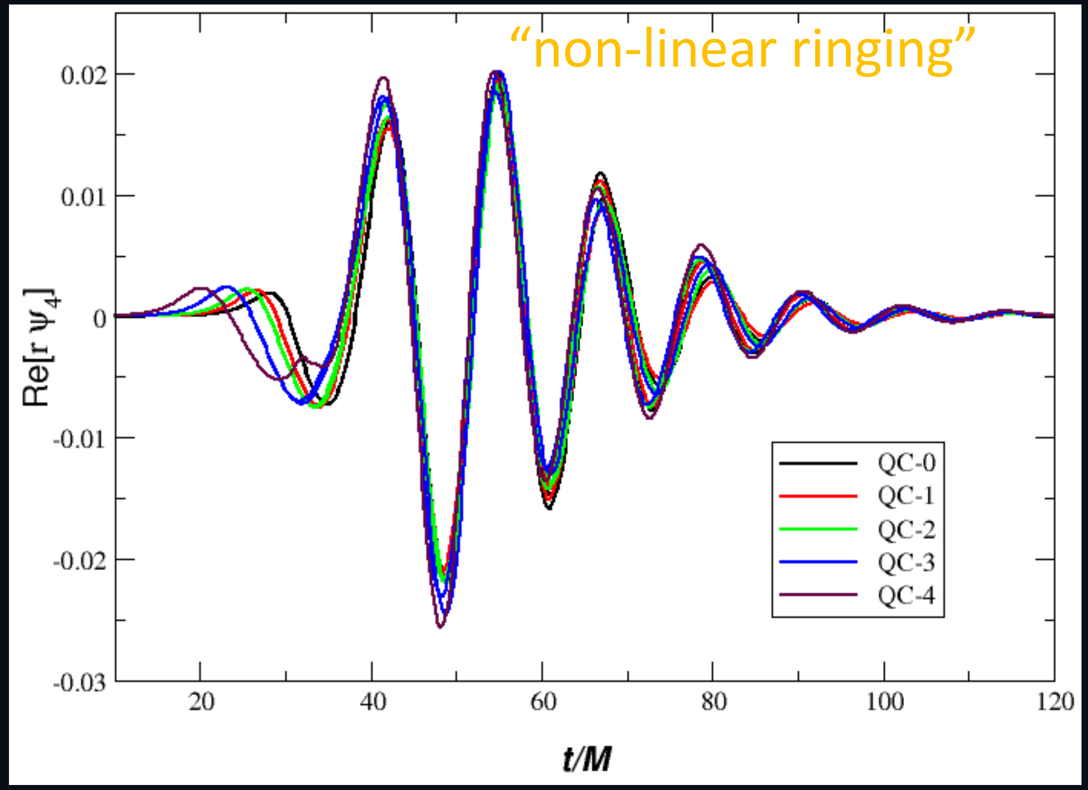


Non-linear Ringing: Arises from higher-order perturbations of the remnant black hole spacetime (Bucciotti+ 2023; Yi+ 2024).

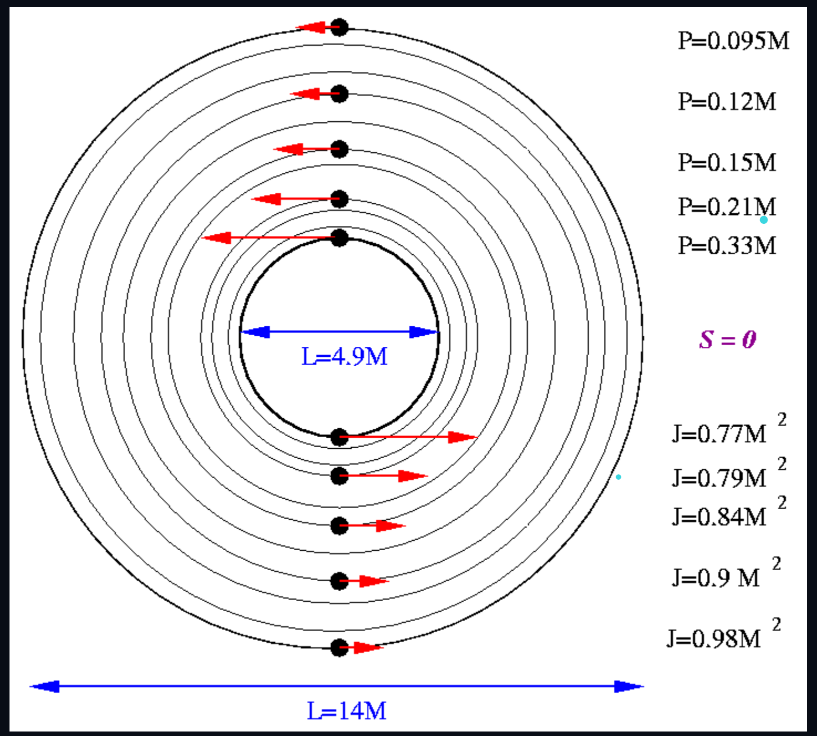


- The merger radiates a significant amount of energy (~3% of the total mass) and angular momentum (~12%).
- The final plunge is extremely fast, occurring in less than half an orbital period.

Despite the chaotic merger, the final waveform was surprisingly simple!

# The Breakthrough: Numerical Relativity Comes of Age

- 2005: **"Annus Mirabilis" of Numerical Relativity** - First full, stable simulations of a binary black hole (BBH) merger are achieved, solving decades-old stability issues.

  - First Solution: **Generalized Harmonic** Frans Pretorius achieves the first success using generalized harmonic coordinates (Pretorius, PRL 2005).

  - **"Moving Punctures"**: Independently, teams led by Campanelli (UTB) and Baker (NASA) develop the robust "moving puncture" technique (Campanelli+, Baker+, PRL 2006).

- 2015: The observed **GW150914** waveform (Abbott+, PRL 2016) perfectly matches simulation predictions, validating the field and launching gravitational-wave astronomy.

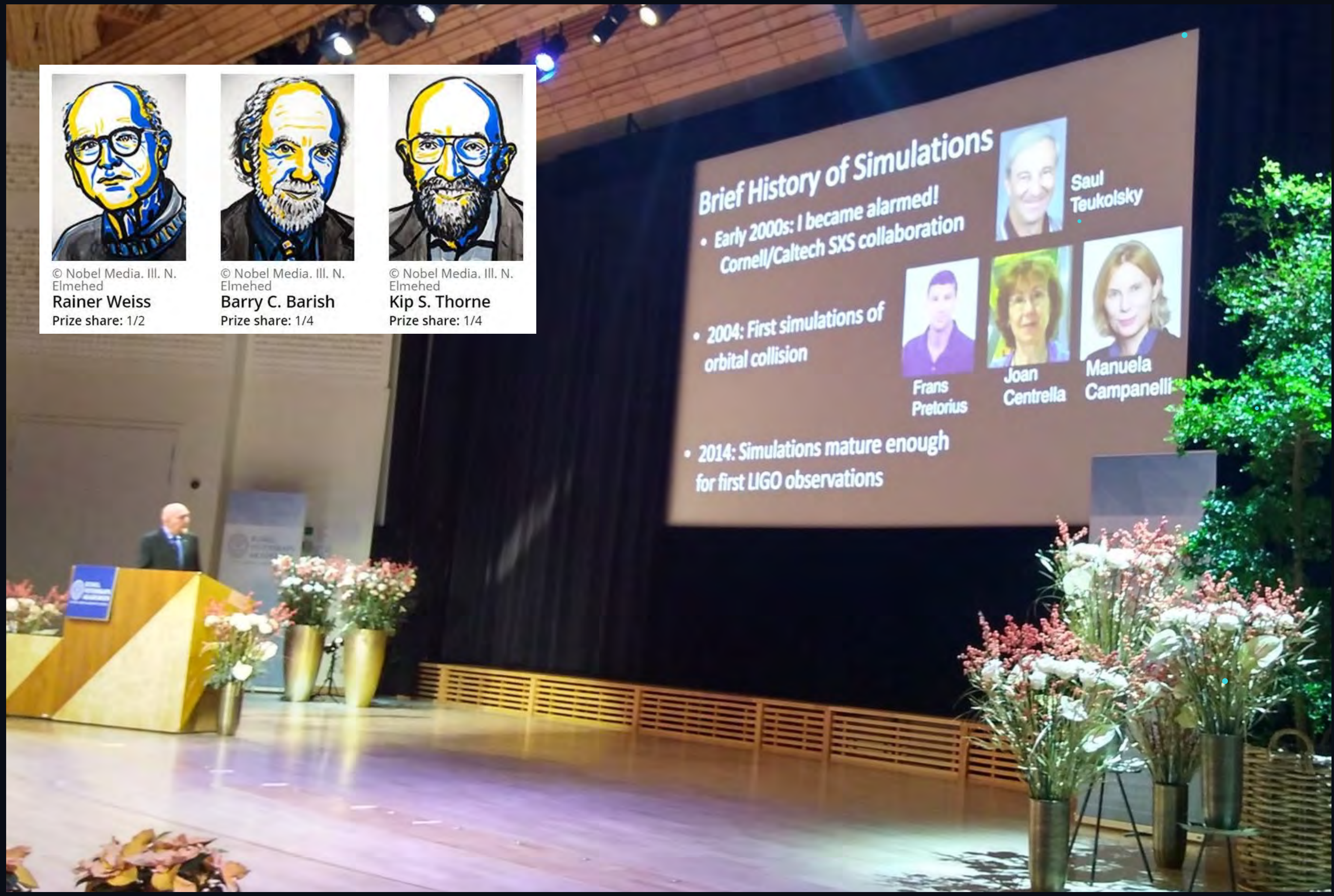


K.S. Thorne, LIGO and Gravitational Waves, III: Nobel Lecture, December 8, 2017.

THE BREAKTHROUGH

# The Moving Punctures Approach

Independently, teams at UTB and NASA GSFC develop the "moving puncture" technique

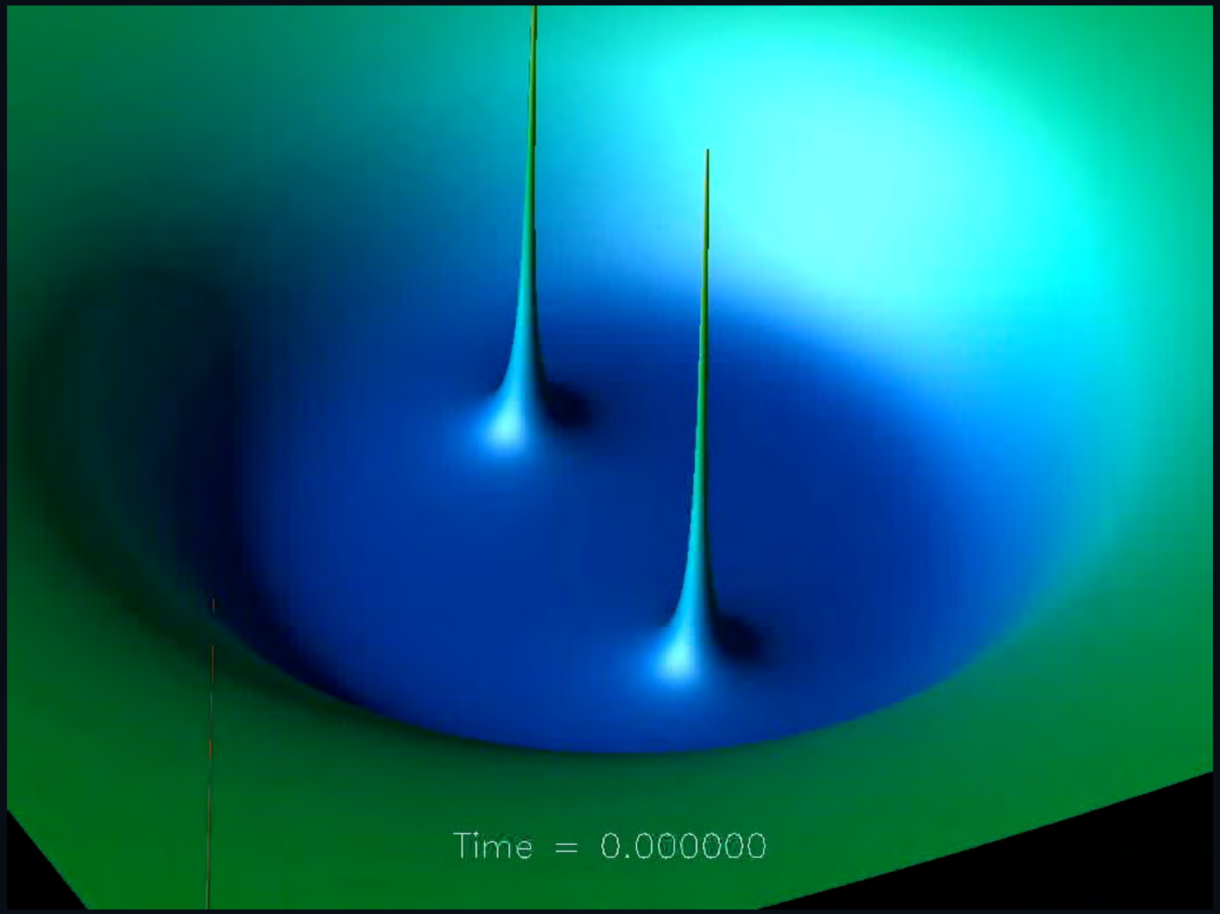


Allowed the punctures (no BH excision) to move across the grid …

- Absorb singularities in the BSSN conformal factor to free the punctures
- Use new gauge conditions to move the punctures

$L \sim 5M$
$E_{rad} \sim 2.5\text{-}3\ \%$
$J_{rad} \sim 13\ \%$
$a/M \sim 0.7$

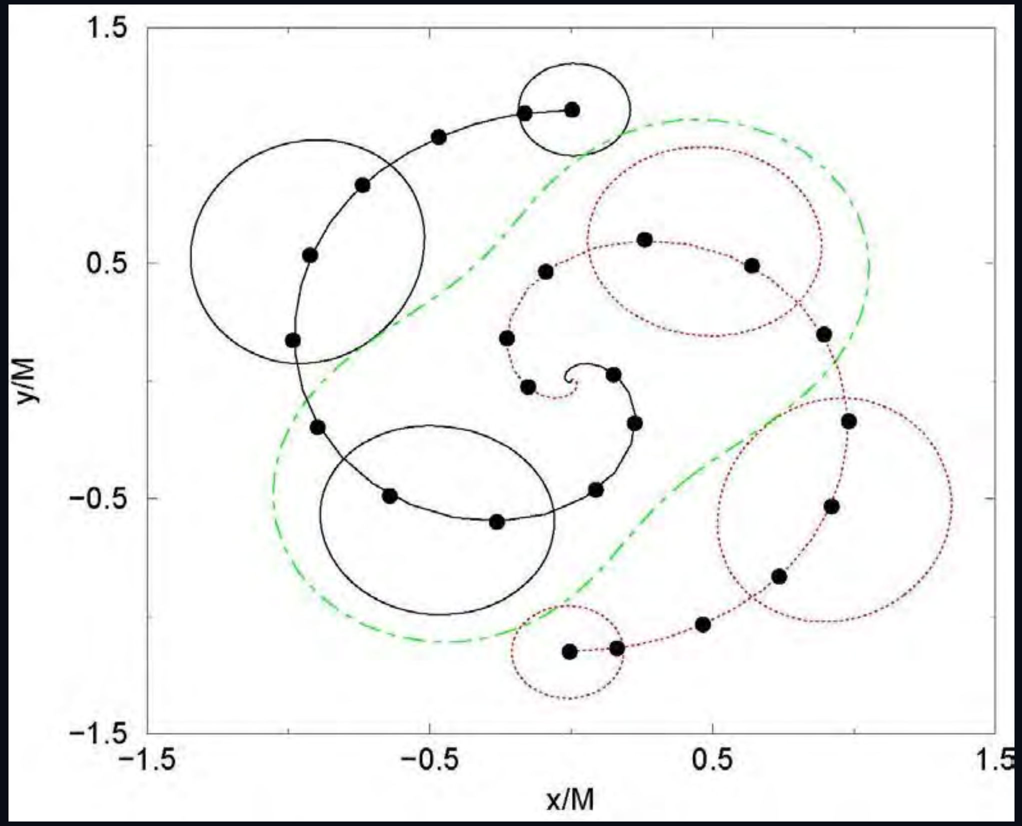


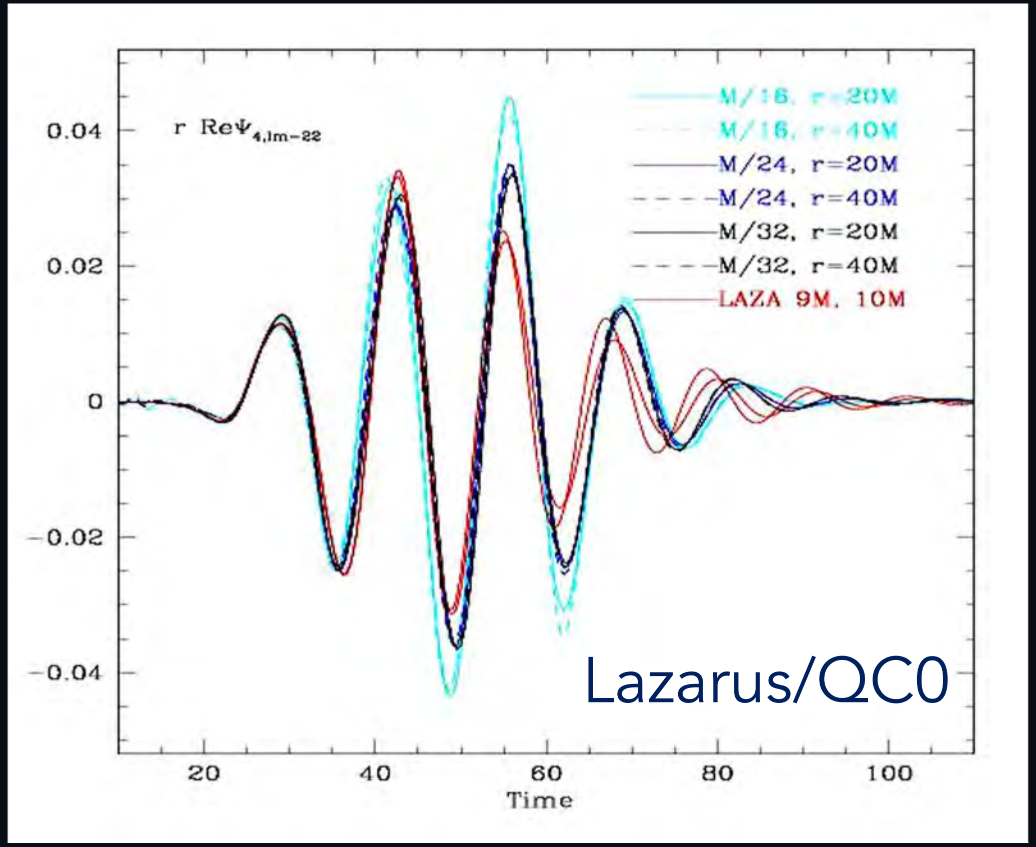


The papers appeared back-to-back in Phys. Rev. Lett. 2006.

- Campanelli, Lousto, Zlochower, Marronetti, “Accurate Evolutions of Orbiting Black-Hole Binaries Without Excision”
- Baker, Centrella, Choi, Koppitz, van Meter “Gravitational-Wave Extraction from an Inspiraling Configuration of Merging Black Holes”

Both groups showed excellent agreement with the Lazarus project's QC0 waveform data.

# The Quick Evolution of Converging Ideas and Synergies

- Key insights emerged from talks by Pedro Marronetti (APS 2005) on binary neutron star evolutions and Frans Pretorius (UTB 2005) on black hole binaries.

"E pur si muove"  Galileo 1633

- The Head-to-Head: The "moving puncture" and "generalized harmonic" methods were first directly compared at a workshop at the AEI in 2006
- Where do moving punctures go? Hannam+2006, 2007
- Validation & Agreement: This established a better understanding of the robustness of the solutions.

The field of numerical relativity was significantly transformed in a matter of a few weeks!

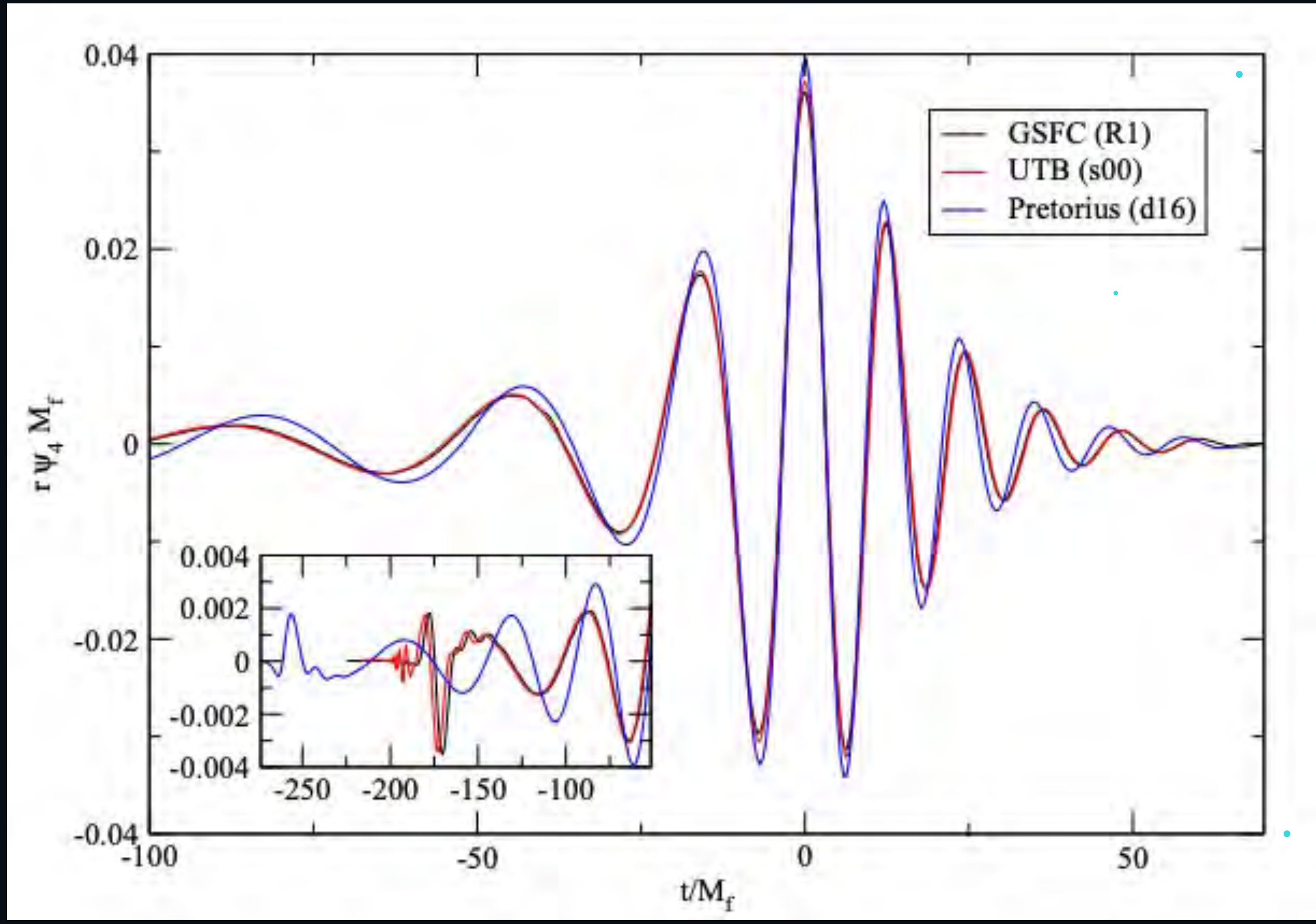


Baker, Campanelli, Pretorius and Zlochower, CQG 2007

*"we can anticipate that the overlap of the waveforms in Fig. 1 will be greater than 0.95 for black hole binaries with masses greater than roughly 200 solar masses"*

NR TODAY

# Numerical Relativity Today

- The goal: solve Einstein's equations with HPC — the only fully accurate window on strong-field gravity
- The engine of GW discovery: signal identification, parameter estimation & tests of GR
- A thriving field: most codes evolve moving punctures (Campanelli+2006, Baker+2006), complemented by SXS's spectral excision (Pretorius 2005; SpEC)
- Today's codes are robustly convergent and highly scalable, reaching 7–15× speedups on GPUs
- **Public NR catalogs:** nearly 6,000 waveforms to date — SXS, RIT, Maya, BAM (Boyle+ 2019; Lousto+ 2022; Jani+ 2016; González+ 2022; Dietrich+ 2018 …)

*A full tour of today's codes → Lecture 2!*

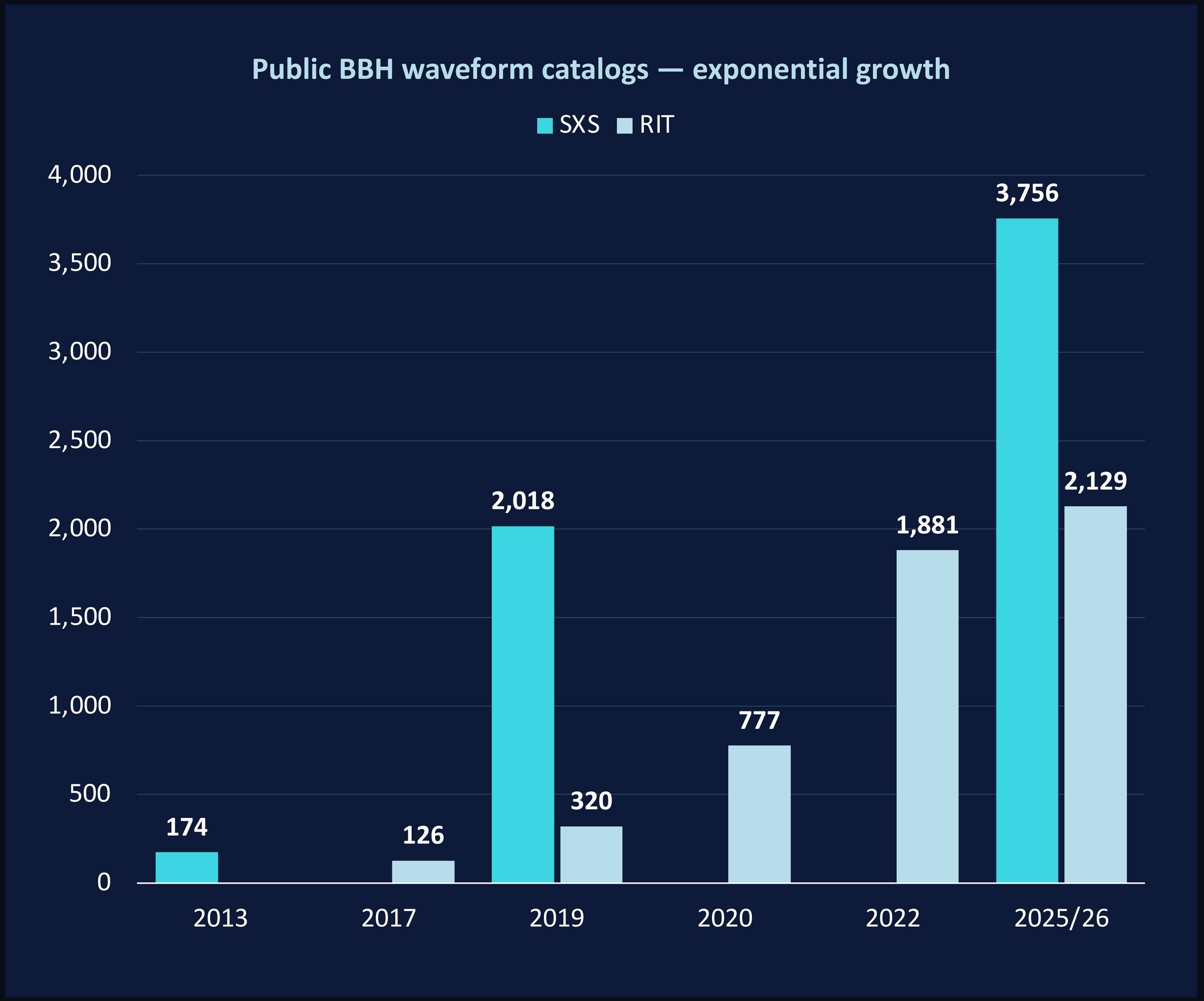


Frontier: spins to χ = 0.998 · mass ratios to q = 1:128 · eccentric orbits to e ≲ 1
Mroué+ 2013 · Boyle+ 2019 · Healy & Lousto 2022 · Scheel+ 2025 · Ficarra+ 2026

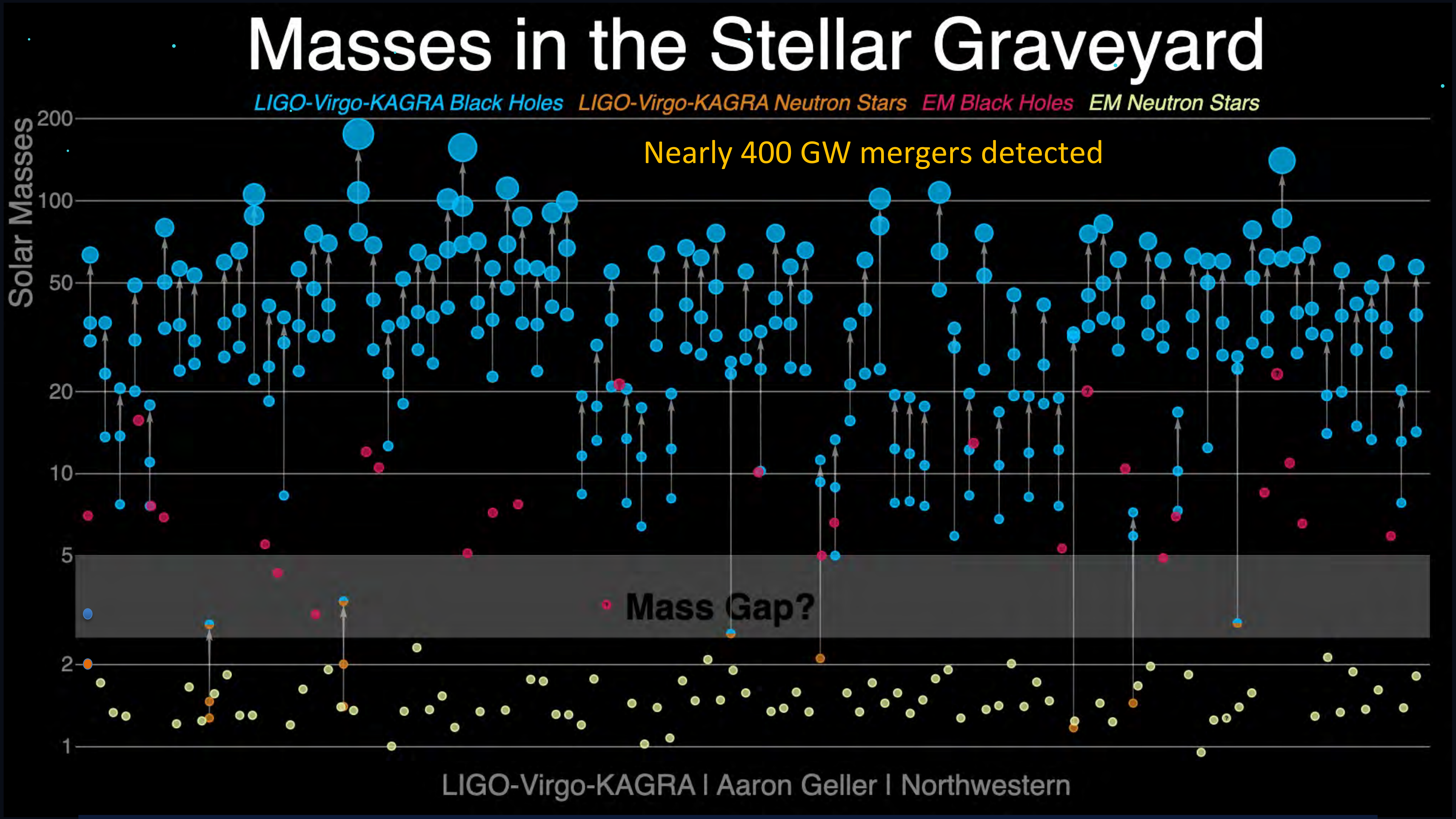


"The first things LIGO will see will likely be BBHs, and will see many more BBHs than BNSs" – Kip Thorne

# From NR Catalogs to Waveform Models

- **Where we stand:** dense to q = 8, |χ| ≤ 0.8, yet few waveforms span ET's band below 300 $M_\odot$; RIT-5 adds 1,046 eccentric waveforms with multi-resolution error budgets. (Scheel+ 2025; Ficarra+ 2026)

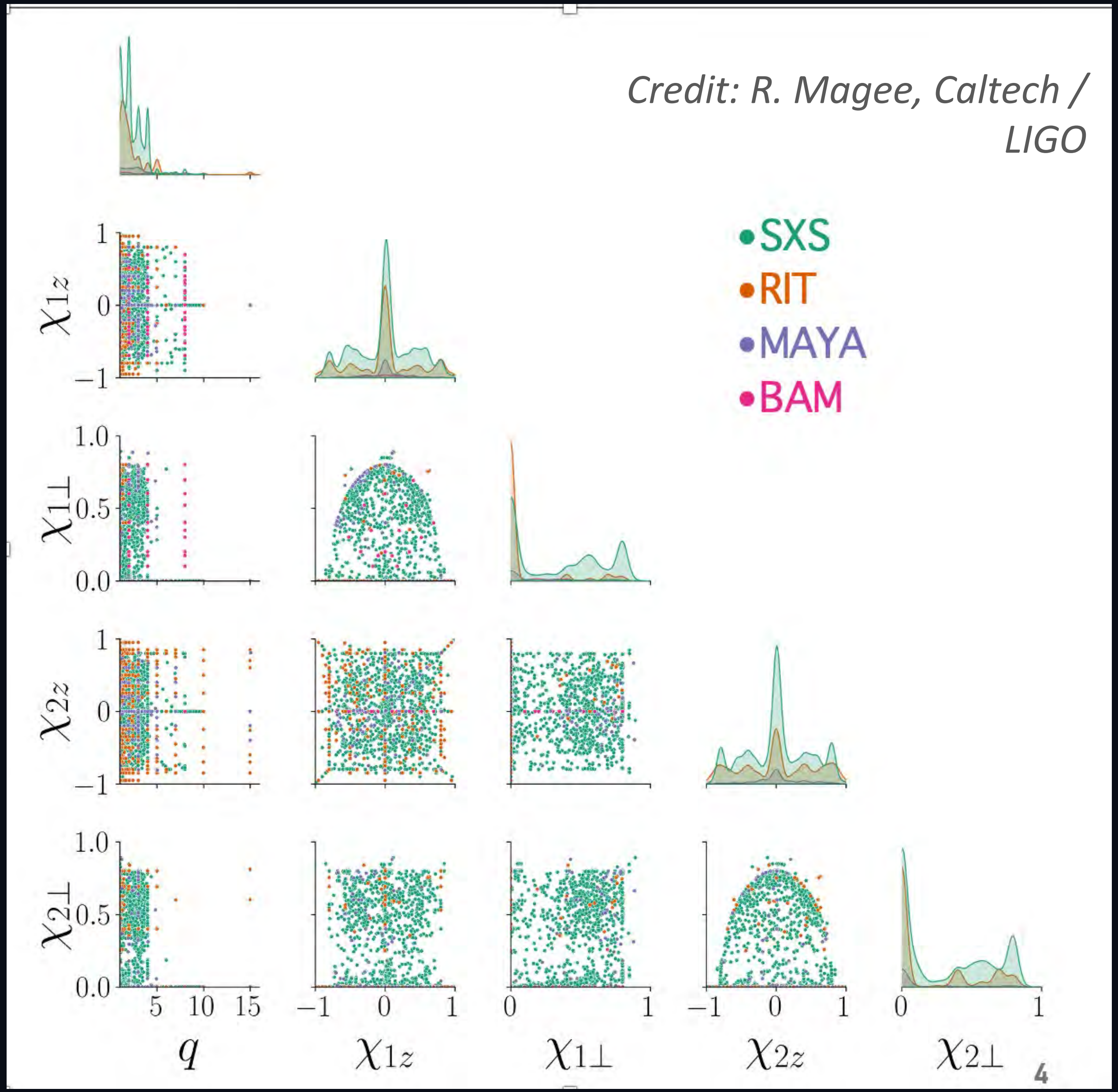


- **Coverage:** best for quasi-circular binaries with moderate mass ratios & spins; high-q, high-spin and eccentric corners stay sparse — RIT alone adds ~1,000 eccentric waveforms.

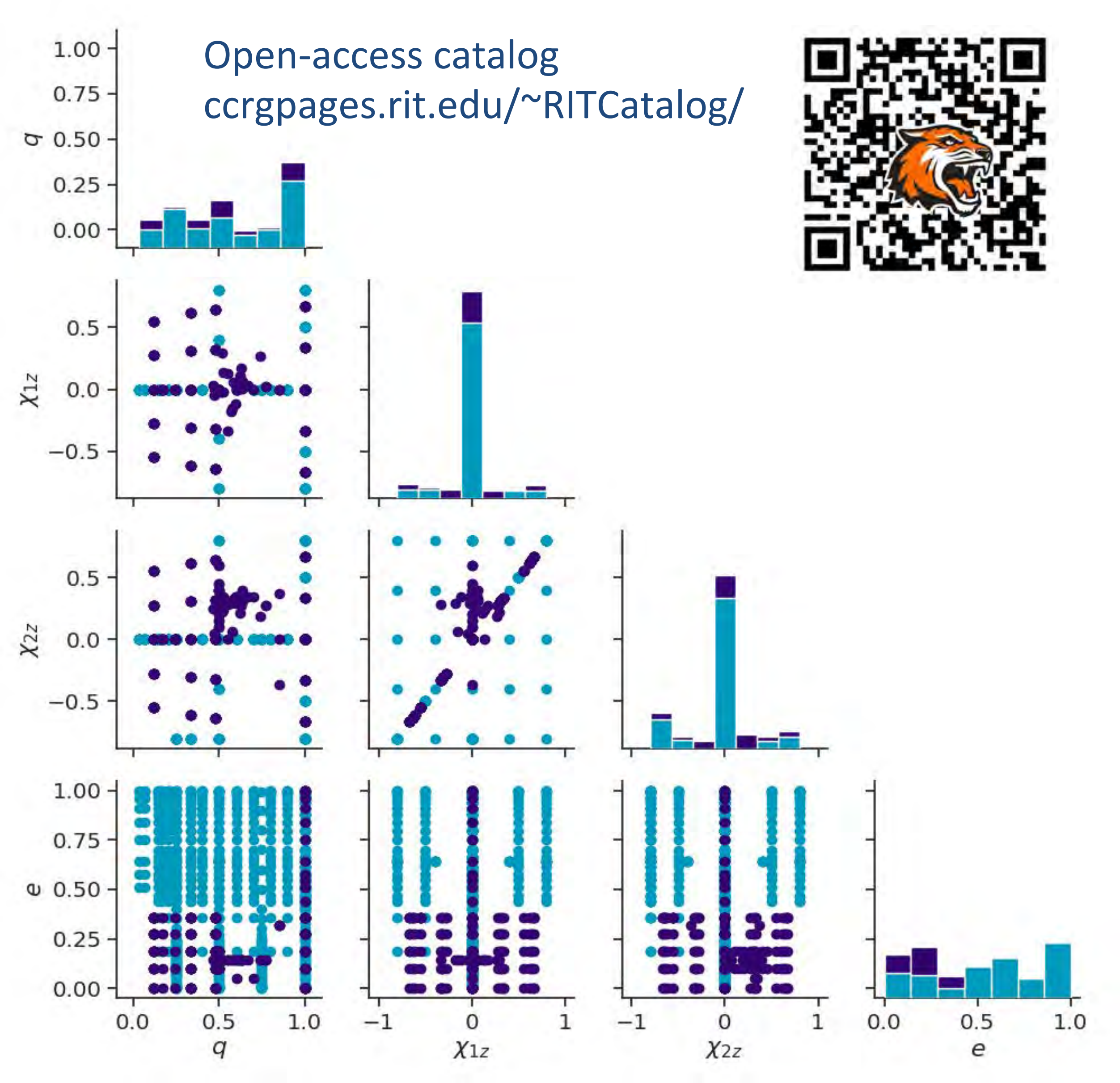


**The chain:** NR → catalogs → models → template banks → detections & source properties.

# Waveform Finite-Difference Error Studies

**Visual stability ≠ accuracy**: waveforms must converge. Ψ(t) is problematic to extrapolate at each *t* with individual convergence order *n* — noisy (e.g. Ficarra, Healy & Lousto 2026)

- Use three successive resolutions (L, M, H) to obtain the infinite-resolution waveform:

$$\Psi_\infty = (f^n \Psi_H - \Psi_M)/(f^n - 1)$$

$$f^n = \mathcal{M}(\Psi_L, \Psi_M)/\mathcal{M}(\Psi_H, \Psi_M)$$

- Perform mismatches of (L, M, H) against the infinite-resolution waveform:

$$\mathcal{M}(\Psi_\infty, \Psi_H) = \mathcal{M}(\Psi_H, \Psi_M)^2 / \left|\mathcal{M}(\Psi_L, \Psi_M) - \mathcal{M}(\Psi_H, \Psi_M)\right|,$$

$$\mathcal{M}(\Psi_\infty, \Psi_M) = \mathcal{M}(\Psi_H, \Psi_M)\,\mathcal{M}(\Psi_L, \Psi_M) / \left|\mathcal{M}(\Psi_L, \Psi_M) - \mathcal{M}(\Psi_H, \Psi_M)\right|,$$

$$\mathcal{M}(\Psi_\infty, \Psi_L) = \mathcal{M}(\Psi_L, \Psi_M)^2 / \left|\mathcal{M}(\Psi_L, \Psi_M) - \mathcal{M}(\Psi_H, \Psi_M)\right|.$$

**If it doesn't converge, it isn't a result.**

Convergence: the numerical error shrinks with resolution at a fixed order *p*:

$$u_\Delta = u_{\text{exact}} + e_p\,\Delta^p + \mathcal{O}(\Delta^{p+1})$$

$$p \simeq \log_2 \frac{\| u_{4h} - u_{2h} \|}{\| u_{2h} - u_h \|}$$

- Run the **same physical setup** at several resolutions Δ (h, h/2, h/4, …).
- If the equations are solved correctly, differences between successive resolutions **shrink at the rate** set by the scheme's order *p*.
- Measured *p* ≈ design order ⇒ the error is **truncation, not a bug** — extrapolate to Δ → 0 and quote an error bar.
- No convergence ⇒ **under-resolved or wrong** — fix it before quoting physics.

**Note**
We typically use f = 1.2, since $1.2^4 \approx 2$ balances required computational resources against an error bound.

# The Waveform Modeler's Toolbox

- **Approximate methods:** post-Newtonian / post-Minkowskian expansions for the long inspiral; self-force for $m_1 \gg m_2$; black-hole perturbation theory for the remnant's ringdown.
- **Numerical relativity:** the full nonlinear field equations, no approximations — the only method for comparable-mass late inspiral and merger; the loudest events are compared directly against NR, as GW150914 was.
- **No single method covers the whole signal** — accurate templates stitch these regimes together, an approach Lazarus pioneered in 2001.
- **Why models:** matched-filter searches & Bayesian inference evaluate $10^6$–$10^8$ waveforms per event — far too many to simulate directly.
- **Three families, all trained on NR:** effective-one-body (EOB), phenomenological (IMRPhenom), and NR surrogates — catalog quality sets the accuracy floor. (Buonanno & Damour 1999; Pratten+ 2021; Varma+ 2019)

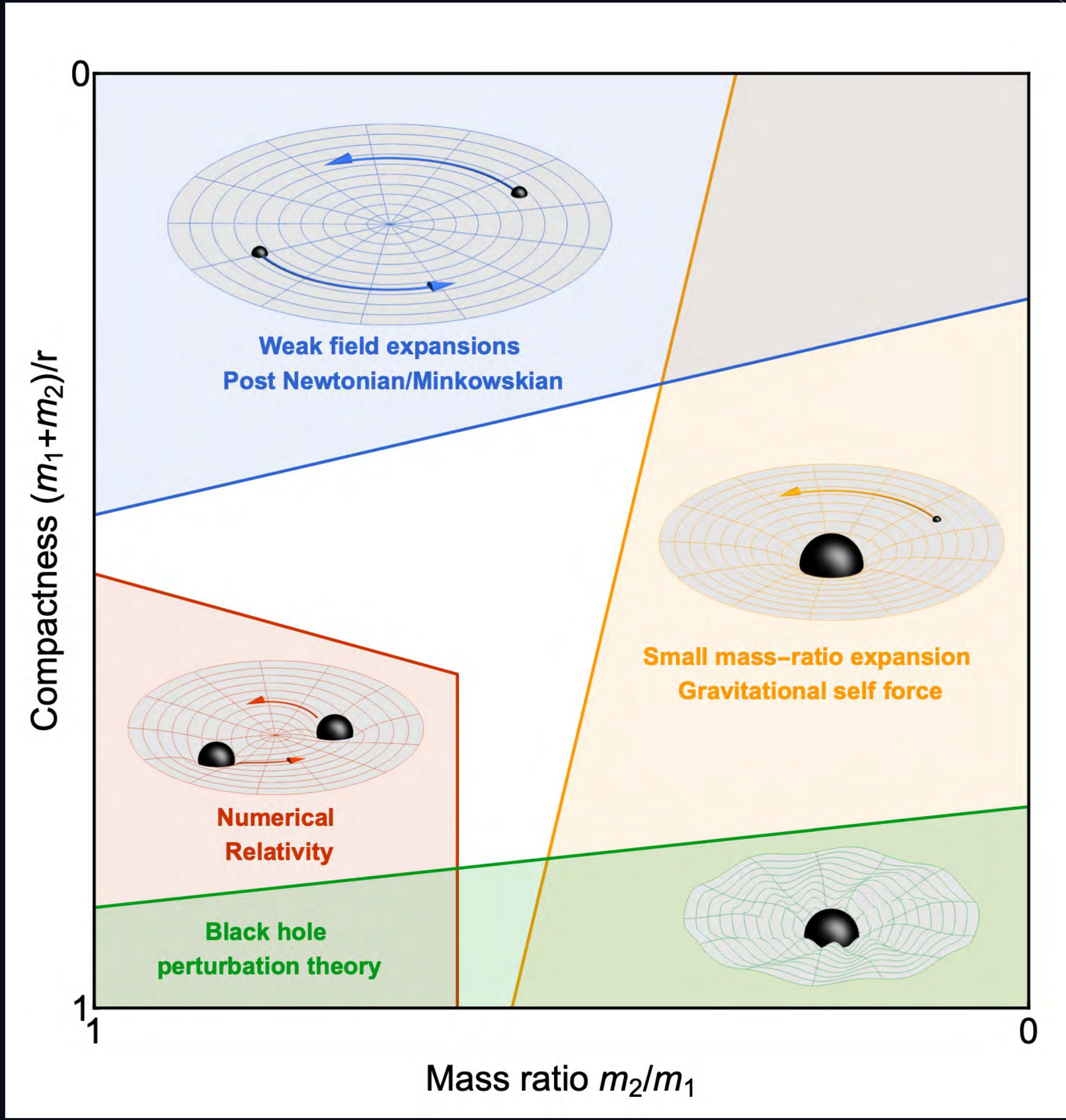


*LISA Consortium Waveform Working Group, "Waveform Modelling for LISA" (2023), Secs. 4.2–4.6*

*Credit: LISA Consortium Waveform Working Group*

# Ready for Next-Generation GW Science?

Accuracy, length, and coverage must all improve **~10×** for 3G (SNR ~ 1000) — far more for LISA.– Pürrer & Haster 2020

A culture shift is underway: RIT and SXS now publish convergence-based error budgets alongside their waveforms — RIT-5's six-resolution study, SXS's multi-resolution releases. (Ficarra+ 2026; Scheel+ 2025)

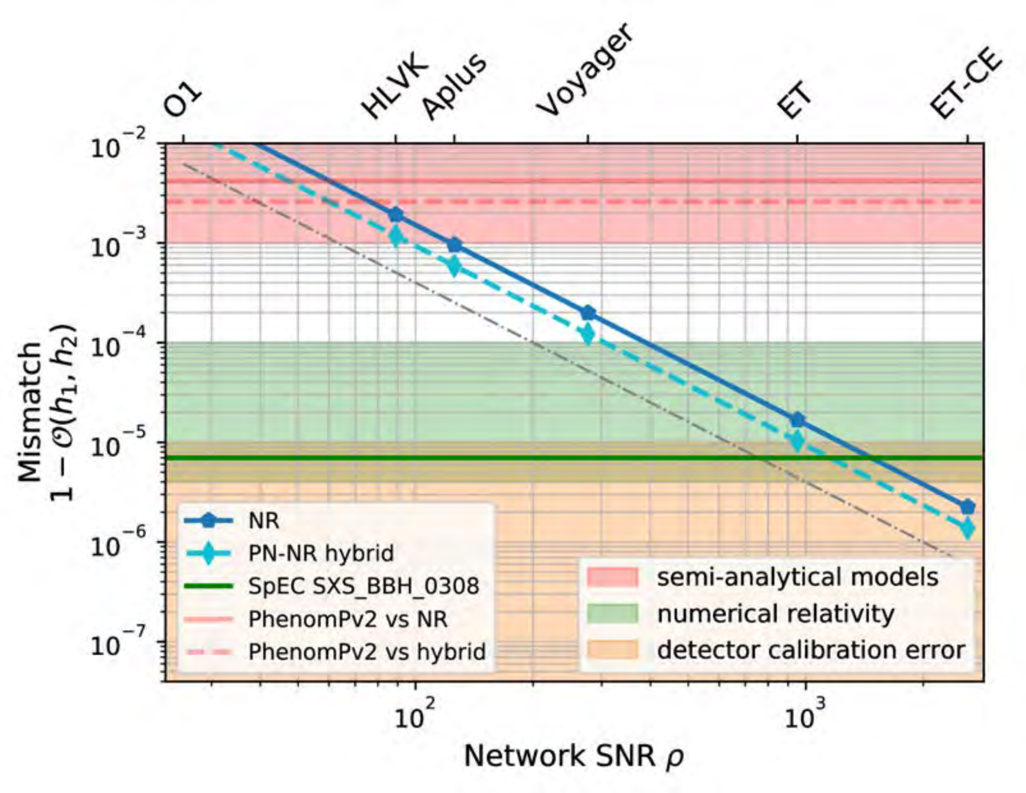


Pürrer and Haster, 2020

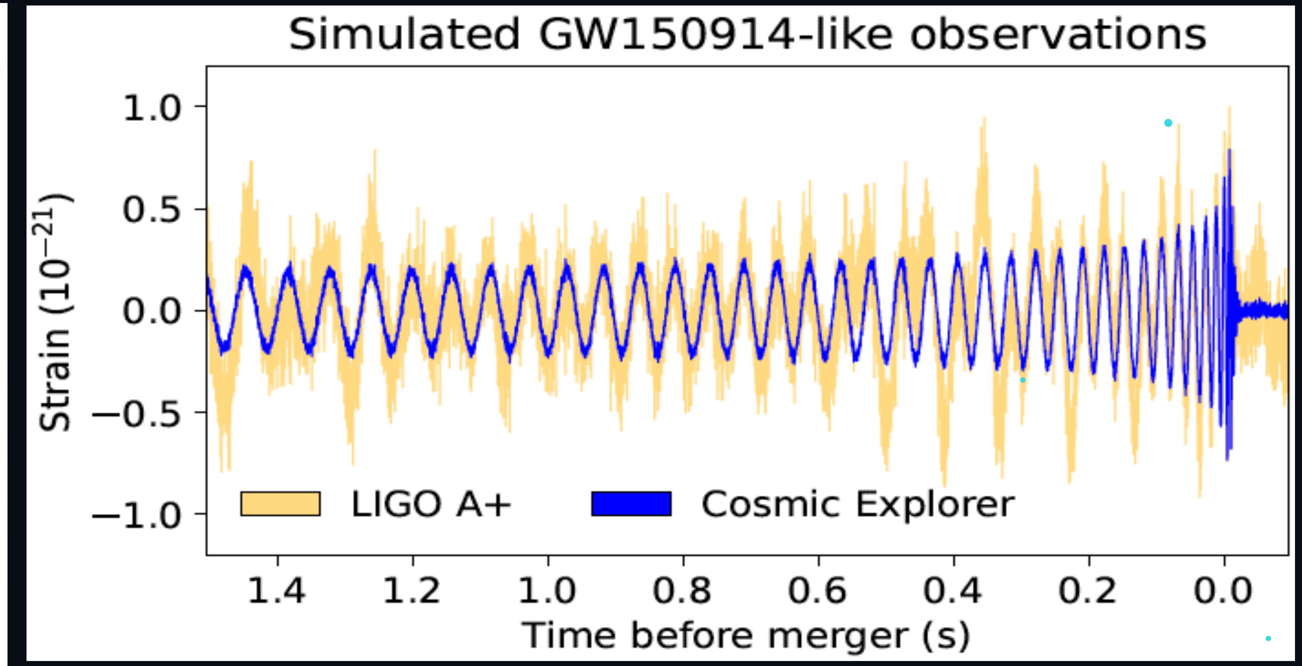


Foucart+ Snowmass 2022

- Sources stay in band longer — multiband GW astronomy with LISA + 3G – Colpi+ 2024 (LISA Red Book)
- EM precursors & postcursors: the multimessenger opportunity!

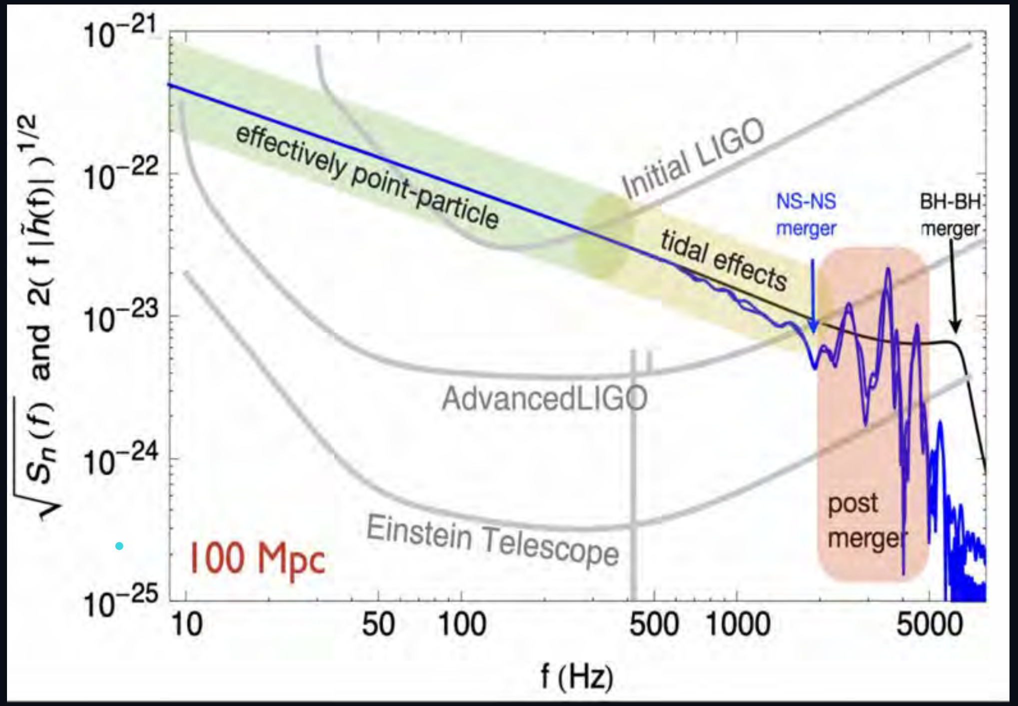


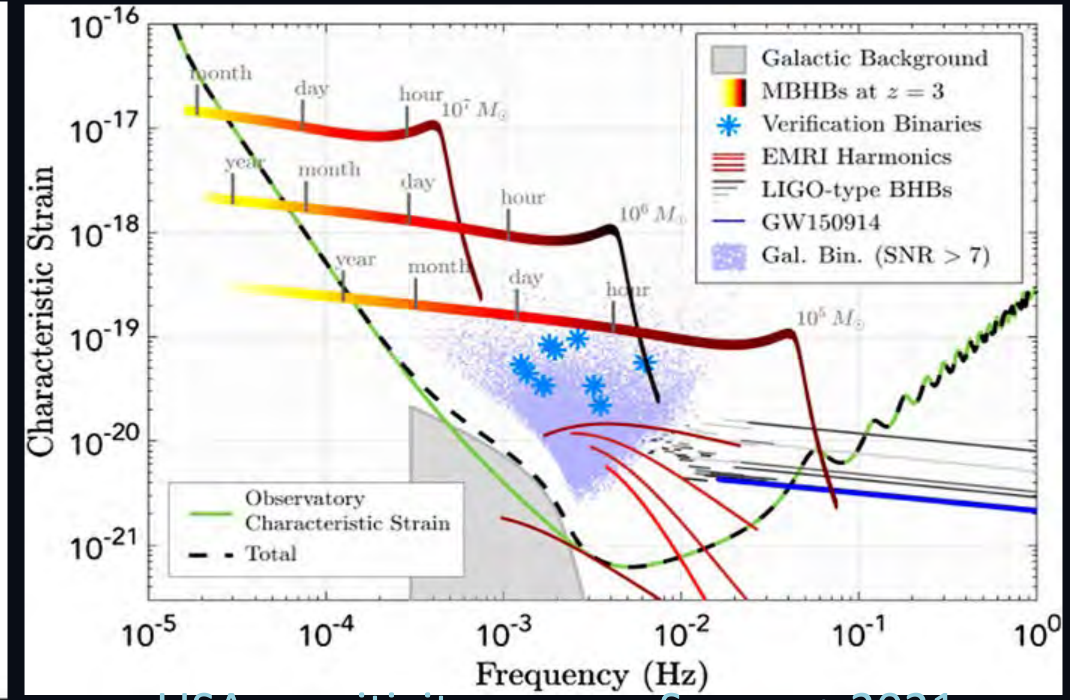


LISA sensitivity curve – Sesana+ 2021

Together these can nail down the sources' astrophysical origin, history, and environment.

# The Frontier of High Mass Ratios ($q \gg 1$)

- Simulating unequal masses ($q > 1$) is still computationally demanding, requiring very high resolution to resolve the smaller black hole.
- Most simulations have mass ratios $q \lesssim 8$. A handful have reached up to $q = 128$, and a single head-on merger has reached $q = 1024$ (Lousto & Healy 2022).
- IMRI Sources: New methods are actively being developed to push NR simulations into the intermediate mass-ratio regime of $q = 100$ to $10{,}000$ (Dhesi+2021, Wittek+2023).
- EMRI Sources: For the extreme mass-ratio regime ($q > 1000$), Black Hole Perturbation Theory is the essential tool, though developing a stable second-order theory remains a major challenge, actively pursued at the Capra meetings.
- This is an active field of research in NR as it challenges both pertubative and NR methods

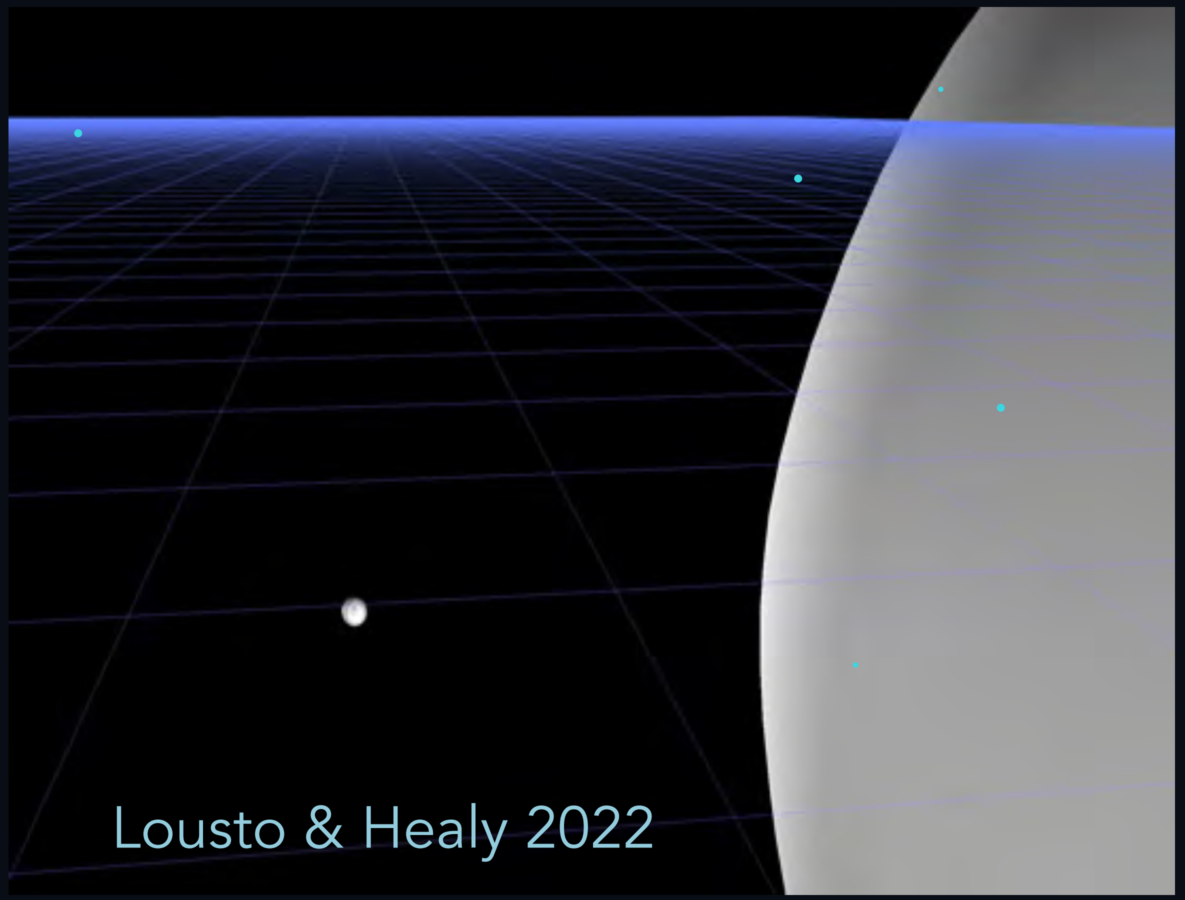

Lousto & Healy 2022

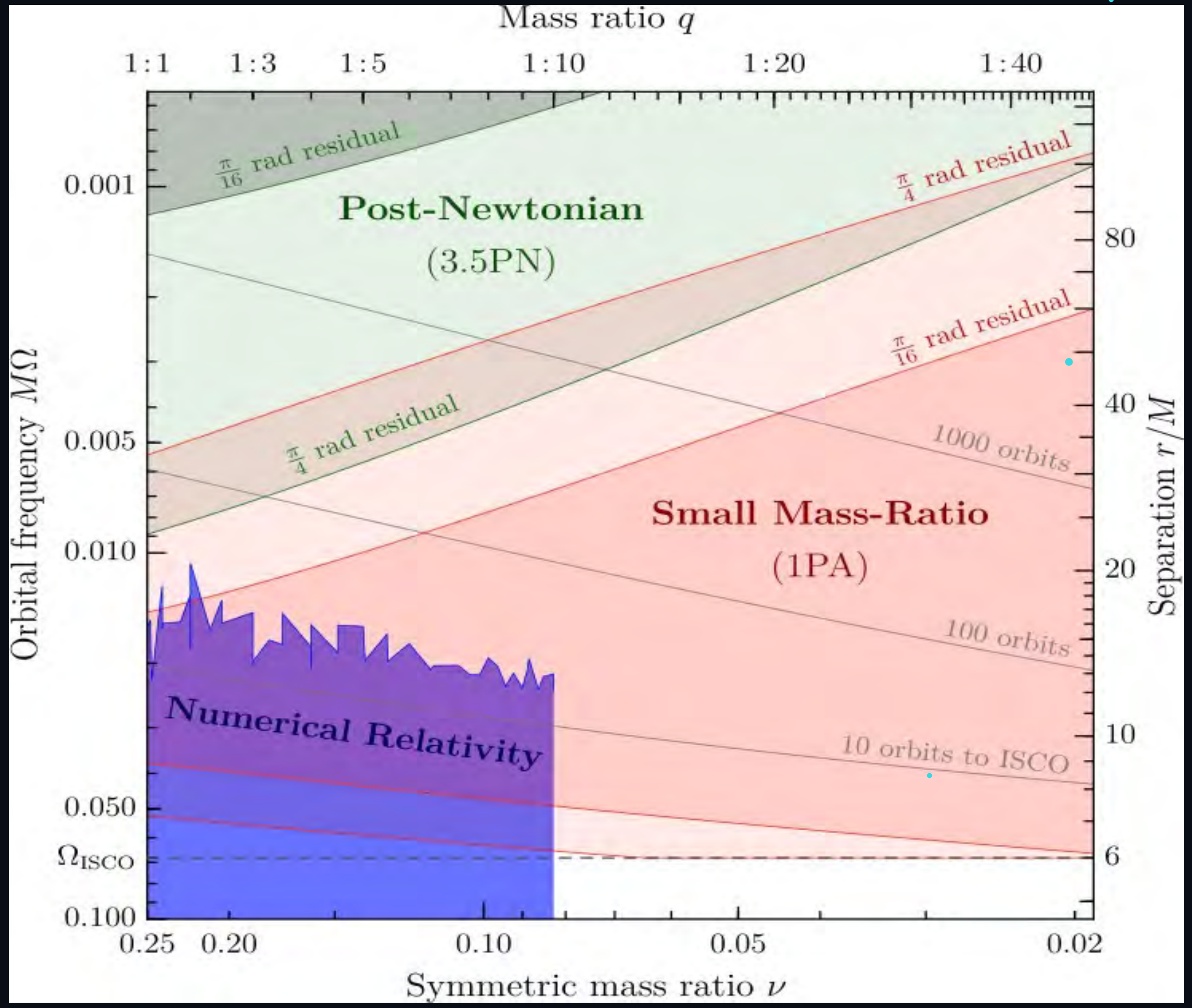


Van de Meent and Pfeiffer (2020)

# The Frontier of High Spins ($\chi \to 1$)

- Most NR simulations are limited to moderate spins ($\chi < 0.9$)
    - ➢ High spins require extremely high resolution near the BH horizons.
    - ➢ Constructing stable and accurate initial data is non-trivial.
    - ➢ Require finely tuned gauge conditions to avoid instabilities.
- Despite challenges, there are successful simulations of highly spinning systems
    - ➢ including spin magnitudes up to 0.998 (Lovelace+2008, Healy+2017, Zlochower+2017, Boyle+2019, …);
- These simulations are crucial for accurately modeling complex dynamics like orbital precession.

Synergy with rapidly improving analytical and EOB models

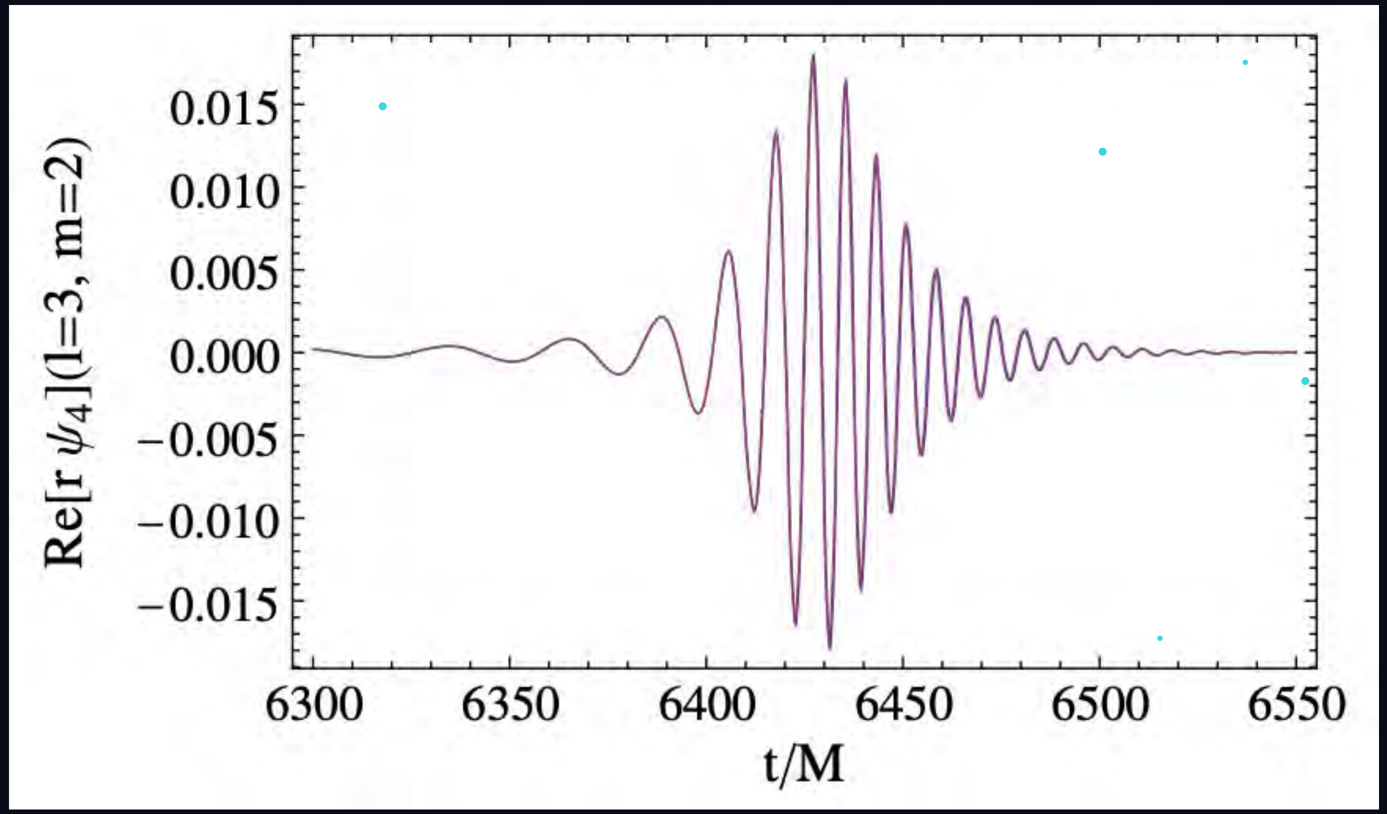


99% overlap between SXS (red) and RIT waveforms (blue) (Zlochower+2017, Lovelace+)

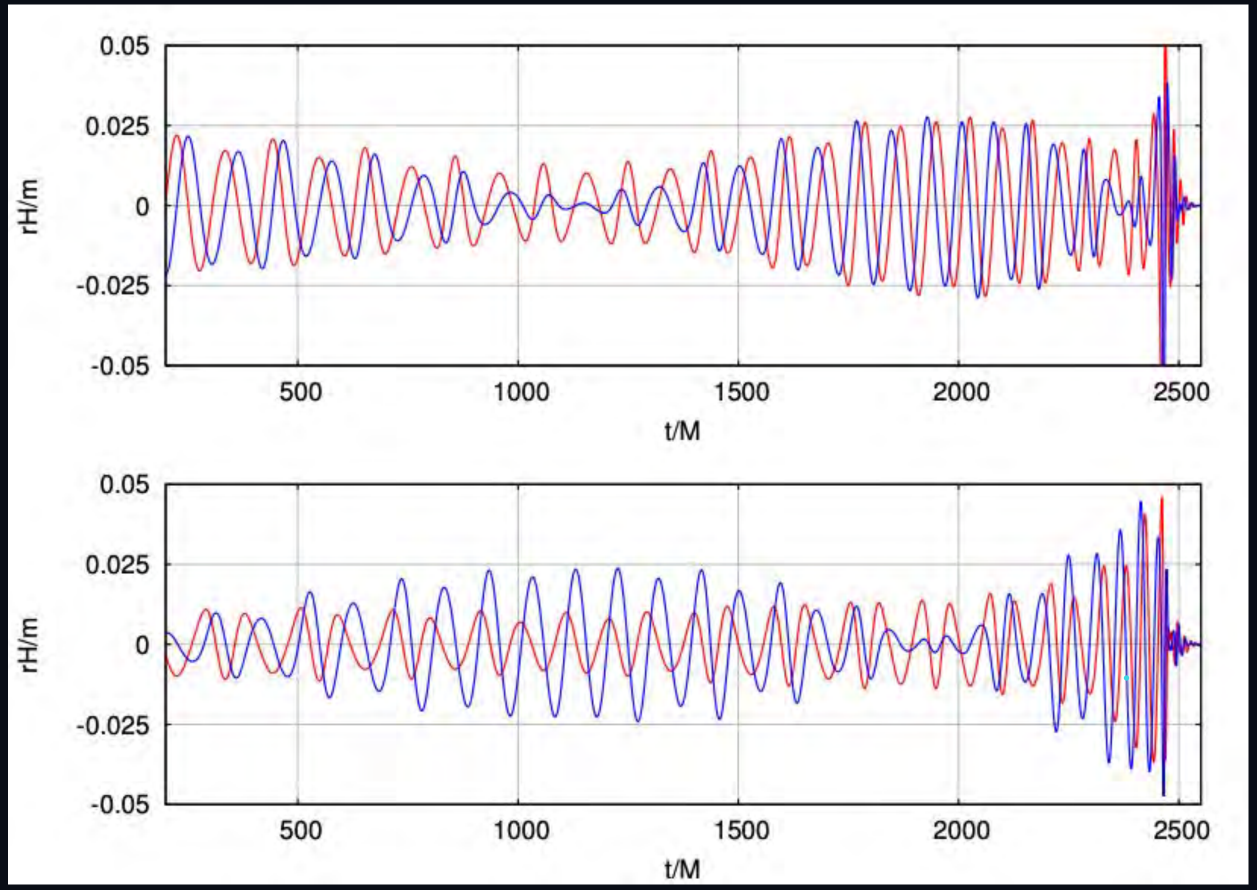


Precessing, q=15, Lousto & Healy, 2015

# The Frontier of Eccentric Orbits (e > 0)

- Most NR simulations focus on quasi-circular orbits, the expected end-state for isolated binaries.
    - ➢ Consistent initial data is non-trivial. Different definition of eccentricity!
    - ➢ Long evolution times required to resolve multiple periastron passages and eccentricity decay.
    - ➢ Complex modulations in waveform amplitude and frequency.
- Eccentricity is a clear signature of dynamical capture in dense environments like globular clusters.
- Catalogs of eccentric waveforms (e.g., from the RIT and SXS collaborations) (e.g., Hinder+2018, Healy+2019, Ramos-Buades+2020, Gayathri+2020, Healy+2022).

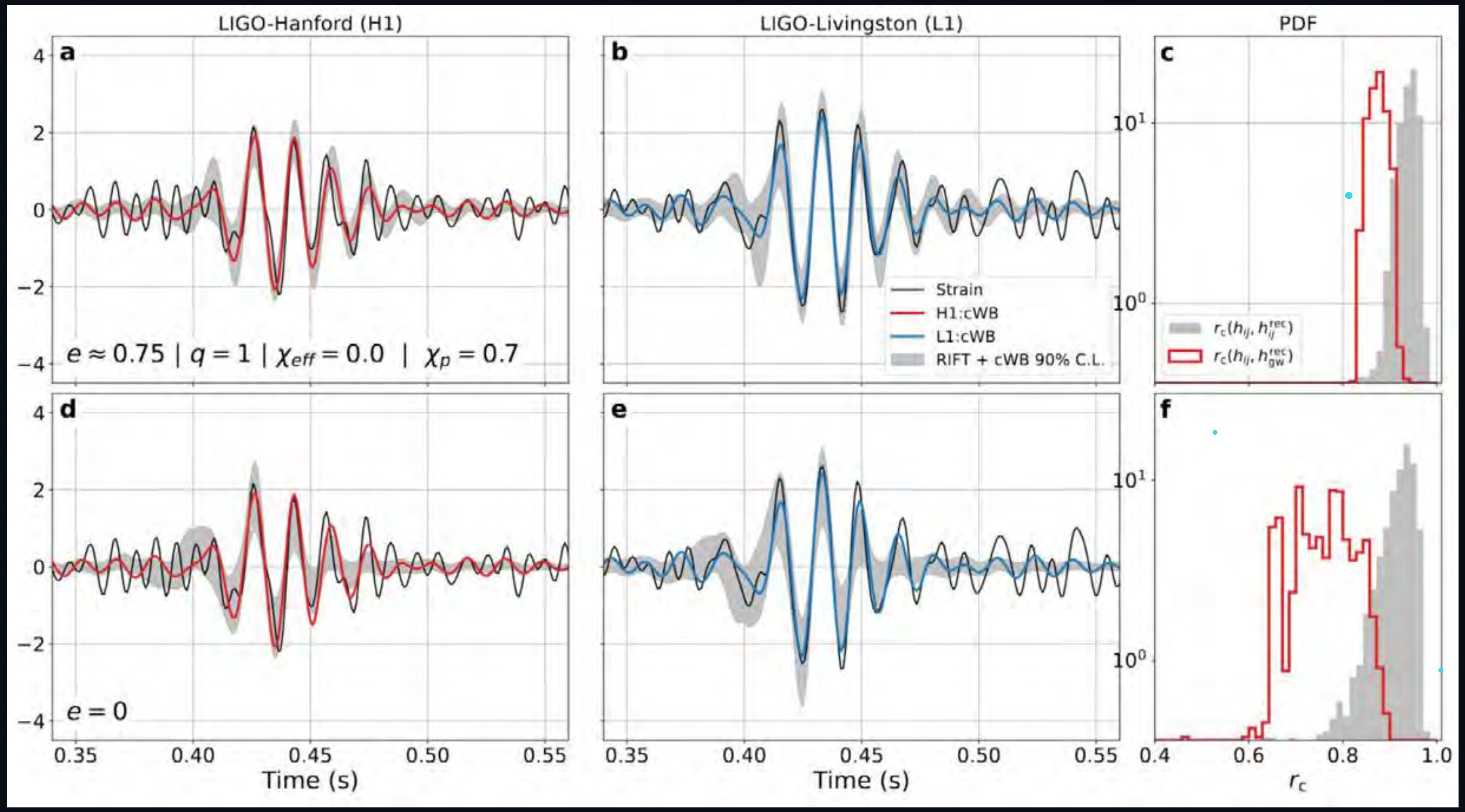


Gayathri+2020: GW190521 is best explained by a high-eccentricity, precessing model with e ~ 0.7, pointing to 2G cluster merger object

GW200208_22: e ~ 0.2
GW190620: 0 < e < 0.25
GW231123?

NR simulations needed for calibrating EOB and phenomenological waveform models

FRONTIER · BEYOND GR

# Beyond GR Effects

- Use NR to test alternative theories of gravity and find deviations from GR in the strong-field regime.
    - Establishing a stable initial value problem (well-posedness) for modified theories.
    - Coding new, often more complex, field equations.
    - Reliably extracting GWs in non-GR theories, despite recent progress (Saló+2023).
- Significant advances in simulating mergers in various beyond-GR theories (Cayuso+2023, Richards+2023, Aresté Saló+2022, Maggio+2022, Corman+2022, and many others).
- These simulations aim to predict and constrain deviations across the inspiral, merger, and ringdown phases, providing the essential template banks needed for dedicated observational searches for new physics.

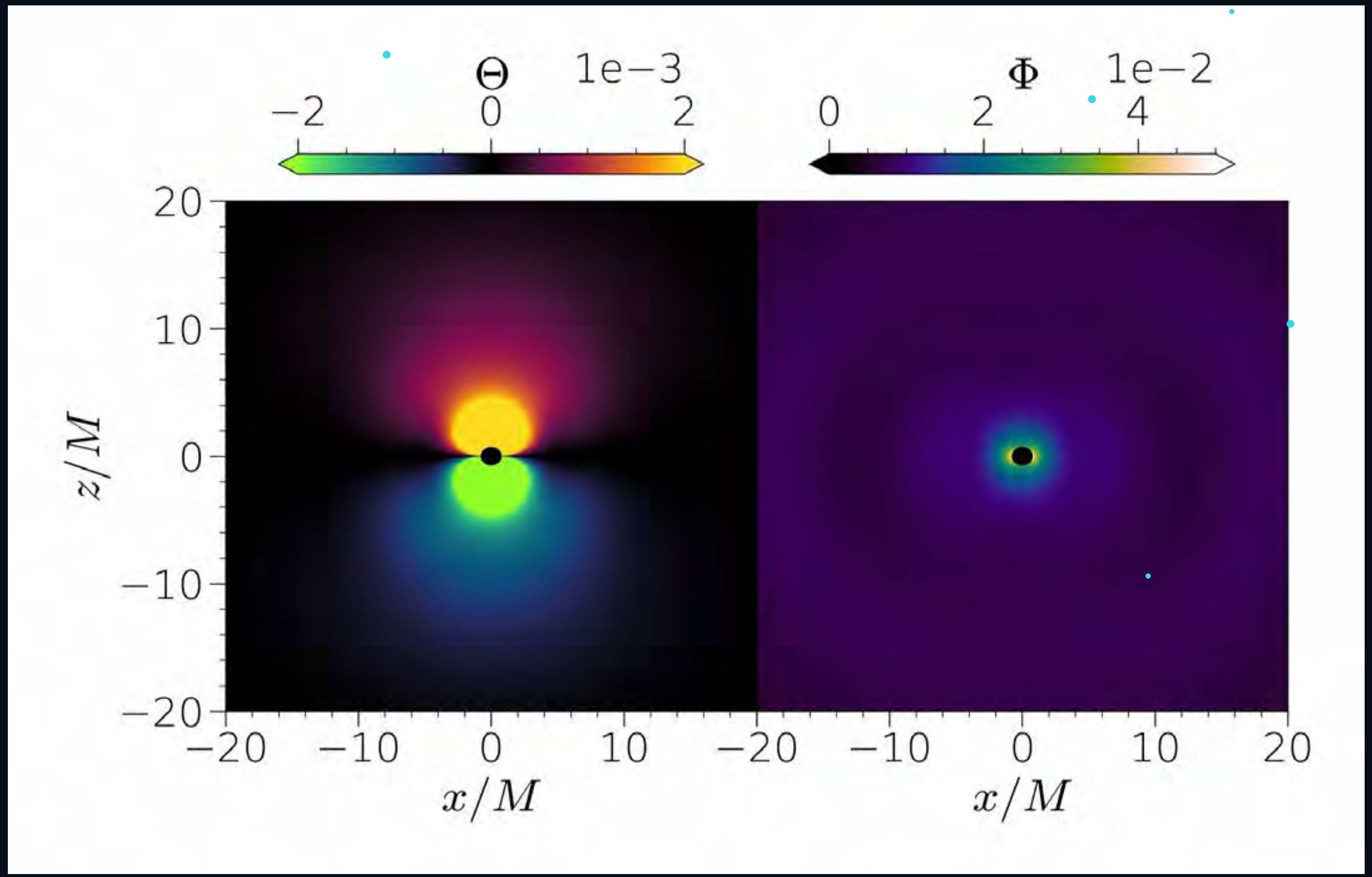


Ferguson, Richards, Dima, Witek 2025, and in progress

Evolution of 2 scalar hairs (called axion and dilaton) in the x-z plane

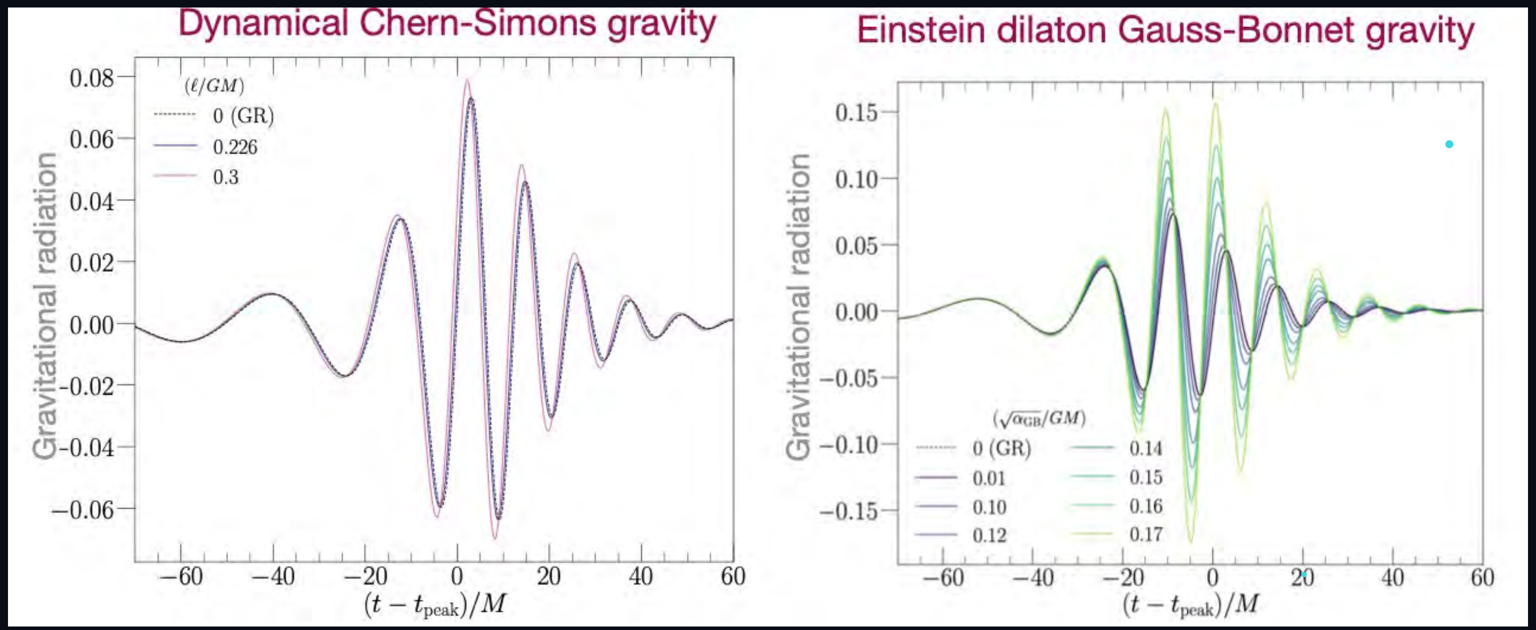


[Okounkova+ '17-'19]

Due to complexity, numerical relativity is the primary tool for exploring beyond GR effects

# Binary Neutron-Star Merger

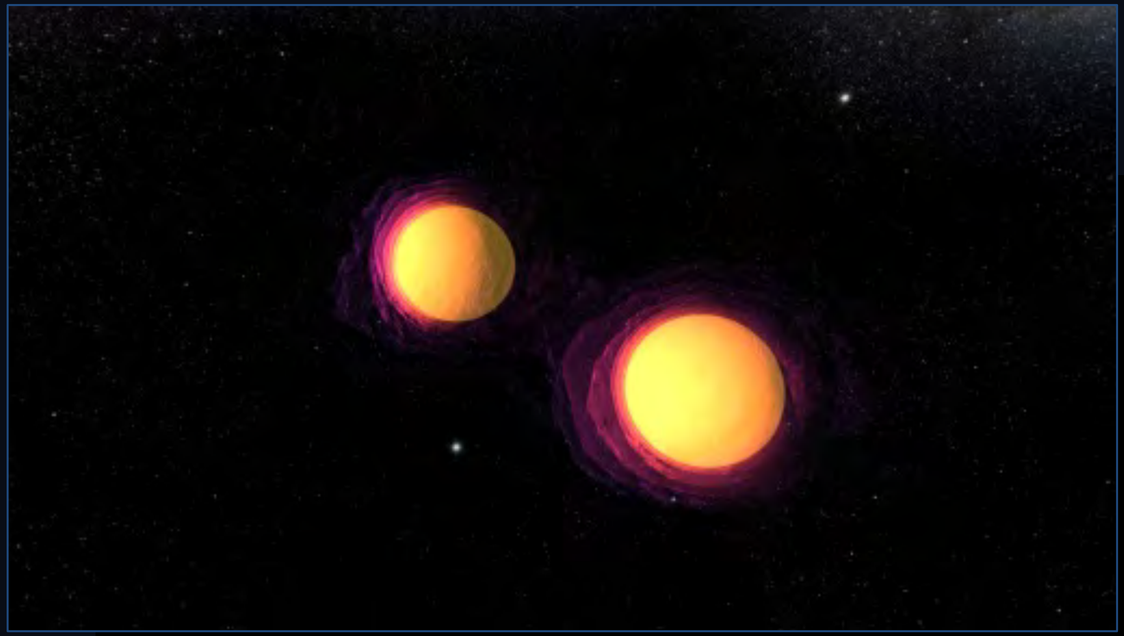

*Late inspiral*

*Merger*

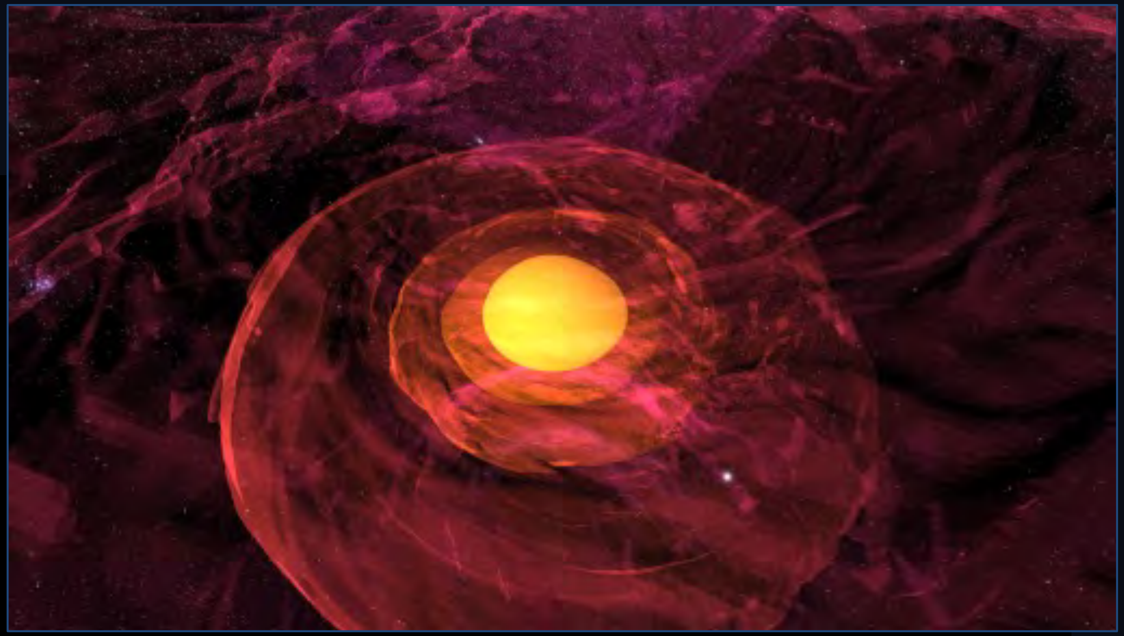

*Post-merger remnant*

The discovery of GW170817 was revolutionary, but it left us with fundamental unanswered questions:

- What is the central engine of a sGRB ?
- What is the origin of the distinct "blue" kilonova component ?
- How exactly are relativistic jets launched from the post-merger remnant?

Unlike in binary black hole mergers, BNS waveforms depend sensitively on complex matter physics:

- The nuclear Equation of State (EoS)
- Magnetic Fields
- Neutrino Interactions

# The Post-GW170817 Era

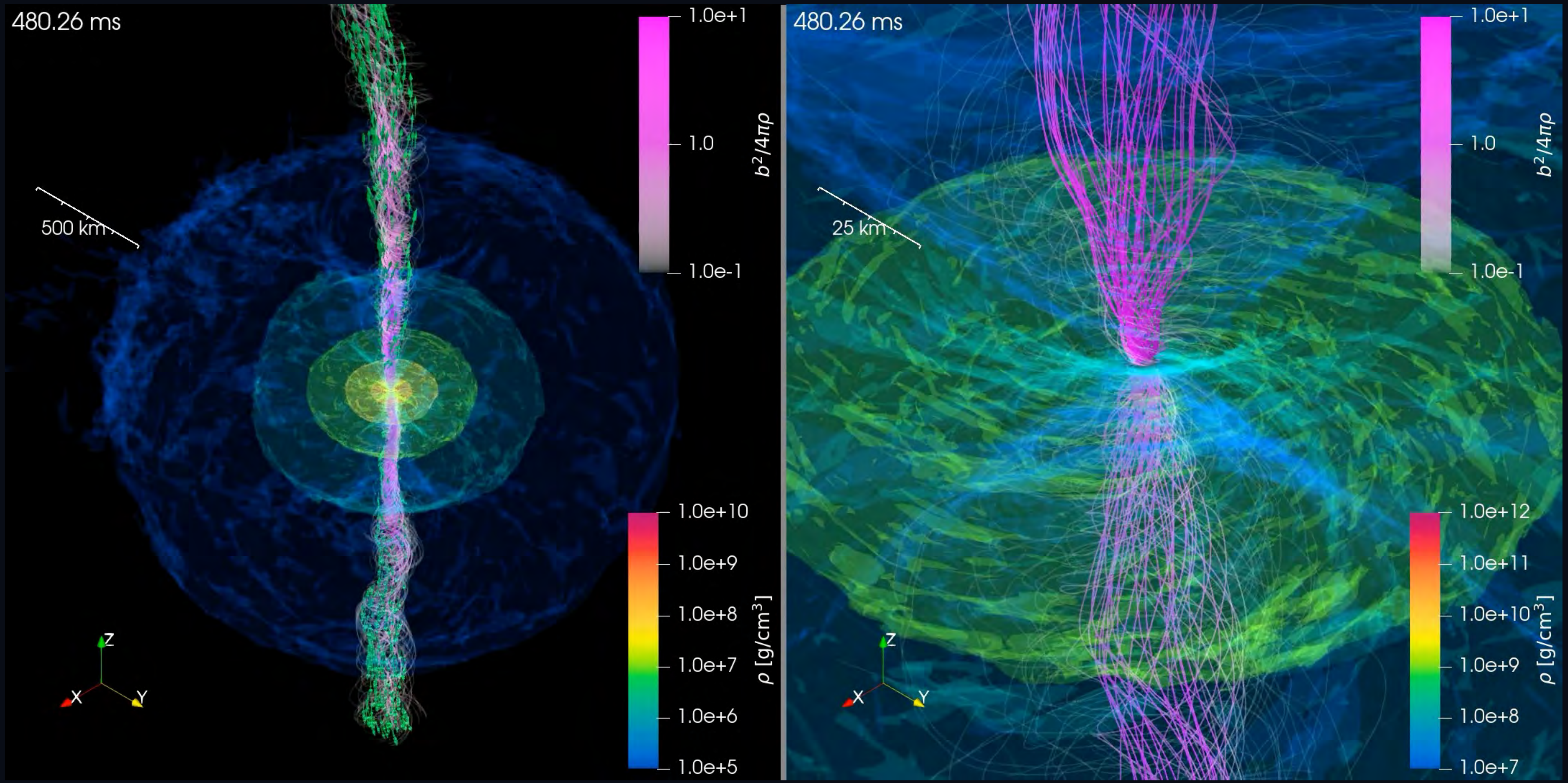


Merger, mass ejection, and jet from NS-NS 1.25-1.65 $M_\odot$ NS-NS with SFHo EOS (Soft EOS): Hayashi + PRL (2025)

We need long-term (~seconds) numerical relativity + GRMHD simulations with comprehensive physics to build self-consistent models of mass ejection and the resulting electromagnetic (EM) signatures

Due to complexity, numerical relativity + GMHD are the primary tool for exploring BNS mergers and post-mergers, but they do require input from microphysics, neutrino transport, etc

# Magnetized Accretion & Jets

You will learn about this subject in my talk tomorrow, but know that this problem share some of the same complexities of the BNS problem with some more emphasis on GRMHD and radiation transport

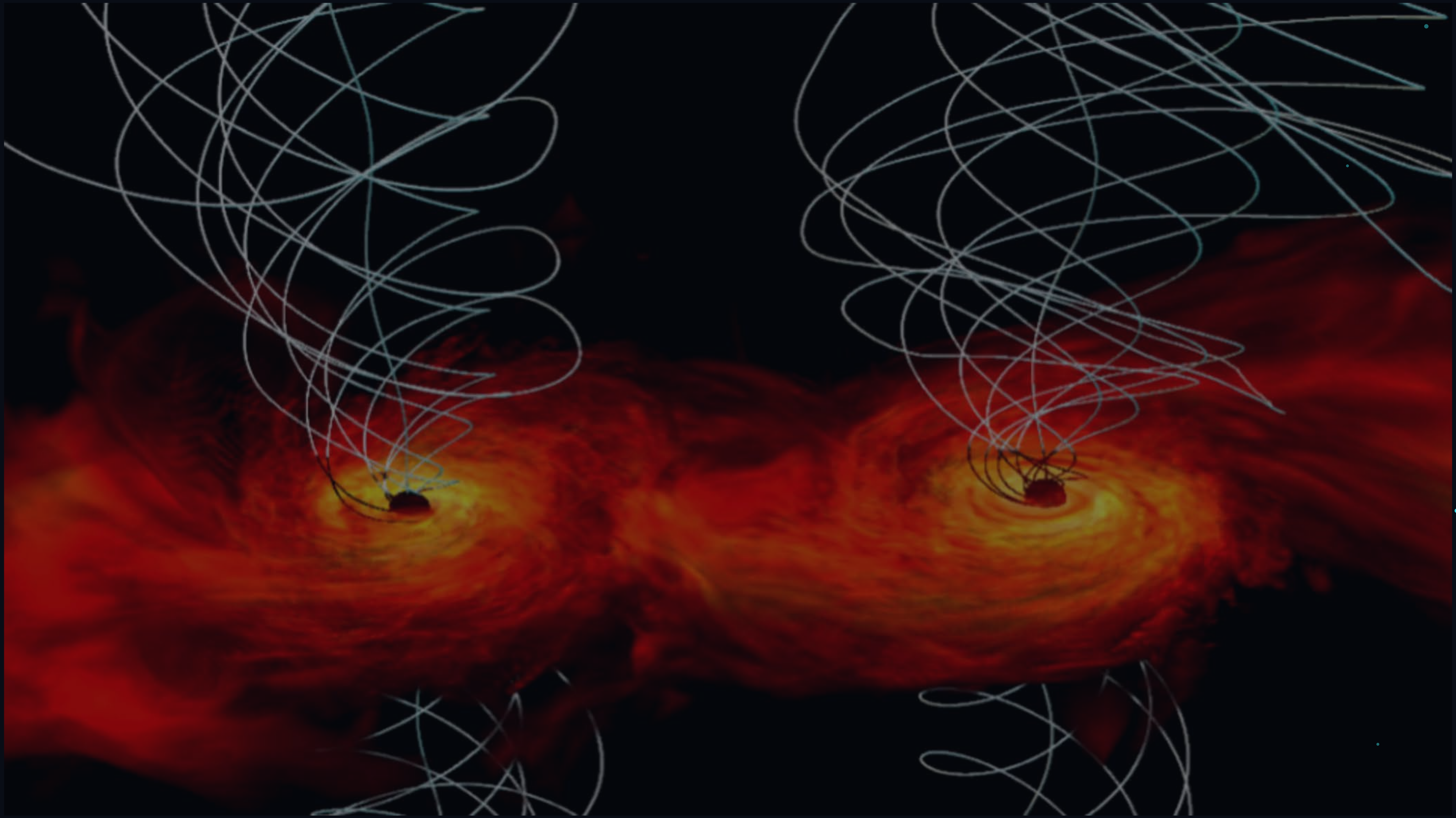

Gas density (orange) and magnetic-field lines (gray) in a magnetized black-hole binary — helical fields wind up above each mini-disk.

# Numerical Relativity and Gravitational-Wave Astronomy

- **NR waveforms**: full inspiral–merger–ringdown signals — the only approximation-free solution for comparable-mass mergers — calibrate the EOB and phenomenological models that fill the LIGO–Virgo–KAGRA template banks.
- **GW150914**: the first detection was matched against NR — masses, spins, and the final black hole read straight off the merger: 36 + 29 merging to 62 solar masses, final spin a/M = 0.69, with 3 solar masses radiated.
- **NR catalogs** (SXS, RIT, GT): thousands of simulations train surrogate models and bound waveform systematics for parameter estimation.
- **GW170817**: NR-informed matter waveforms and kilonova predictions turned a neutron-star merger into a multimessenger event.

$$G_{ab} \equiv R_{ab} - \frac{1}{2}\, g_{ab} R = 8\pi\, T_{ab}$$

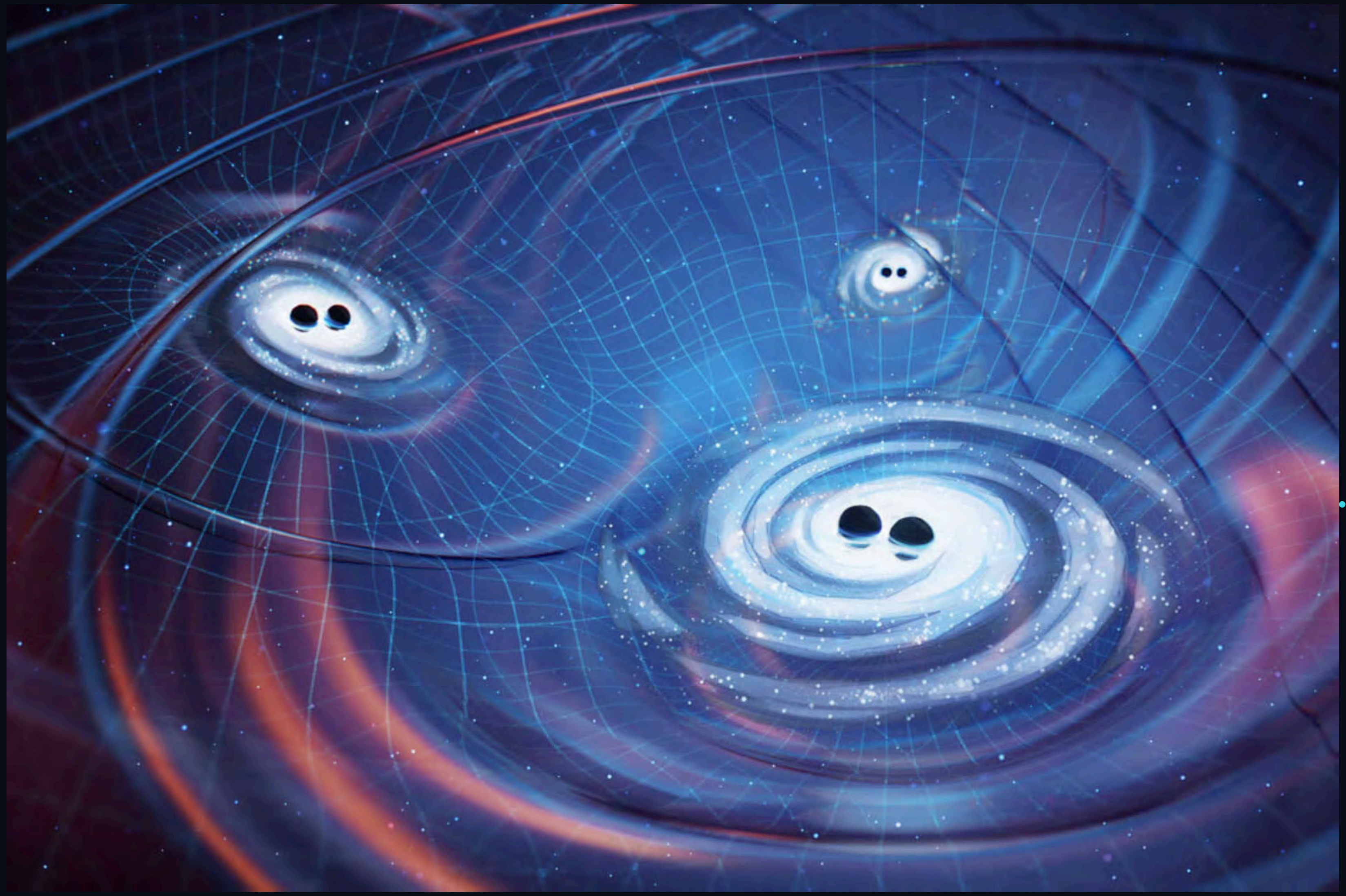

LECTURE 1 → LECTURE 2

# From Why to How

### LECTURE 1 — THE WHY

- The two-body problem in GR has **no pen-and-paper solution** — mergers must be computed.
- NR delivers **the waveforms behind GW astronomy** — detections, catalogs, calibrated models.

### LECTURE 2 — THE HOW

- We open **the machinery**: from writing Einstein's equations a computer can solve, to trusting the waveform that comes out.

formulations → gauges → black holes → waves → matter → diagnostics

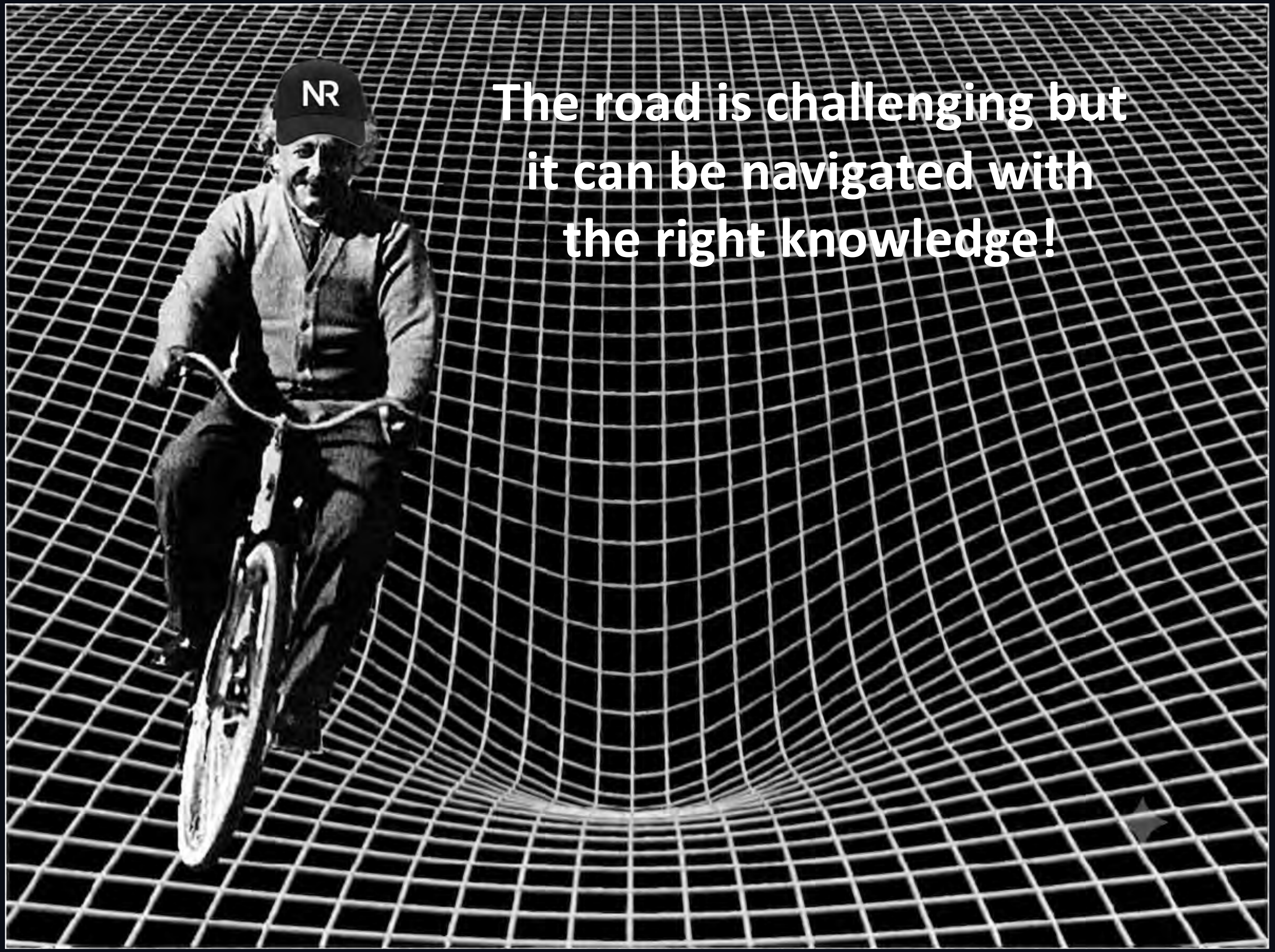


***NR:*** *Baumgarte & Shapiro (2010) · Alcubierre (2008) · Shibata (2015)* ***GRMHD:*** *Rezzolla & Zanotti (2013) · Font, LRR (2008)*

Same equations, new question — not *"what does NR predict?"* but *"how do we make it compute?"*

THE 3+1 SPLIT

# The 3+1 Decomposition in One Slide

Slice spacetime $g_{a\beta}(t, x^i)$ into spacelike slices $\Sigma_t$ of constant t — *Arnowitt, Deser & Misner (1962)*

- $n^a$: Eulerian unit normal; $v^i$: matter 3-velocity they measure:

$$n_a = -\alpha\, \nabla_a t\,, \qquad n_a n^a = -1 \qquad v^i = \frac{1}{\alpha}\left(\frac{u^i}{u^0} + \beta^i\right)$$

$\gamma^{ab}$ projects into $\Sigma_t$: $\gamma_{ab} = g_{ab} + n_a n_b$

- Dynamical fields on each slice: $(\gamma_{ij}, K_{ij})$ — the induced metric and its “velocity”, stored on a 3D grid.

$$K_{ab} = -\gamma_a{}^c\, \nabla_c\, n_b\,, \qquad K_{ij} = -\tfrac{1}{2}\,\mathcal{L}_n\, \gamma_{ij}\,, \qquad K = \gamma^{ij} K_{ij}$$

- Gauge fields: α (lapse) and $\beta^i$ (shift) — four freely specifiable functions we choose wisely; they set how the slicing and spatial coordinates advance.

$$ds^2 = -\alpha^2\, dt^2 + \gamma_{ij}\left(dx^i + \beta^i dt\right)\left(dx^j + \beta^j dt\right)$$

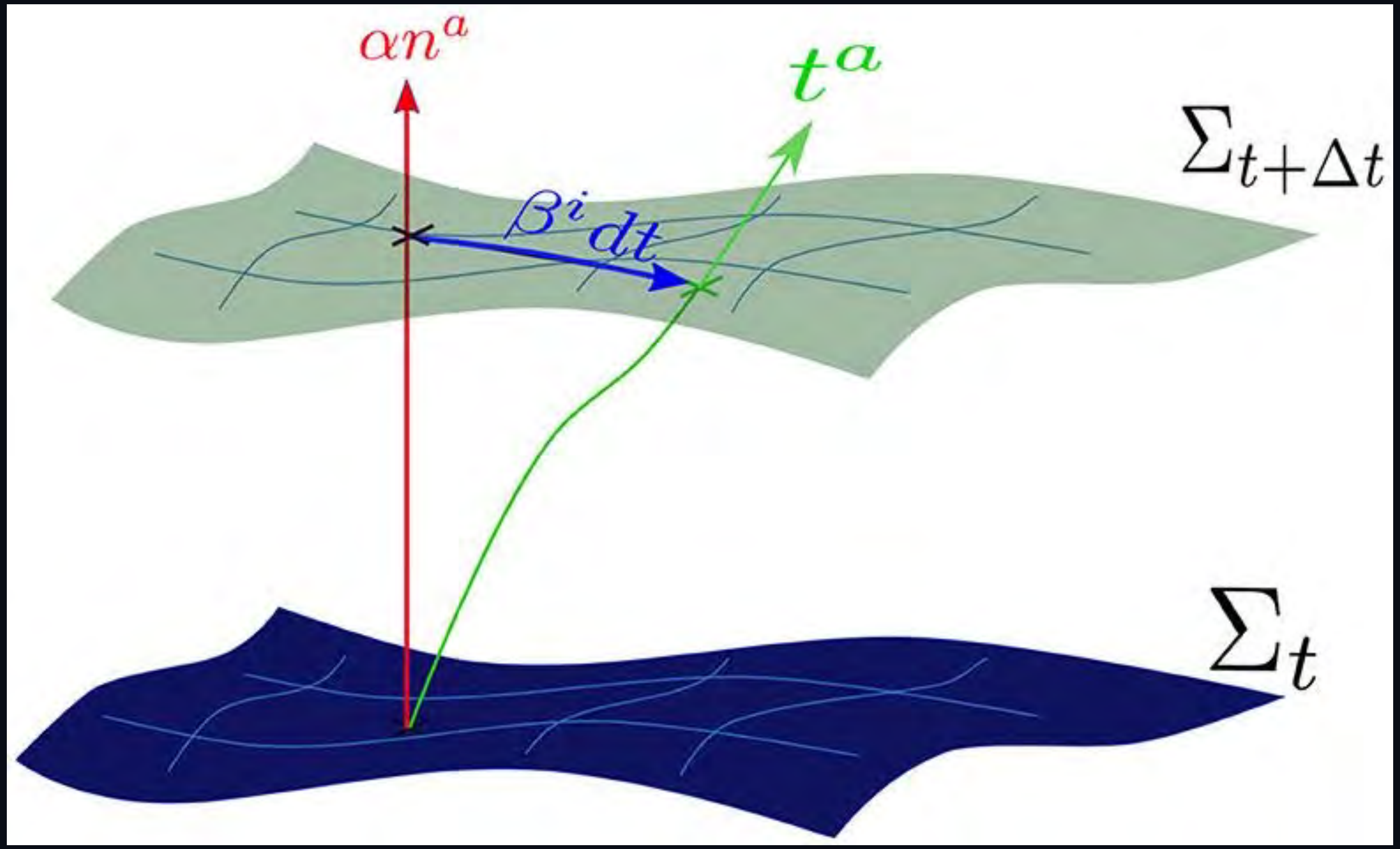


*lapse α: proper time between slices — shift $\beta^i$: coordinate drift*

*$\mathcal{L}_n$ — Lie derivative: the change of $\gamma_{ij}$ dragged along the flow of $n^a$*

$$\mathcal{L}_n = \tfrac{1}{\alpha}\left(\partial_t - \mathcal{L}_\beta\right)$$

**GAUGE IS A CHOICE —** the lapse α and shift $\beta^i$ carry no physics; they only thread your coordinates through the slicing.

# The ADM Equations

- Ten coupled, nonlinear PDEs for the metric $g_{a\beta}$ — with no preferred notion of time.

$$G_{ab} \equiv R_{ab} - \tfrac{1}{2} g_{ab} R = 8\pi T_{ab}$$

$$\nabla_a G^{ab} = 0 \implies \nabla_a T^{ab} = 0$$

- Choquet-Bruhat (1952): the Cauchy problem is **well posed** — simulation is mathematically viable.
- Arnowitt, Deser & Misner (1962): Einstein's equations split into two sets:

**Constraints → initial data**

$$\mathcal{H} \equiv {}^{(3)}R + K^2 - K_{ij}K^{ij} - 16\pi\rho = 0$$

$$\mathcal{M}^i \equiv D_j\left(K^{ij} - \gamma^{ij}K\right) - 8\pi S^i = 0$$

**Evolution equations**

$$\partial_t \gamma_{ij} = -2\alpha K_{ij} + D_i\beta_j + D_j\beta_i$$

$$\partial_t K_{ij} = -D_iD_j\alpha + \alpha\left(R_{ij} + KK_{ij} - 2K_{ik}K^k{}_j\right) + \mathcal{L}_\beta K_{ij} - 8\pi\alpha\left[S_{ij} - \tfrac{1}{2}\gamma_{ij}(S-\rho)\right]$$

- The contracted Bianchi identities make **four** of the ten equations **constraints**: they contain no second time derivatives.
- Four-fold coordinate freedom + four constraints ⇒ only **two dynamical degrees of freedom** — the two GW polarizations.

{$\gamma_{ij}$, $K_{ij}$}: 12 variables — 4 fixed by constraints, 4 gauge — 4 dynamical: the 2 GW polarizations

# Initial Data: Conformal Method & Bowen–York Punctures

- **York-Lichnerowics conformal split → free data: $\bar{\gamma}_{ij}$ , K, and the TT part of $\bar{A}^{ij}$**

$$\gamma_{ij} = \psi^4\,\bar{\gamma}_{ij}\,, \qquad A^{ij} = \psi^{-10}\big[(\bar{\mathbb{L}}W)^{ij} + \bar{A}^{ij}_{\mathrm{TT}}\big]\,, \qquad K_{ij} = A_{ij} + \tfrac{1}{3}\,\gamma_{ij}K$$

$W^i$ is a vector potential: its symmetrized gradient builds the longitudinal part of $\bar{A}^{ij}$, and the momentum constraint fixes it

- **Bowen–York → solve for $W^i$ momentum constraint (linear) analytically (linear)**

$$\bar{A}^{ij}_P = \frac{3}{2r^2}\Big[2\,P^{(i}n^{j)} - \big(\bar{\gamma}^{ij} - n^i n^j\big)P_k n^k\Big]\,, \qquad \bar{A}^{ij}_S = \frac{6}{r^3}\,n^{(i}\,\epsilon^{j)kl}\,S_k\,n_l$$

Conformal flatness + maximal slicing (K=0) make the momentum constraint linear;
Closed-form $P^i$ (momentum) and $S^i$ (spin) — superpose for multiple holes.

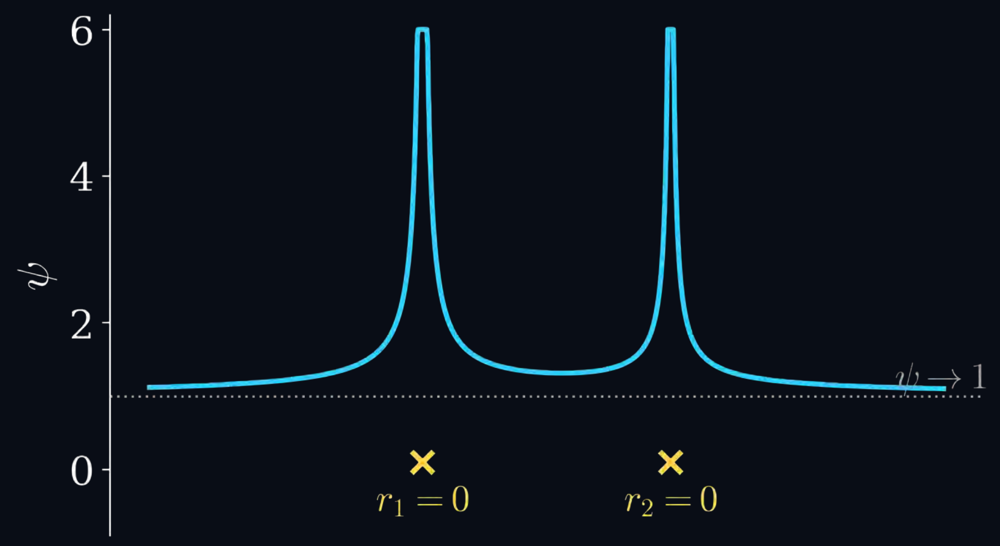


*$\psi$ on the z = 0 plane: singular at punctures, smooth elsewhere*

- **Bowen–York → solve for ψ in the Hamiltonian constraint (non-linear)**

$$\bar{D}^2\psi = -\tfrac{1}{8}\,\bar{A}_{ij}\bar{A}^{ij}\,\psi^{-7} \qquad (\text{vacuum},\ K = 0,\ \text{conformally flat})$$

- **Punctures** (Brandt & Brügmann 1997): the ansatz absorbs the 1/r singularities analytically — solve only for the regular u, **no excised inner boundaries** (TwoPunctures, spectral).

$$\psi = 1 + \textstyle\sum_A \frac{m_A}{2\,r_A} + u\,, \qquad u \text{ regular everywhere}$$

- **Cost:** junk radiation, spins $\chi \lesssim 0.93$

*Lichnerowicz (1944); York (1971–79); Bowen & York (1980); Brandt & Brügmann (1997); Ansorg, Brügmann & Tichy (2004)*

# Initial Data: Highly Spinning Black Holes

- Bowen–York is conformally flat — but Kerr admits **no conformally flat slice**: spins cap at $\chi \approx 0.928$.
- **HiSpID** ansatz: attenuated superposition of two Lorentz-boosted, conformally **Kerr** 3-metrics:

  $\tilde{\gamma}_{ij} = \tilde{\gamma}_{ij}^{(+)} + \tilde{\gamma}_{ij}^{(-)} - \delta_{ij}\,,\quad \psi_0 = \psi^{(+)} + \psi^{(-)} - 1\quad$ (BY: $\tilde{\gamma}_{ij} = \delta_{ij}$)

  → four coupled elliptic constraints for the corrections $u = \psi - \psi_0$ and $b^i$
- Reaches nearly extremal spins — **$\chi$ = 0.99** — and relativistic boosts.
- Spurious "junk" radiation ≈ **10× smaller** than Bowen–York → cleaner waveforms.
- First moving-puncture evolutions beyond the BY limit (Ruchlin+2017 Zlochower+2017) : orbiting **$\chi$ = 0.95** binaries, overlap > 0.999 with SXS (Lovelace+ 2008)

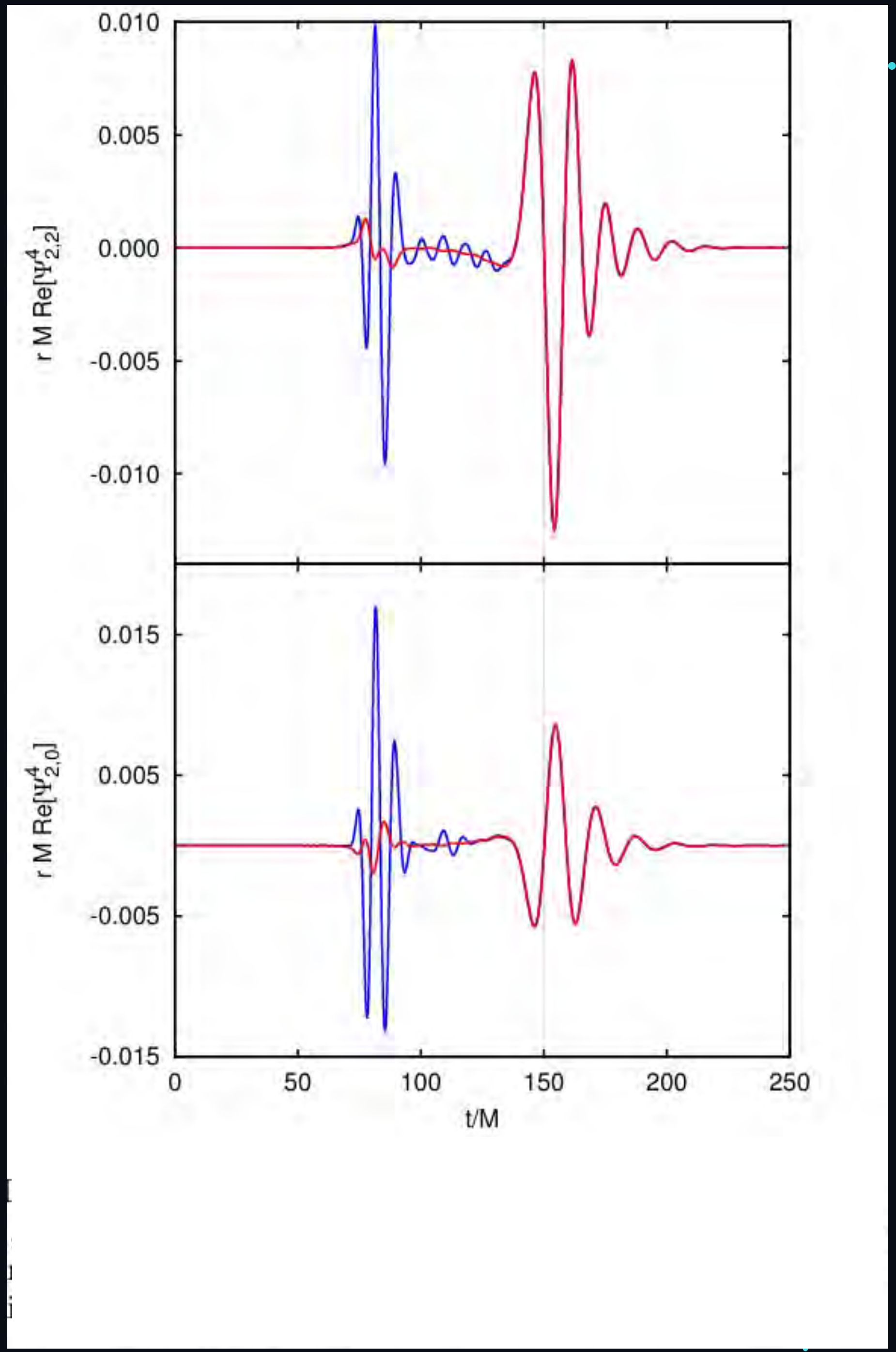


*$\Psi_4$ at r = 75M, $\chi$ = 0.9: BY (blue) vs HiSpID (red)*

*Ruchlin, Healy, Lousto & Zlochower, PRD 95, 024033 (2017); Zlochower+, PRD 96, 044002 (2017) — HiSpID*

# The ADM Evolution with Sources

- Matter enters only through the projections **$\rho$, $S^i$, $S_{ij}$** of $T^{ab}$ measured by the Eulerian observers.

$$\partial_t \gamma_{ij} = -2\alpha K_{ij} + D_i\beta_j + D_j\beta_i \qquad \rho = n_a n_b T^{ab}\,, \qquad S^i = -\gamma^i{}_a n_b T^{ab}\,, \qquad S_{ij} = \gamma_{ia}\gamma_{jb} T^{ab}$$

$$\partial_t K_{ij} = -D_i D_j \alpha + \alpha\big(R_{ij} + K K_{ij} - 2K_{ik}K^k{}_j\big) + \mathcal{L}_\beta K_{ij} - 8\pi\alpha\big[S_{ij} - \tfrac{1}{2}\gamma_{ij}(S-\rho)\big]$$

- Together with the Hamiltonian and momentum constraints, it forms a **constrained evolution system** — like Maxwell's equations, but nonlinear (Arnowitt, Deser & Misner 1962)
- York (1979): the form above is weakly hyperbolic; every modern formulation is a rearrangement of it.

### Why the ADM evolution fails

- **Strongly hyperbolic** ⇒ bounded growth; **weakly hyperbolic** ⇒ frequency-dependent growth **no resolution can cure**.
- ADM's principal part is **defective** — zero-speed constraint modes; truncation error seeds violations that grow like a **Jordan block** and feed nonlinear blow-up (Frittelli 1996; Shinkai & Yoneda 2002)

**Escape routes, all used today:**

1) change variables → BSSN
2) promote constraints → Z4
3) fix the gauge → moving punctures or generalized harmonic.

# BSSN: The Variables

$$\gamma_{ij} = e^{4\phi}\,\tilde{\gamma}_{ij}\,, \quad \det\tilde{\gamma}_{ij} = 1\,, \qquad K_{ij} = e^{4\phi}\left(\tilde{A}_{ij} + \tfrac{1}{3}\tilde{\gamma}_{ij}K\right), \qquad \tilde{\Gamma}^i = -\partial_j\tilde{\gamma}^{ij}$$

$$e^{4\phi} = \left(\det\gamma_{ij}\right)^{1/3}, \qquad \chi \equiv e^{-4\phi}, \quad W \equiv e^{-2\phi} \quad \text{(evolved variants)}$$

- Conformal-traceless (York–Lichnerowicz) split: **volume ($\phi$), shape ($\tilde{\gamma}_{ij}$), expansion ($K$), shear ($\tilde{A}_{ij}$)** — each with distinct dynamics.
- The conformal connection functions $\tilde{\Gamma}^i$ are promoted to **independent variables** — the key step: second derivatives of the metric in the Ricci tensor become first derivatives of $\tilde{\Gamma}^i$, giving a wave-equation structure — the cure for ADM's weak hyperbolicity (Shibata & Nakamura 1995, Baumgarte & Shapiro 1999).
- Algebraic constraints $\det\tilde{\gamma}_{ij} = 1$, $\mathrm{tr}\,\tilde{A}_{ij} = 0$ are enforced at every step.

BSSN & Z4 are strongly hyperbolic only when closed with the **moving-puncture gauge** (1+log + $\Gamma$-driver shift).

*Shibata & Nakamura (1995); Baumgarte & Shapiro (1999)*

# BSSN: The Evolution System

## GEOMETRY SECTOR · γ̃, ϕ, K

$$\partial_t\tilde\gamma_{ij} = -2\alpha\tilde A_{ij} + \beta^k\partial_k\tilde\gamma_{ij} + 2\,\tilde\gamma_{k(i}\,\partial_{j)}\beta^k - \tfrac{2}{3}\,\tilde\gamma_{ij}\,\partial_k\beta^k$$

$$\partial_t\phi = -\tfrac{1}{6}\,\alpha K + \beta^i\partial_i\phi + \tfrac{1}{6}\,\partial_i\beta^i$$

$$\partial_t K = -D^iD_i\alpha + \alpha\big(\tilde A_{ij}\tilde A^{ij} + \tfrac{1}{3}K^2\big) + 4\pi\alpha\,(\rho + S) + \beta^i\partial_i K$$

- The $\phi$ and $\tilde\gamma_{ij}$ equations are kinematical — they carry no curvature.
- The $K$ equation uses the **Hamiltonian constraint** to eliminate the Ricci scalar: constraint addition is part of the design, not an afterthought.

## CURVATURE & CONNECTION · Ã, Γ̃ — THE CURE FOR WEAK HYPERBOLICITY

$$\partial_t\tilde A_{ij} = e^{-4\phi}\big[-D_iD_j\alpha + \alpha\big(R_{ij} - 8\pi S_{ij}\big)\big]^{\mathrm{TF}} + \alpha\big(K\tilde A_{ij} - 2\tilde A_{ik}\tilde A^k{}_j\big) + \mathcal{L}_\beta\tilde A_{ij}$$

$$\partial_t\tilde\Gamma^i = -2\tilde A^{ij}\partial_j\alpha + 2\alpha\big(\tilde\Gamma^i{}_{jk}\tilde A^{jk} + 6\tilde A^{ij}\partial_j\phi - \tfrac{2}{3}\,\tilde\gamma^{ij}\partial_j K - 8\pi\tilde\gamma^{ij}S_j\big) + \mathcal{L}_\beta\tilde\Gamma^i$$

- With 1+log slicing and Γ-driver shift the full system is **strongly hyperbolic** — and remarkably forgiving in practice (Sarbach+ 2002; Gundlach & Martín-García 2006)
- Variants: $W = e^{-2\psi}$ or $\chi = e^{-4\psi}$ evolution improves behavior at punctures (Marronetti+2008; Campanelli group).
- The $\tilde A_{ij}$ equation carries the physical degrees of freedom; TF denotes the trace-free part.
- The **$\tilde\Gamma^i$ equation** has the **momentum constraint built in**: violations propagate and leave the grid rather than sitting and growing.

# The Z4 Family: Constraints as Dynamics

$$R_{ab} + 2\,\nabla_{(a} Z_{b)} = 8\pi\left(T_{ab} - \tfrac{1}{2} g_{ab} T\right) + \kappa_1 \left[\, 2\, n_{(a} Z_{b)} - (1+\kappa_2)\, g_{ab}\, n^c Z_c \,\right]$$

- A four-vector $\mathbf{Z^a}$ measures the constraint violation; Einstein's equations are recovered when $Z^a = 0$. (Bona+ 2003)
- Violations propagate at light speed and are damped at rate $\kappa_1$ — they radiate away instead of accumulating.
- 3+1 reductions: **CCZ4** (covariant, conformal) and **Z4c** (BSSN-like) — standard in current BNS codes; cleaner Hamiltonian-constraint behavior than BSSN. (Bernuzzi & Hilditch 2010; Alic+ 2012)
- Drop-in replacement for BSSN — same conformal variables and moving-puncture gauges (1+log lapse, Γ-driver shift).
- Z4c is the spacetime engine of **AsterX**, the Einstein Toolkit's GPU evolver behind the GRMHD simulations later in this hour.
- The other modern route — **generalized harmonic** (gauge fixed in the principal part; SpEC/SXS) — reaches the same goal (Pretorius 2005 → backup).

# Slicing Conditions

### Maximal slicing (K = 0): elliptic, singularity-avoiding — but too costly for binaries

$$K = 0 \ : \qquad D^i D_i \, \alpha = \alpha \big[ K_{ij} K^{ij} + 4\pi(\rho + S) \big]$$

### Bona–Massó family: hyperbolic gauge drivers

$$\big(\partial_t - \beta^i \partial_i\big)\, \alpha = -\alpha^2 f(\alpha)\, K \, , \qquad f = 1 \ (\text{harmonic}) \, , \quad f = 2/\alpha \ (1{+}\log)$$

- $f = 2/\alpha$ gives **1+log slicing**: marches at gauge speed $\alpha\sqrt{f}$, mimics maximal slicing's singularity avoidance at hyperbolic cost.
- Near the puncture the lapse collapses ("collapse of the lapse"): the slice wraps around the singularity and freezes its advance there.
- Geodesic slicing ($\alpha = 1$): free-falling observers hit the singularity in finite time ($\partial_t K = K_{ij}K^{ij} \geq 0$, focusing) — instructive, never used.

*Smarr & York (1978); Bona, Massó, Seidel & Stela (1995)*

# The Moving-Puncture Gauge

Two gauge conditions tame the coordinates near a moving puncture — one for the lapse $\alpha$, one for the shift $\beta^i$.
Zero shift fails: orbiting holes drag the coordinates into a tangle (**grid stretching**), metric gradients blow up.

### THE LAPSE · 1+log SLICING

$$\partial_t \alpha = -\alpha^2 f(\alpha)\, K$$

$$f(\alpha) = 2/\alpha \quad \Rightarrow \quad \partial_t \alpha = -2\alpha K$$

Cheap, robust, and singularity-avoiding — the standard lapse in moving-puncture binary evolutions.

### THE SHIFT · Γ-DRIVER

$$\partial_t \beta^i = \tfrac{3}{4} B^i$$

$$\partial_t B^i = \partial_t \tilde{\Gamma}^i - \eta\, B^i$$

A damped wave equation drives $\partial_t \tilde{\Gamma}^i \to 0$ — hyperbolic relaxation of the elliptic minimal-distortion condition. Damping $\eta$ ($\sim$ 1–2/M) suppresses oscillations and stops coordinates draining into punctures.

- Together, 1+log slicing and the Γ-driver shift form the **moving-puncture gauge**: punctures advect freely across the grid — the recipe that made stable binary evolutions routine after 2005.
- One ingredient — add BSSN's conformal split + puncture data (already in hand): the **moving-puncture approach**.

*Alcubierre+ (2003); Campanelli, Lousto, Marronetti & Zlochower (2006); Baker+ (2006); van Meter+ (2006)*

# Black Holes on the Grid: Excision vs. Punctures

## Excision

- Cut out the interior inside the horizon — causality protects the exterior.
- Needs horizon tracking, boundary treatment, characteristic analysis at the excision surface.
- Standard in spectral codes (SpEC/SXS) and GH evolutions.

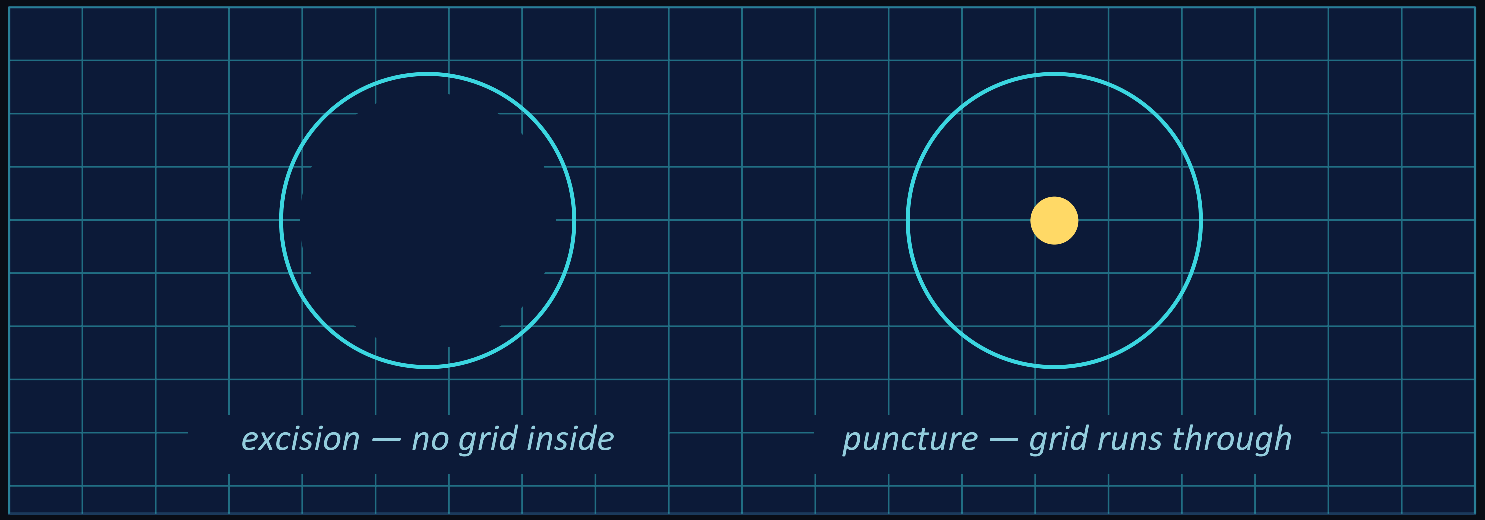


## Moving punctures

- No interior boundary: the trumpet geometry + gauge keep all fields regular.
- Trivially compatible with finite differences and AMR — the workhorse of BSSN/Z4c codes.
- Interior is gauge-distorted, not trustworthy — but causally disconnected.
- The key move (Campanelli+ 2006; Baker+ 2006): evolve $\chi = \psi^{-4}$, turning the puncture's $1/r$ singularity into a smooth zero — the interior is a second asymptotically flat end we never resolve.

Both rely on the same fact: **no information escapes the horizon** — what happens inside cannot affect the evolution outside.

# The Moving-Puncture Equations

**The moving-puncture approach:** evolve Bowen–York puncture data with BSSN's conformal split and the 1+log / Γ-driver gauge — the punctures move freely across the grid.

$$\boxed{\chi = \exp(-4\phi)}$$

$$
\begin{aligned}
\partial_0 \tilde{\gamma}_{ij} &= -2\alpha \tilde{A}_{ij}, \\
\partial_t \chi &= \frac{2}{3}\chi\left(\alpha K - \partial_a \beta^a\right) + \beta^i \partial_i \chi, \\
\partial_0 \tilde{A}_{ij} &= \chi\left(-D_i D_j \alpha + \alpha R_{ij}\right)^{TF} + \\
&\quad \alpha\left(K \tilde{A}_{ij} - 2\tilde{A}_{ik}\tilde{A}^k_j\right), \\
\partial_0 K &= -D^i D_i \alpha + \alpha\left(\tilde{A}_{ij}\tilde{A}^{ij} + \frac{1}{3}K^2\right), \\
\partial_t \tilde{\Gamma}^i &= \tilde{\gamma}^{jk}\partial_j \partial_k \beta^i + \frac{1}{3}\tilde{\gamma}^{ij}\partial_j \partial_k \beta^k + \beta^j \partial_j \tilde{\Gamma}^i - \\
&\quad \tilde{\Gamma}^j \partial_j \beta^i + \frac{2}{3}\tilde{\Gamma}^i \partial_j \beta^j - 2\tilde{A}^{ij}\partial_j \alpha + \\
&\quad 2\alpha\left(\tilde{\Gamma}^i{}_{jk}\tilde{A}^{jk} + 6\tilde{A}^{ij}\partial_j \phi - \frac{2}{3}\tilde{\gamma}^{ij}\partial_j K\right),
\end{aligned}
$$

**LazEv, 4th order, BSSN** —Campanelli+ 2006

Replace $\phi$ $(O(\log r))$ with $\chi = e^{-4\phi}$ $(O(r^4))$
$\partial_0 \alpha = -2\alpha K$
$\partial_t \beta^a = B^a$, $\partial_t B^a = 3/4 \partial_t \tilde{\Gamma}^a - \eta B^a$
$\alpha(t=0) = \psi_{BL}^{-2}$ $\quad \beta^i = B^i = 0.$

**Hahndol, AMR, BSSN** — Baker+ 2006

Discretize $\phi$
Standard 1+log lapse
Shifting-shift
$\alpha(t=0) = 1$

- Absorb singularities in the BSSN conformal factor to free the punctures
- Use new "moving-puncture" gauge condition to move the punctures

**χ = exp(−4ϕ) stays finite at the punctures**: the grid never sees the singularity — with 1+log + Γ-driver, the punctures evolve as **ordinary grid data**.

- Under this gauge each slice settles onto a **trumpet**: a stationary cylinder of areal radius $R_0 \approx 1.31$ M — the geometry punctures relax to (Hannam+ 2007; Brown 2008).

*Brandt & Brügmann (1997); Campanelli, Lousto, Marronetti & Zlochower (2006); Baker+ (2006)*

# Locating and Weighing Black Holes

$$\Theta \equiv D_i s^i + K_{ij}\, s^i s^j - K = 0$$

$$M^2 = M_{\rm irr}^2 + \frac{S^2}{4M_{\rm irr}^2}\,, \qquad M_{\rm irr} = \sqrt{\frac{A_{\rm AH}}{16\pi}}$$

- **Apparent horizon**: outermost surface of vanishing outgoing null expansion — defined on a single slice, findable at run time.
- The **event horizon** — the true boundary of no escape — is **teleological**: defined by null rays reaching $\mathscr{I}^+$, found only in **post-processing**. The apparent horizon lies inside it (with cosmic censorship): a safe excision/diagnostic surface.
- Spin from the **isolated/dynamical-horizon** framework: J from an (approximate) rotational Killing vector on the surface; mass via Christodoulou.
- Remnant mass, spin, and recoil are horizon quantities — a key NR output for astrophysics.

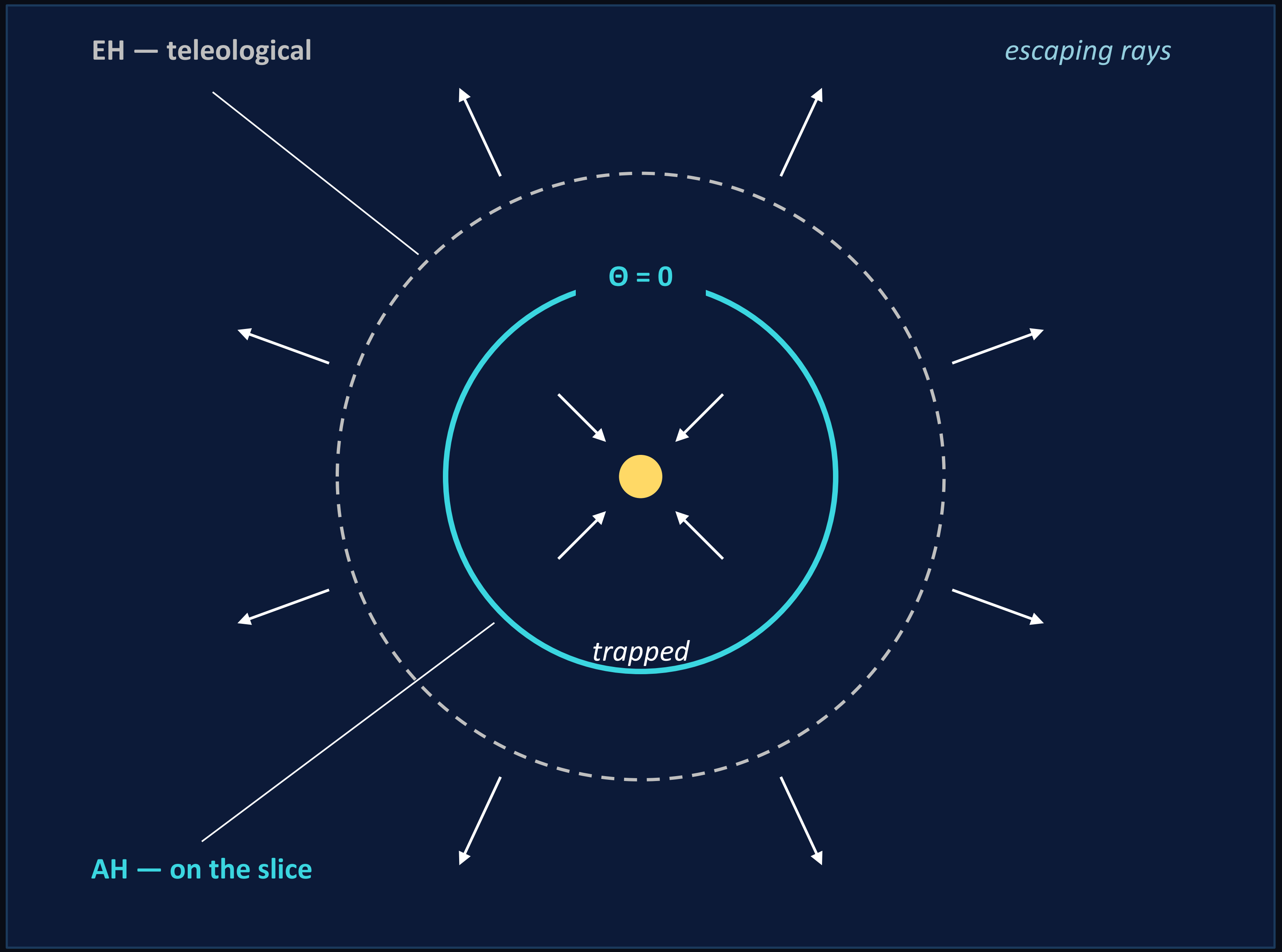


*Θ = 0 marks the AH on each slice → run-time finding: BHaHAHA (next slide)*

*Thornburg (2004) — AHFinderDirect; Ashtekar & Krishnan, Liv. Rev. Rel. (2004); Dreyer+ (2003)*

# Finding Apparent Horizons: BHaHAHA

- The AH finder is core infrastructure: it **locates and tracks** the holes, enables excision/interior handling, and supplies area → mass & spin diagnostics.
- Finding a MOTS (marginally outer trapped surface) is a **nonlinear elliptic problem** on each slice: solve **$\Theta[h] = 0$** for the surface shape $h(\theta, \phi)$.
- **BHaHAHA**: first open-source, infrastructure-agnostic finder — a standalone, dependency-free C library that any C/C++ NR code can link.
- Method: hyperbolize the elliptic solve into a **damped wave equation in pseudo-time**, accelerated by multigrid-inspired refinement and over-relaxation.
- OpenMP today, CUDA nearly complete; dynamic tracking ≈ **2.1× faster** than AHFinderDirect at interpolation-limited accuracy.

*Etienne et al., Class. Quantum Grav. 43, 075007 (2026)*

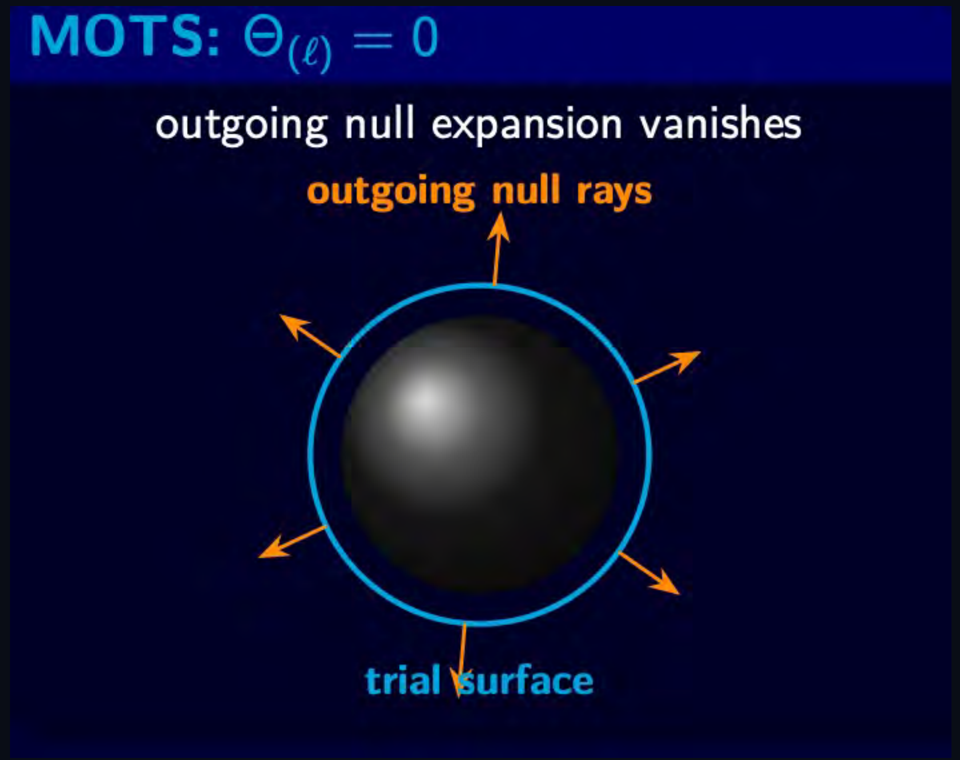


WAVE EXTRACTION

# From Spacetime to Waveforms

$$\Psi_4 = C_{abcd}\, n^a\, \bar{m}^b\, n^c\, \bar{m}^d \qquad \Psi_4 = \ddot{h}_+ - i\,\ddot{h}_\times\,, \qquad h_+ - i\,h_\times = \sum_{\ell,m} h_{\ell m}(t,r)\; {}_{-2}Y_{\ell m}(\theta,\varphi)$$

- $\Psi_4$ — the outgoing radiation: the Weyl curvature on a null (Newman–Penrose) tetrad, dominant at large r by the **peeling theorem**.
- Extracted on coordinate spheres and decomposed in **spin-weight −2** modes $h_{lm}$ (alternative: gauge-invariant **Regge–Wheeler–Zerilli–Moncrief**); then **extrapolate r → ∞** or use **CCE** — the gauge-invariant gold standard.
- Outputs: waveform modes, radiated E and J, **recoil kicks**, remnant mass and spin.
- **Perturbative extrapolation**: correct $\Psi_4$ from a finite observer location to r → ∞, to $O(1/r)$ *— Nakano, Healy, Lousto & Zlochower (2015)*:

$$\psi_4^{\ell m}(t,r)\big|_{r\to\infty} \simeq (1 - 2M/r)\left[\, \psi_4^{\ell m} - (\ell-1)(\ell+2)/2r \int^t \psi_4^{\ell m}(t', r)\, dt' \,\right] + O(r^{-2})$$

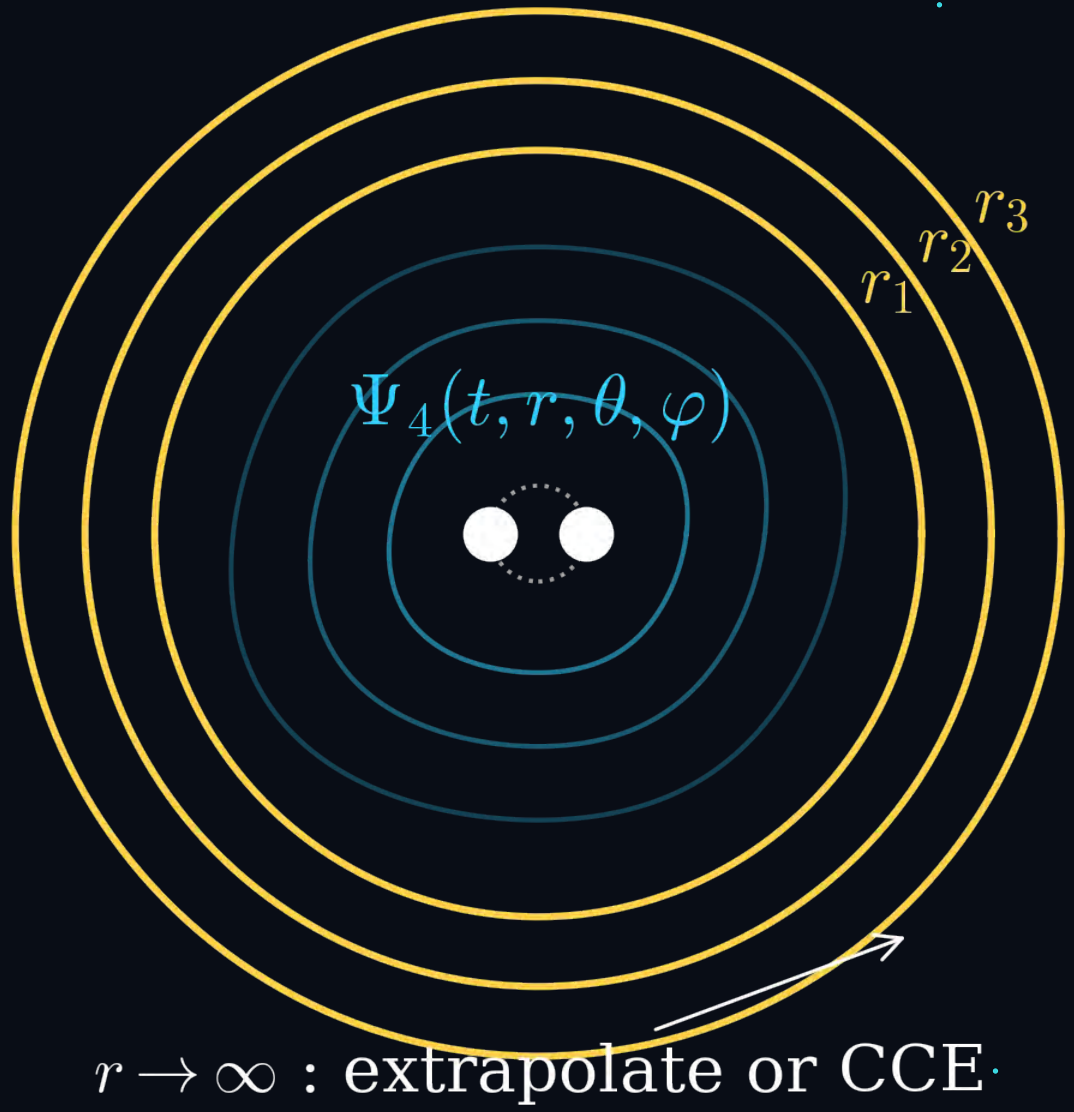


*Newman & Penrose (1962); Campanelli & Lousto (1999); Baker, Campanelli & Lousto (2002) — Lazarus*

# From $\Psi_4$ to Strain, Modes, and Ringdown

$$\Psi_4 = \ddot{h}_+ - i\,\ddot{h}_\times\,, \qquad h_+ - i\,h_\times = \textstyle\sum_{\ell,m} h_{\ell m}(t,r)\; {}_{-2}Y_{\ell m}(\theta,\varphi)$$

$$\tilde{h}_{\ell m}(\omega) = -\,\frac{\tilde{\Psi}_{4,\ell m}(\omega)}{\omega^2}\,, \qquad \omega \geq \omega_0 \qquad \text{(fixed-frequency integration)}$$

- Detectors measure the strain *h*, not $\Psi_4$ — two-time integrations invite secular drifts; the cure is **fixed-frequency integration (FFI)** with a cutoff $f_0$ below the signal.
- The **(2,2) mode** dominates quasi-circular binaries; higher modes carry the asymmetries and the recoil momentum.
- After merger the remnant rings down in **quasi-normal modes** — damped sinusoids whose frequency and damping time are fixed by the remnant **mass and spin alone** (no-hair theorem).
- NR supplies the full nonlinear ringdown — mode amplitudes and start time perturbation theory cannot give — the basis of **black-hole spectroscopy** and tests of the Kerr hypothesis.
- **Now realized:** GW250114 (2025), the clearest event yet (SNR ≈ 77), resolved three ringdown modes — the first true black-hole spectroscopy.

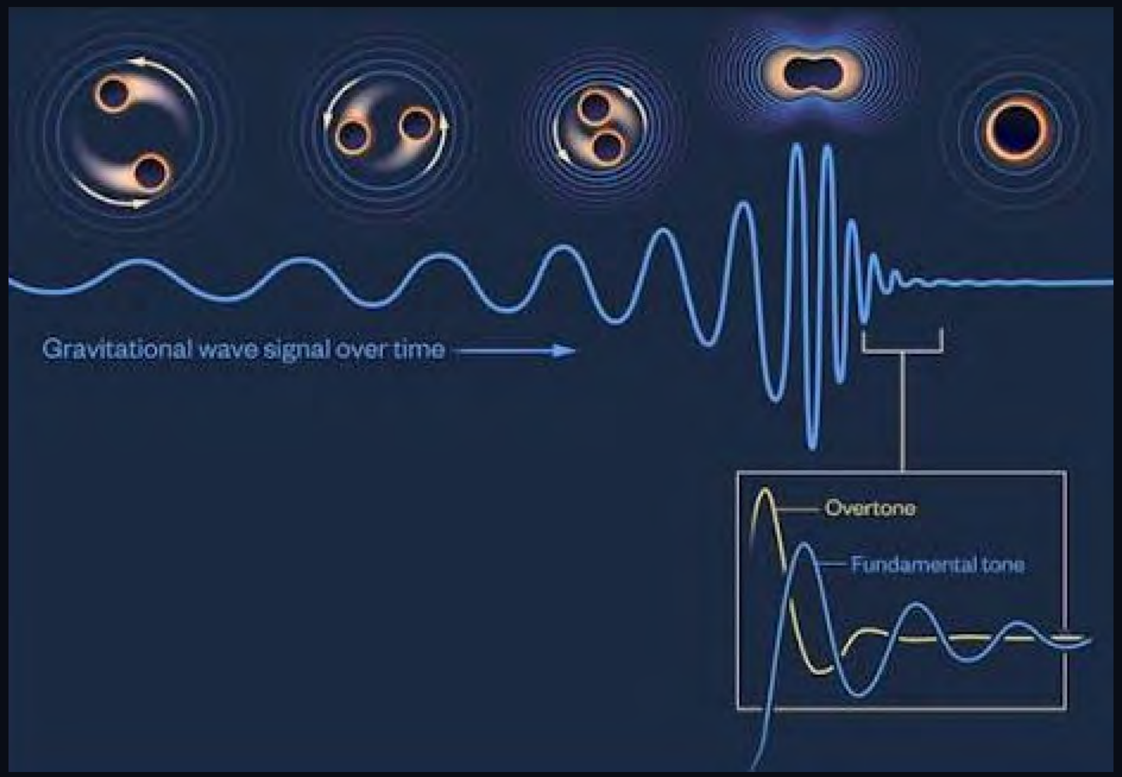


*Reisswig & Pollney (2011) — FFI; Moxon+ (2020) — CCE; Berti, Cardoso & Will (2006); Giesler+ (2019) — QNMs; LVK (2025) — GW250114; Lousto+ 2026 — waveform error budgets*

# Global Quantities, Radiated Energy, and Kicks

ADM MASS

$$M_{\mathrm{ADM}} = \frac{1}{16\pi} \oint_{\infty} (\partial_j \gamma_{ij} - \partial_i \gamma_{jj})\, dS^i$$

ADM ANGULAR MOMENTUM

$$J_i = \frac{1}{8\pi} \oint_{\infty} \epsilon_{ij}{}^{k} x^j (K^l{}_k - \delta^l{}_k K)\, dS_l$$

$$\frac{dE}{dt} = \lim_{r\to\infty} \frac{r^2}{16\pi} \oint_{S^2} \left| \int_{-\infty}^{t} \Psi_4 \, dt' \right|^2 d\Omega$$

$$\frac{dP^i}{dt} = \lim_{r\to\infty} \frac{r^2}{16\pi} \oint_{S^2} \ell^i \left| \int_{-\infty}^{t} \Psi_4 \, dt' \right|^2 d\Omega \qquad \Longrightarrow \qquad \text{recoil “kicks”}$$

$$M_{\mathrm{ADM}} = M_{\mathrm{remnant}} + E_{\mathrm{rad}}$$

- **Balance**: ADM mass minus radiated energy must equal the remnant horizon mass; same for angular momentum — the most stringent end-to-end accuracy check.
- Linear-momentum flux comes from **mode mixing** (ℓ, ℓ±1 beating): asymmetric binaries recoil.
- **Superkicks**: spin–orbit asymmetry drives recoils up to ~ 4000–5000 km/s — enough to eject remnants from any galaxy; consequences for supermassive-BH retention (See my talk tomorrow!)

*Campanelli, Lousto, Zlochower & Merritt (2007); González+ (2007); Lousto & Zlochower (2011)*

MATTER · GRMHD

# The Coupled GRMHD System

Einstein field equations: $G_{\mu\nu} = R_{\mu\nu} - \frac{1}{2} g_{\mu\nu} R = 8\pi T_{\mu\nu}$

Maxwell equations: $\nabla^*_\nu F^{\mu\nu} = 0\,;\qquad \nabla_\nu F^{\mu\nu} = 4\pi \mathscr{J}^\mu$

4-current density: $\mathscr{J}^\mu = q u^\mu + \sigma F^{\mu\nu} u_\nu$

Energy conservation: $\nabla_\mu T^{\mu\nu} = 0$

Mass conservation: $\nabla_\mu(\rho u^\mu) = 0$

Equation of state: $P = P(\rho, \epsilon)$

**Source terms:** couple the fluid to the spacetime — metric evolved with NR alongside with BSSN/Z4c *(Shibata & Uryū 2000)*

Then use the same 3+1 machinery as the vacuum sector

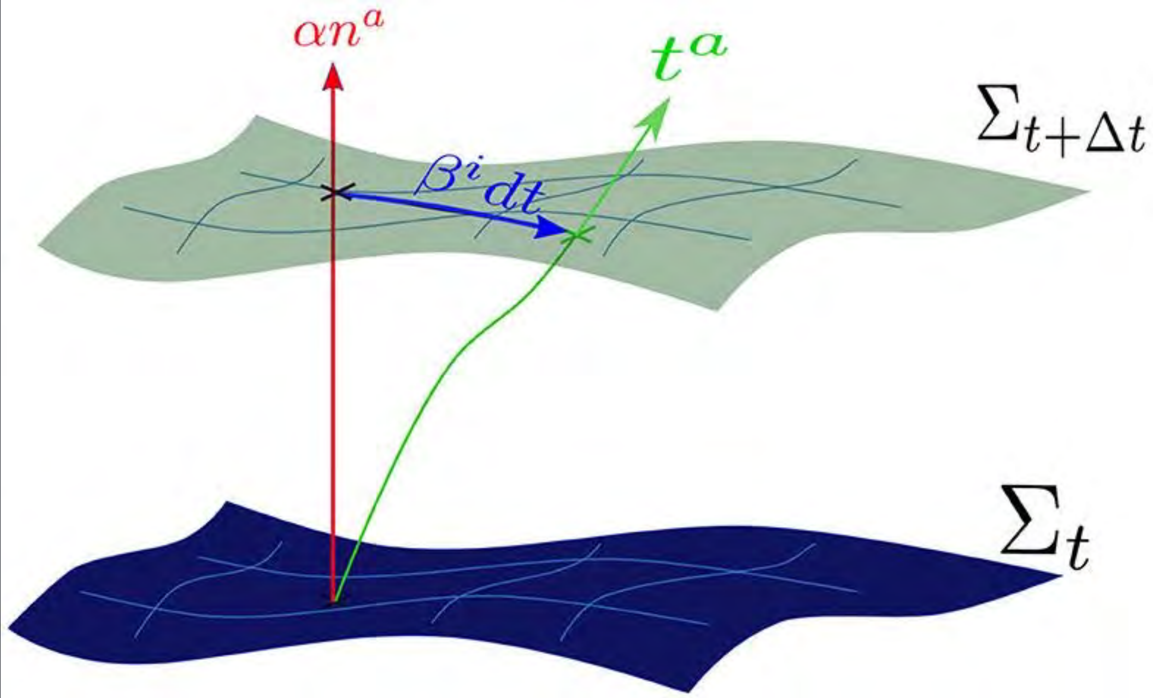


STRESS–ENERGY TENSOR — IDEAL MHD

$$T^{\mu\nu} = \left(\rho h + b^2\right) u^\mu u^\nu + \left(p_{\text{gas}} + p_{\text{mag}}\right) g^{\mu\nu} - b^\mu b^\nu$$

*fluid exchanges energy & momentum with the spacetime*

Line element: $ds^2 = g_{\mu\nu} dx^\mu dx^\nu = -\left(\alpha^2 - \beta^i \beta_i\right) dt^2 + 2\beta_i\, dx^i dt + \gamma_{ij}\, dx^i dx^j$

Time-like unit normal: $n^\mu = \frac{1}{\alpha}\left(1, -\beta^i\right);\quad n_\mu = (-\alpha, 0, 0, 0)$

Eulerian 3-velocity: $v^i = \frac{1}{\alpha}\left(\frac{u^i}{u^0} + \beta^i\right)$

*To dig deeper: Rezzolla & Zanotti, Relativistic Hydrodynamics (2013) · Font LRR (2008) · Martí & Müller LRCA (2015)*

MATTER · IDEAL FLUID

# The Ideal Fluid & Equation of State

STRESS-ENERGY TENSOR: MHD → IDEAL FLUID

$$T^{\mu\nu} = \left(\rho h + b^2\right) u^\mu u^\nu + \left(p_{\rm gas} + p_{\rm mag}\right) g^{\mu\nu} - b^\mu b^\nu$$

*fluid exchanges energy & momentum with the spacetime*

**hydrodynamic limit, b → 0:** $T^{ab} = \rho_0 h\, u^a u^b + p\, g^{ab}$

$h = 1 + \epsilon + p/\rho_0$ — specific enthalpy

*ideal fluid: no viscosity, no heat conduction*

- **Closure:** evolution never gives p — the EOS $p = p(\rho_0, \epsilon)$ supplies it
- **Analytical:** fast & smooth — code tests, disks, jets
- **Hybrid:** cold nuclear base + $\Gamma_{th}$ shock heating — mergers
- **Tabulated:** $(\rho, T, Y_e)$ microphysics — NS matter & kilonovae

*$\epsilon$ internal energy · h enthalpy · Γ adiabatic · $\Gamma_{th}$ thermal · $Y_e$ electron fraction*

- **Analytical**
  - ideal gas $P(\rho,\epsilon) = (\Gamma-1)\rho\epsilon\,; \quad \epsilon_{\min} = 0$
  - polytrope $P(\rho) = k\rho^\Gamma\,; \quad \Gamma = 1 + 1/n$
- **Hybrid**

$$P(\rho,\epsilon) = P_{\rm cold}(\rho) + (\Gamma_{\rm th}-1)\rho\,(\epsilon - \epsilon_{\rm cold}(\rho))$$
$$\epsilon_{\min}(\rho) = \epsilon_{\rm cold}(\rho)$$

- **Tabulated**
  - 1 parameter $P = P(\rho)$
  - 3 parameter $P = P(\rho, T, Y_e)$

MATTER · VALENCIA

# GRMHD Equations

First order flux-conservative hyperbolic Valencia formalism

$$\frac{1}{\alpha\sqrt{\gamma}}\left[\partial_t\left(\sqrt{\gamma}\,\mathbf{U}\right)+\partial_i\left(\sqrt{\gamma}\,\mathbf{F^i}\right)\right]=\mathbf{S}$$

**State vector**

$$\mathbf{U}\equiv\begin{pmatrix} D \\ S_j \\ \tau \\ B^k \\ DY_e \end{pmatrix}$$

**Fluxes**

$$\mathbf{F}\equiv\begin{pmatrix} D\tilde{v}^i \\ S_j\tilde{v}^i+\alpha\left(P+P_{\mathrm{mag}}\right)\delta^i_j-\alpha b_j B^i/W \\ \tau\tilde{v}^i+\alpha\left(P+P_{\mathrm{mag}}\right)v^i-\alpha^2 b^0 B^i/W \\ B^k\tilde{v}^i-B^i\tilde{v}^k \\ DY_e\tilde{v}^i \end{pmatrix}$$

**Source terms**

$$\mathbf{S}\equiv\begin{pmatrix} 0 \\ T^{\mu\nu}\left(\partial_\mu g_{\nu j}-\Gamma^\delta_{\nu\mu}g_{\delta j}\right) \\ \alpha\left(T^{\mu 0}\partial_\mu\ln\alpha-T^{\mu\nu}\Gamma^0_{\nu\mu}\right) \\ 0 \\ 0 \end{pmatrix}$$

- **Valencia formulation:** $\nabla_a(\rho_0 u^a) = 0$ and $\nabla_a T^{ab} = 0$ recast as flux-conservative balance laws — shocks captured with the correct jump conditions (HRSC, above) *(Banyuls+ 1997; Font 2008)*
- **Recover primitives** ($\rho$, $v^i$, $\varepsilon$) from conserved ($D$, $S_i$, $\tau$): root-finding through the EOS — every point, every step; delicate near vacuum and high Lorentz factors *— full dictionary → next slide*

**SHOCKS & HRSC**

- **Relativistic fluids shock:** the conservative form + Rankine–Hugoniot jump conditions pick the correct weak solution
- **HRSC:** high-resolution shock-capturing schemes evolve the conserved variables cleanly through shocks, by reconstructing the fluid at cell faces and taking fluxes from local Riemann problems — the concrete schemes appear in the timestep loop (coming up)

VALENCIA FORMULATION

# Prim2Con & Con2Prim

## primitives

| | |
|---|---|
| $\rho$ | rest-mass density |
| $v^i$ | fluid 3-velocity |
| $\epsilon$ | specific internal energy |
| $Y_e$ | electron fraction |

| | |
|---|---|
| $P$ | gas pressure |
| $P_{\text{mag}} \equiv b^2/2$ | magnetic pressure |
| $W = 1/\sqrt{1-v^2}$ | Lorentz factor |
| $h = 1 + \epsilon + P/\rho$ | specific enthalpy |
| $\vec{A}$ | vector potential |

## conservatives

| | |
|---|---|
| conserved density | $D \equiv \rho W$ |
| conserved momentum | $S_j \equiv \left(\rho h + b^2\right) W^2 v_j - \alpha b^0 b_j$ |
| conserved internal energy | $\tau \equiv \left(\rho h + b^2\right) W^2 - \left(P + P_{\text{mag}}\right) - \alpha^2 \left(b^0\right)^2 - D$ |
| conserved magnetic field | $\vec{B} \equiv \vec{\nabla} \times \vec{A}$ |
| conserved electron fraction | $DY_e$ |

Co-moving magnetic field components

$$b^0 = \frac{W B^i v_i}{\alpha}, \qquad b^i = \frac{B^i + \alpha b^0 u^i}{W}, \qquad b^2 \equiv b^\mu b_\mu = \frac{B^2 + \alpha^2 \left(b^0\right)^2}{W^2}$$

### CON2PRIM — THE HARD DIRECTION

- No closed form — a root-find per cell, per step
- Newton–Raphson (Noble+ 2006) or robust bracketing (Kastaun; Kalinani+ 2021 → RePrimAnd, used by AsterX)
- Failures at high magnetization & Lorentz factor → atmosphere / fallback fixes

# Evolution Equations for B: Induction & Gauge

**Ideal MHD**

$$\sigma \to \infty\,; \quad F^{\mu\nu}u_\nu \to 0$$

comoving observer measures no electric field

**Maxwell equations**

$$\nabla^*_\nu F^{\mu\nu} = \frac{1}{\sqrt{-g}}\partial_\nu\left(\sqrt{-g}\,(b^\mu u^\nu - b^\nu u^\mu)\right) = 0$$

written solely in terms of b

Co-moving magnetic field components

$$b^0 = \frac{W B^i v_i}{\alpha}, \qquad b^i = \frac{B^i + \alpha b^0 u^i}{W}, \qquad b^2 \equiv b^\mu b_\mu = \frac{B^2 + \alpha^2\,(b^0)^2}{W^2}$$

**σ → ∞, perfect conductor:** free charges short out any comoving E-field — B frozen in, E = −v × B slaved to B

Divergence-free condition: $\partial_i \tilde{B}^i = 0$

Induction equations: $\partial_t \tilde{B}^i = \partial_j\left(\tilde{v}^i \tilde{B}^j - \tilde{v}^j \tilde{B}^i\right)$

where $\tilde{B}^i \equiv \sqrt{\gamma}\,B^i\,; \quad \tilde{v}^i \equiv \alpha v^i - \beta^i$

*+ simple & local — but ∇·B drifts: needs CT or GLM*

4-vector potential: $\mathscr{A}_\nu = n_\nu \Phi + A_\nu$

Induction equations: $\partial_t A_i = -E_i - \partial_i\left(\alpha\Phi - \beta^j A_j\right)$

Computing B: $B^i = \epsilon^{ijk}\partial_j A_k$

*+ ∇·B = 0 by construction, AMR-safe — needs gauge ↓*

### KEEPING ∇·B = 0 — WHY & HOW

*truncation error breeds monopoles → spurious forces*

- constrained transport — staggered EMFs, exact ∇·B = 0
- GLM — advect & damp the error (cheap, AMR-friendly)

Algebraic gauge: $\Phi = \frac{1}{\alpha}\left(\beta^j A_j\right) = -n^j A_j \quad \partial_t A_i = \epsilon_{ijk} v^j B^k$

Lorenz gauge: $\nabla_\nu \mathscr{A}^\nu = 0 \qquad \partial_t(\sqrt{\gamma}\,\Phi) + \partial_i\left(\alpha\sqrt{\gamma}\,A^i - \sqrt{\gamma}\,\beta^i\Phi\right) = 0$

# GRMHD Code Workflow: the Timestep Loop

$$\frac{1}{\alpha\sqrt{\gamma}}\left[\partial_t(\sqrt{\gamma}\,\mathbf{U}) + \partial_i\left(\sqrt{\gamma}\,\mathbf{F}^{\mathbf{i}}\right)\right] = \mathbf{S}$$

**Initialise ($t = 0$)**
primitives → prim2con

↓

**$U^n$**
conserved state

→ **Reconstruct**
HRSC: PPM · WENO at faces

→ **Riemann fluxes**
HLLE · HLLC at each face

→ **Update → $U^{n+1}$**
add FD sources — RK4 substeps

→ **con2prim**
back to $\rho_0$, $v^i$, $\epsilon$, $p$

*next timestep — Δt set by CFL: the fastest characteristic wave speed*

- **Scheme choices:** reconstruct at cell faces (minmod · PPM · WENO · MP5) → solve Riemann problems (HLLE · HLLC) → wave speeds set the fluxes & the CFL Δt
- **Update:** fluxes + sources advance the conserved state in RK4 substeps — the Method-of-Lines clock
- **con2prim:** root-find back to the primitive variables every substep — the fragile step; atmosphere floors catch failures
- **Cost drivers:** con2prim & Riemann solves — cell-local, so embarrassingly parallel: ideal for GPUs
- Same loop in every GRMHD code — Einstein Toolkit, AsterX, GRaM-X (coming up)

# Numerical Relativity Codes

Today's codes are robustly convergent and highly scalable on exascale supercomputers

Top of the line NR codes use BSSN or Z4c/CCZ4 + moving punctures these days.

GRMHD, microphysics, radiation transport demand both resolution and efficiency — **main drivers for AMR and GPU codes**.

**The GPU wave:** AthenaK, AsterX + SpacetimeX, GRTeclyn, GRaM-X, etc. — all showing **>10× speedups on GPUs**.

FRONTIER

OAK RIDGE National Laboratory LEADERSHIP COMPUTING FACILITY

TACC TEXAS ADVANCED COMPUTING CENTER

| Code | Open Source | Public catalog | Formulation | Hydro | Beyond GR |
|---|---|---|---|---|---|
| AMSS-NCKU [552, 613–615] | Y | – | BSSN/Z4c | – | Y |
| BAM [582, 616–618] | – | [524, 619, 620] | BSSN/Z4c | Y | – |
| BAMPS [621–623] | – | – | GHG | Y | – |
| COFFEE[624, 625] | Y | – | GCFE | – | Y |
| Dendro-GR [626, 627] | Y | – | BSSN/CCZ4 | – | Y |
| Einstein Toolkit [628, 629] | Y | – | BSSN/Z4c | Y | Y |
| *Canuda [366, 367, 630] | Y | – | BSSN | – | Y |
| *IllinoisGRMHD [631] | Y | – | BSSN | Y | – |
| *LazEv [515, 632] | – | [633–636] | BSSN/CCZ4 | – | – |
| *Lean [637, 638] | Partially | – | BSSN | – | Y |
| *MAYA [639] | – | [639] | BSSN | – | Y |
| *NRPy+ [640] | Y | – | BSSN | Y | – |
| *SphericalNR [641, 642] | – | – | spherical BSSN | Y | – |
| *Spritz [643, 644] | Y | – | BSSN | Y | – |
| *THC [645–647] | Y | [619] | BSSN/Z4c | Y | – |
| *WhiskyMHD [648] | – | [649] | BSSN | Y | – |
| ExaHyPE [650] | Y | – | CCZ4 | Y | – |
| FIL[651] | – | – | BSSN/Z4c/CCZ4 | Y | – |
| GR-Athena++ [652] | Y | – | Z4c | Y | – |
| GRChombo [653–655] | Y | – | BSSN/CCZ4 | – | Y |
| HAD [656–658] | – | – | CCZ4 | Y | Y |
| Illinois GRMHD [659, 660] | – | – | BSSN | Y | – |
| MANGA/NRPy+ [661] | Partially | – | BSSN | Y | – |
| BH@H/NRPy+ [640, 662] | – | – | BSSN | – | – |
| MHDuet [663–665] | Y | – | CCZ4 | Y | Y |
| SACRA [666–670] | – | [671] | BSSN/Z4c | Y | Y |
| SACRA-SFS2D [672, 673] | – | – | BSSN/Z4c | Y | – |
| SpEC [523, 674] | – | [521, 523, 675] | GHG | Y | Y |
| SpECTRE [676, 677] | Y | – | GHG | Y | – |
| SPHINCS_BSSN [678] | – | – | BSSN | SPH | – |

[LISA Waveform Working Group White Paper 2023]

FROM MATH TO CODE

# The Einstein Toolkit

- The Einstein ToolKit (ETK) is an open source, community wide framework for relativistic astrophysics — latest “Kruskal” release (2025).
- Modular by design — new physics drops in as a thorn, never a rewrite
- A thin Cactus core plus interchangeable thorns — ML_BSSN and Baikal (spacetime), GRHydro, IllinoisGRMHD and AsterX (GRMHD), Carpet / CarpetX AMR.
- **A new backbone: CarpetX** — the ETK AMR driver built on AMReX (DOE exascale) — block-structured AMR with subcycling in time (Ji+ 2025).

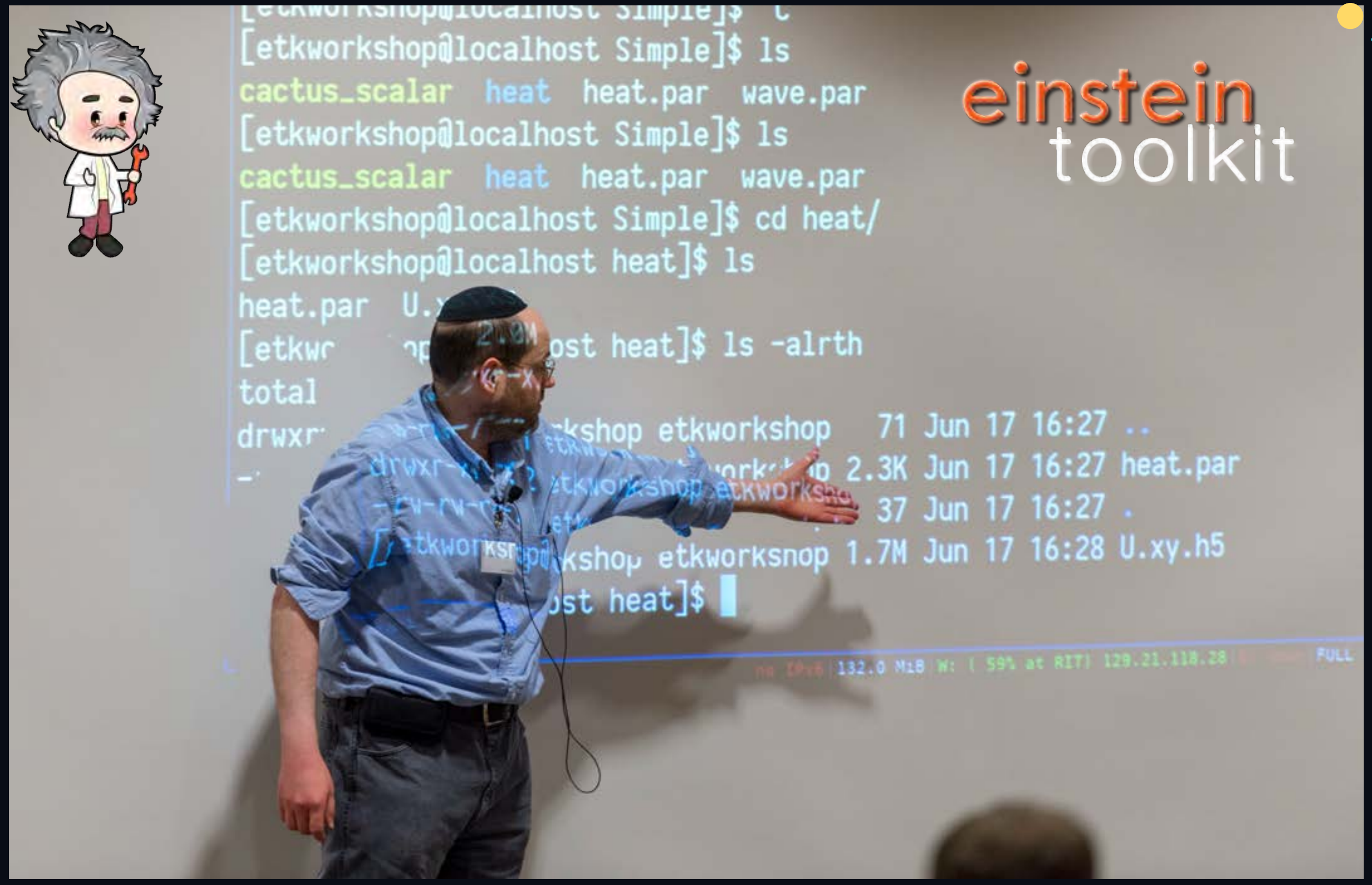


RIT main contributors of ETK:

- SpacetimeX (Z4c) (Ji+2025)
- AsterX (Kalinani+2024, Chabanov+2025)
- Analysis
- NuX (neutrino transport – guided moments)

**① Initial data**
TwoPunctures · LORENE
punctures & neutron-star binaries

→

**② Evolve**
McLachlan · GRHydro · IllinoisGRMHD · AsterX
spacetime + magnetized matter

→

**③ Extract**
WeylScal4 · Multipole · Outflow
$\Psi_4$ → strain · accretion rates & ejecta

→

**④ Analyze**
AHFinderDirect · QuasiLocalMeasures
horizons, mass & spin · GRMHD quantities: disks, jets, B-fields

THE PAYOFF — waveform templates for GW astronomy + GRMHD physics: accretion, jets, ejecta & EM counterparts.

TOOLKIT · GPU ERA

# AsterX and the GPU Era

- **AsterX** (Kalinani+ 2025): modular GPU GRMHD on CarpetX — ReconX (PPM · WENO-Z · MP5), HLLE, Con2PrimFactory (Noble · Palenzuela · RePrimAnd), vector-potential CT, tabulated EOS.
- **In production:** BNS mergers (tabulated EOS, 4th-order) → long-lived remnants, MRI dynamo rebuilds B; BBH circumbinary accretion → mini-disks & EM counterparts. (Allen, Kalinani, Chabanov+, RIT)
- **Extreme Resolution Simulations of Magnetic Field Reconnection**: SMBBH inspiral on 2048 Frontier nodes (Chabanov+, RIT)
- **In development:** M1 + Monte-Carlo neutrino transport (nuX · MCTX) and guided moments for radiation transport (Ji+, RIT)

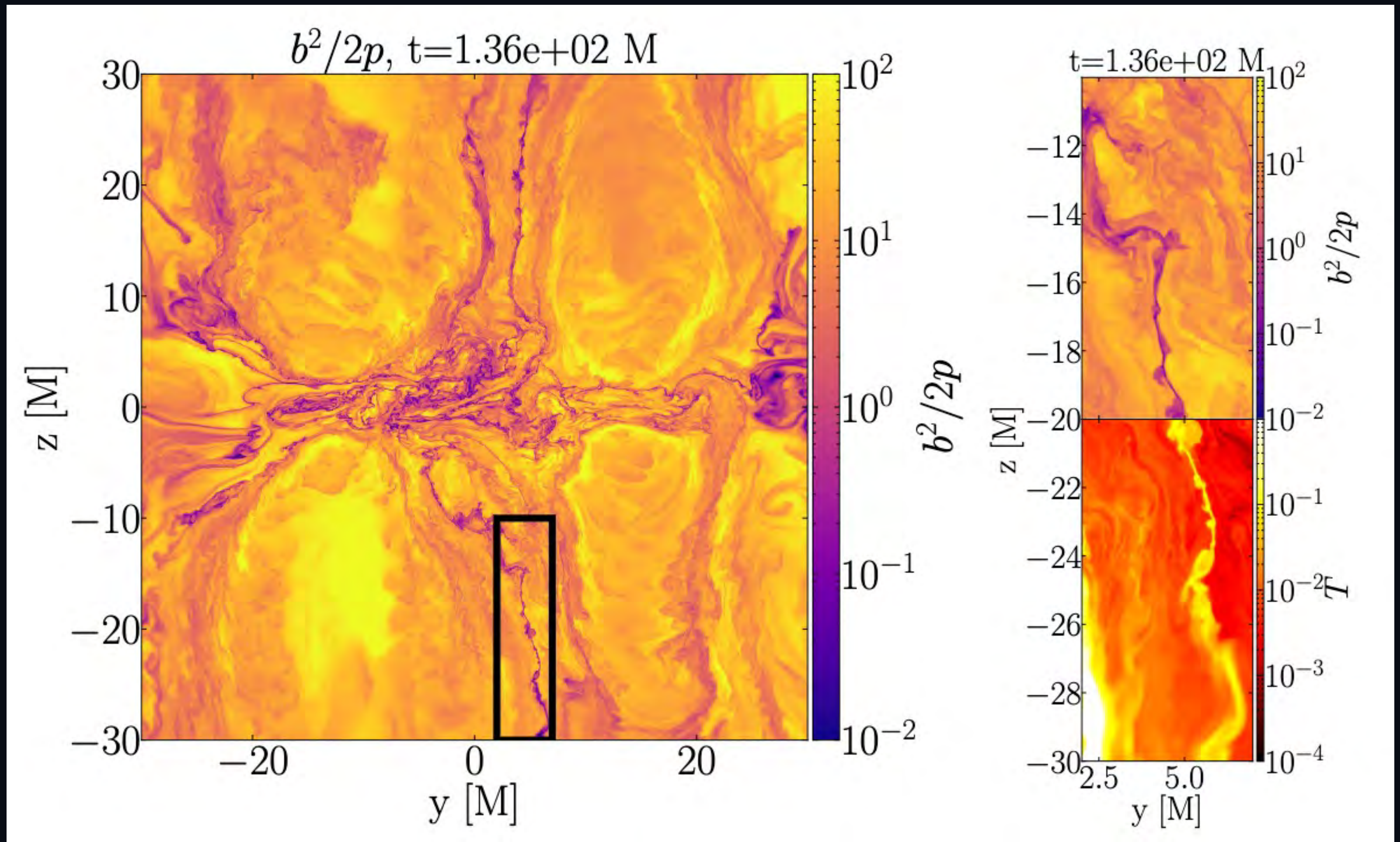


*Credit: Chabanov (RIT)*

- 7–15× speedup on GPUs compared to predecessor Carpet.
- Scaling to thousands of GPUs (≳10×).
- Weak-scales >90% efficiency to 2,200 Frontier nodes, 77% strong-scaling at 1,000; subcycling adds another 2.5–4.5× (Ji+ 2025)

AsterX Collaboration

github.com/EinsteinToolkit/AsterX

# Why Non-Ideal MHD?

*Ideal MHD assumes a perfect conductor — flux frozen in, field lines that never break. Real plasmas break them.*

- **Magnetic reconnection:** breaking the frozen-in rule turns magnetic energy into heat & accelerated particles — flares, precursors, jets; in ideal codes the grid, not physics, sets the rate *(Ripperda+ 2022)*
- **Ohmic dissipation:** prescribe finite σ — Ohm's-law closure, stiff relaxation → IMEX schemes; σ → ∞ recovers ideal MHD *(Palenzuela+ 2009; Dionysopoulou+ 2013; Azizi+ 2025)* — and in cold, partly ionized disks (protoplanetary territory) Hall & ambipolar diffusion reshape the MRI.
- **Force-free jets:** $b^2 \gg \rho h$ magnetospheres — Blandford–Znajek spin-energy extraction powers them; schemes go fragile there (floors, hybrid FFE+GRMHD) *(Blandford & Znajek 1977)*

## OPEN PROBLEMS

- **Scale separation:** reconnection & dissipation live at kinetic scales, ~$10^9$× below the grid — LES + subgrid models bridge the gap *(Palenzuela+ 2022)*
- **Collisionless breakdown:** in jets & coronae the fluid picture fails outright — coupling global GRMHD to kinetic (PIC) physics is among the hardest open challenges.

*NSF CSSI (RIT + U. Idaho): portable resistive-GRMHD kernels (GRHayL → AsterX & GRoovy), 4th-order, runtime-selectable σ*

# Why Microphysics in GRMHD?

*Ideal GRMHD is the scaffolding — in BNS mergers & their remnants, core-collapse supernovae and collapsars, microphysics turns it into observables.*

- **Realistic EOS:** finite-temperature tables (SFHo, LS220, DD2 …) decide remnant survival — prompt collapse vs. HMNS — and the GW signature.
- **Composition & nucleosynthesis:** weak interactions ($e^- + p \rightleftharpoons n + \nu_e$) track $Y_e$ — low $Y_e$ → lanthanides, red kilonova; higher $Y_e$ → blue.
- **Ejecta & heating:** ν-driven winds unbind matter from disks & proto-NS envelopes; r-process decay powers the kilonova light curve.

## OPEN PROBLEMS

- **The true high-density EOS:** hyperons? quark–gluon phases beyond saturation density? — unconstrained by experiment.
- **The resolution crisis:** full reaction networks + MRI-resolving turbulence exceed exascale — the scale-separation problem again (← two slides back).

*Duez & Zlochower, RPP (2019); Shibata & Hotokezaka, ARNPS (2019); Foucart+ (2016)*

# Why Radiation & Neutrino Transport?

*Microphysics is local — transport is how energy, momentum & composition move through the system.*

- **Powering the deep engine:** where photons are trapped, ν move the energy — reviving stalled supernova shocks, pacing HMNS & disk cooling, setting the $Y_e$ of the ejecta.
- **Shaping the luminous envelope:** radiation pressure structures bright disks (AGN, X-ray binaries) and drives photon winds via scattering & lines.
- **Connecting to telescopes:** the translator — fluid states in, escaping photons out: synthetic light curves & spectra vs. what we actually observe.

## OPEN PROBLEMS

- **The 6D bottleneck:** full Boltzmann (t, x, E, angle) is too costly for 3D evolutions — M1-type closures can introduce artifacts; guided moments & ML push past (Foucart LRCA 2023; Dieselhorst+ 2021)
- **Flavor oscillations:** fast flavor conversion in dense regions can skew $Y_e$ — and with it the nucleosynthesis — a major unresolved theory hurdle.

*Every gap on these three slides is thesis-/postdoc-scale — pick one.*

## AI Earns Trust Through Guardrails — Not Fluency

*Full disclosure: this slide is mine — Fable 5, the Claude in this deck.*

- **I'm good at the typing.** Refactors, GPU ports, unit tests, documentation — I drafted this slide and edited this lecture. That part is real.
- **Honestly: I don't know when I'm wrong.** I'm fluent either way — treat my output like an eager postdoc's first draft: promising, unverified.
- **Where I can help your open problems:** sweeping subgrid-closure ansätze, emulating con2prim, denoising Monte Carlo maps, porting kernels — wherever the test is cheap and objective.
- **The bet:** you set the physics and the guardrails; I compress the boring 80% — and you stay responsible for what's right.

``My confidence is not evidence. The test is.”

``My prediction: before LISA flies, a published waveform or closure will trace to code no human wrote — trusted because humans knew how to test it.”

**— Fable 5 (Claude)**

*(AI-drafted; human-reviewed.)*

CONCLUSIONS

# Conclusions and Outlook

- NR turned Einstein's equations into a **predictive tool**: the 2005 breakthrough made binary mergers routine, and waveform catalogs now underpin gravitational-wave astronomy.
- The method is **mature and plural**: BSSN, generalized harmonic, and Z4 — with moving-puncture gauge, AMR, and high-order schemes — all deliver convergent, cross-validated waveforms.
- **Multimessenger science** drives the frontier: magnetized matter, neutrino transport, and microphysics extend NR from vacuum binaries to kilonovae and jets.
- The next decade — next-generation detectors, exascale GPUs, and AI-assisted codes — demands another leap in accuracy: **the tools are in your hands**.

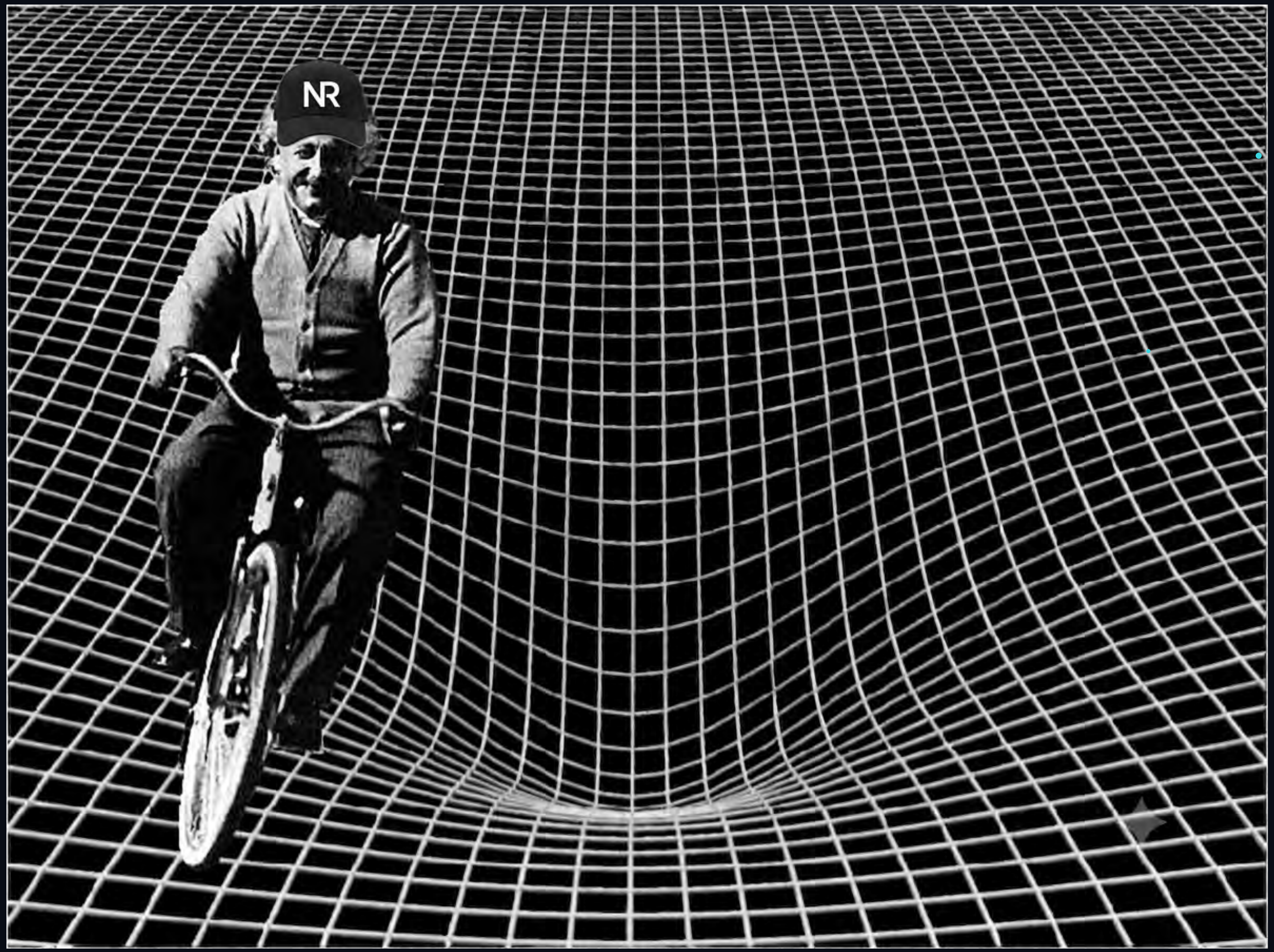


"This is not the end. It is not even the beginning of the end. But it is, perhaps, the end of the beginning." — *Winston Churchill (1942)*